CHARACTERIZATION OF CLINICALLY IMPORTANT MUTANTS OF HUMAN SECRETAGOGIN

M.Sc. Thesis
2017

Submitted to

CENTRAL DEPARTMENT OF BIOTECHNOLOGY
Tribhuvan University
Institute of Science and Technology
Kirtipur, Kathmandu, Nepal

For partial fulfilment of requirement for the degree of
2 year M.Sc. in Biotechnology

By

Rashmi Thapa
Roll No: 212/071
T.U. Regd. No.: 5-2-33-130-2010

Supervisors

Prof. Dr.Tilak R. Shrestha
Central Department of Biotechnology
Trivuwan University
Kirtipur, Kathmandu

Yogendra Sharma, Ph.D, FASc, FNASc
Chief Scientist and Group Leader
Professor of Biology, AcSIR

ACKNOWLEDGEMENTS

First I want to express my deepest gratitude towards **Prof. Dr.Tilak R. Shrestha**, Central Department of Biotechnology for overall supervision of my work in CCMB. It was because of his support and constant efforts that I had an opportunity to carry out my dissertation there in CCMB. His suggestions were very helpful to increase my knowledge, both in practical and theoretical aspects. I am very thankful to **Dr. Yogendra Sharma** for accepting me in his lab to carry out my dissertation. As my external supervisor, he not only guided me in my work but also provided me favourable environment to work in CCMB.

I am very grateful to **Prof. Dr. Krishna Das Manandhar**, the HOD of Central Department of Biotechnology, Tribhuvan University for granting me permission to carry out my dissertation in CCMB. I would also like to thank the former HOD, **Prof. Dr.Rajani Malla** for her support.

I would like express my profound appreciation towards the present Director of CCMB, **Dr. Rakesh K Mishra** for giving me an opportunity to be the part of the esteemed organization.

I am very truly thankful to my mentors**, Anand Sharma and Radhika Khandelwal**, senior PhD students in my lab for designing the project and guiding me through each and every step in my research work. They had been great guides, great friends as well as my local guardians during my stay there.

I want to thank **Amrutha HC**, PhD student in my lab, who had been a great companion, source of encouragement and helped me understand the lab practices. I would like to thank all the labmates, **Dr. Shanti, Dr. Venu, Asmita, Aditya, Swati and Uday** for their suggestions, help and support. I am very thankful to **Mr.Sumit Paliwal** for providing me total RNA sample of human pancreatic cell from which I could start up my work.

I am thankful to **Alok Kumar** and **Dr. Shadiya Praveen** for making my stay there comfortable and for all their moral support. I also want to express my gratitude to **Navin Adhikari**, my classmate, who had been with me to CCMB and supported me like a family.

My deepest gratitude towards those who have coordinated directly or indirectly with me to accomplish my work. Thanks to all the professors, faculties, staff members, my seniors and juniors of Central Department of Biotechnology for their cooperation and support. Lastly, I would be thanking me family for all their love, blessings and investment throughout my educational career.

ABBREVIATIONS

µg	micro gram
µl	micro litre
A	Absorbance
ANS	8-Anilinonapthalene-1-sulfonic acid
Ca^{2+}	Calcium ion
CD	Circular Dichroism
DF	Dilution Factor
DMEM	Dulbecco's Modified Eagle's Media
DTT	Dithioreitol
EDTA	Ethylenediaminetetraacetic acid
EGTA	Ethylene glycol-bis(β-aminoethyl ether)-N,N,N',N'-tetraacetic acid
F.I.	Fluorescence Intensity
F.U.	Fluorescence Unit
GdmCl	Guanidium Hydrochloride
GF	Gel Filtration
HIC	Hydrophobic interaction chromatography
hSCGN	human Secretagogin
IPTG	Isopropyl β–D-1-thiogalactopyranoside
ITC	Isothermal Titration Calorimetry
LB	Luria Bertani
mg	milligram
ml	milliliter
MRE	Mean Residual Elipticity
MQ	Milli-Q-water
mSCGN	mouse Secretagogin

ng	nanogram
OD	Optical Density
PBS	Phosphate Buffer Saline
PCR	Polymerase Chain Reaction
PMSF	Phenylmethylsulfonylfluoride
rpm	rotation per minute
SCGN	Secretagogin
SDM	Site Directed Mutagenesis
SDS PAGE	Sodium Dodecyl sulphate Polyacrylamide Gel Eletrophoresis
SNPs	Single Nucleotide Polymorphism
WT	Wild type
λ	Wavelength
UC	Ulcerative Colitis
TCEP	Tris(2-carboxyethyl)phosphine

List of Tables

List of Figures

ABSTRACT

Secretagogin, a hexa EF-hand family protein, is recently discovered protein which is abundance in pancreatic, neuronal and neuroendocrinal cells. This protein is present in all vertebrates with its known function in pancreas and neurons. Secretagogin, being considered as multifunctional protein, its defect might lead to multiple system disorder. Secretagogin is already identified as the marker of various cancer and tumors. This protein is directly found to be associated with diabetes. The protein is found in various cellular locations including cytoplasm, nucleus, endoplasmic reticulum where it is believed to be involved in different function. Many mutations in this gene are enlisted in database which are rare and related to pathologies but are not well studied. Addressing these problems, "Characterization of clinically important mutants of human Secretagogin" was designed as an approach to improve our understanding towards the consequences of such mutation on the structure and function of the protein as a whole using different biophysical techniques. For the same purpose, wild type human secretagogin as well as its three mutants A216V, R77H and V108M were successfully cloned in pET-21b vector. Wild type as well as mutant proteins were overexpressed and purified. Biophysical characterizations of the proteins were carried out using fluorescence spectroscopy, circular dichroism, isothermal titration calorimetry and analytical gel filtration. Further, the behavior of these proteins was studied by partial trypsin digestion, glutaraldehyde crosslinking of proteins and chemical unfolding of protein. Interaction of the proteins with insulin was further accessed through Far western blot, tryptophan fluorescence and circular dichroism. It was found that some of the mutants showed altered structural and functional properties in interaction with insulin. The mutants show different oligomeric states than that of the wild type protein. The stability of apo form of R77H mutant was lowest ($C_{1/2}$ 2.46M) and that of A216V was similar to hSCGN WT ($C_{1/2}$ 2.65M) and in all these cases the stability was higher in holo form of protein whereas in case of V108M mutant, stability of holo form of protein ($C_{1/2}$ 2.66M) was similar to its apo form ($C_{1/2}$ 2.68M). Though the calcium binding properties in mutants were not completely destroyed, there was some alteration in the affinity for calcium along with the mechanism of binding calcium. The calcium sensor site of Secretagogin seems to have been lost because of the mutation. Specifically in case of V108M mutant, the calcium dependent redox switch seems to have been reversed as dimeric form seemed to be more Calcium responsive. The mutant V108M shows the characters completely different from other proteins in terms of structure and calcium binding properties by virtue of which V108M can be considered as the most affected protein among all the mutant human secretagogin.

Keywords: Secretagogin, apo, holo, oxidized, reduced, oligomer, spectra

CHAPTER 1

INTRODUCTION

1.1 Background

Secretagogin, as the name suggests, is the protein that induces secretion. The protein is expressed most abundantly in neurons, pancreatic β-cells, neuroendocrine cells and to some extent in the epithelial cells of gastrointestinal tract (stomach, intestine and colon). The protein is localized in different cellular locations including cytoplasm, nucleus, cell membrane and endoplasmic reticulum. Structurally the protein resembles calretinin (38% sequence identity) and belongs to the Calmodulin group i.e. EF-hand protein family (Wagner *et al*., 2000). It is a hexa EF-hand calcium binding sensor protein that undergoes conformational change upon binding Calcium. Out of 6 EF-hands present, only four binds calcium with one site having very high affinity for calcium (Rogstam *et al*., 2007). Human secretagogin shows 73% identity to the secretagogin of *Danio rerio* whose crystal structure has been solved. The protein has 3 globular domains arranged in a V-shaped structure with 2 EF-hand motifs in each domain. The EF hand motifs 1 and 2 are non-functional whereas the EF hand motifs 3, 4, 5 and 6, being highly conserved are competent in binding calcium. The domains are linked together by linker region. Domain II and III forms the core and are associated closely whereas domain I is poorly attached to the core (Bitto *et al*., 2010).

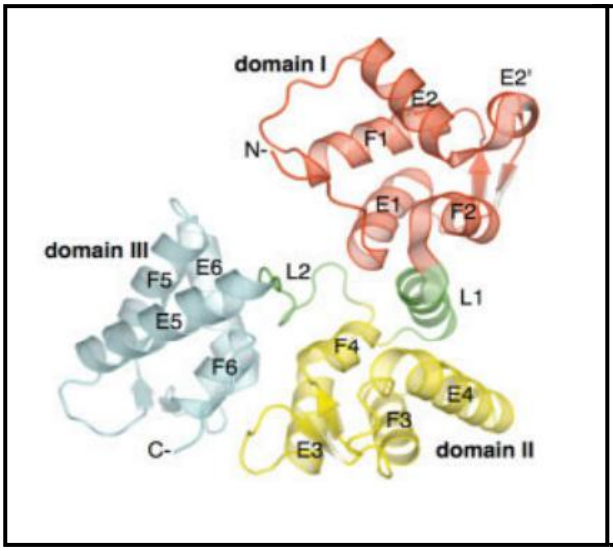

Figure 1.1: Crystal structure of Secretagogin o*f Danio rerio* (Bitto *et al*., 2010).

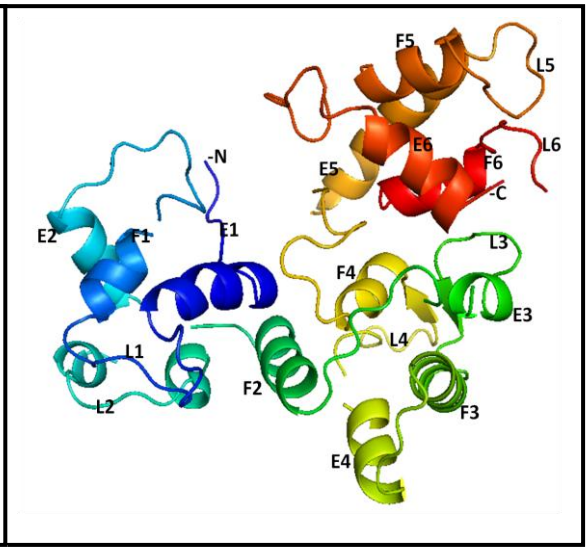

Figure 1.2: Crystal structure of Secretagogin o*f* human designed from phyre taking secretagogin of *Danio rerio* as template for homology modelling

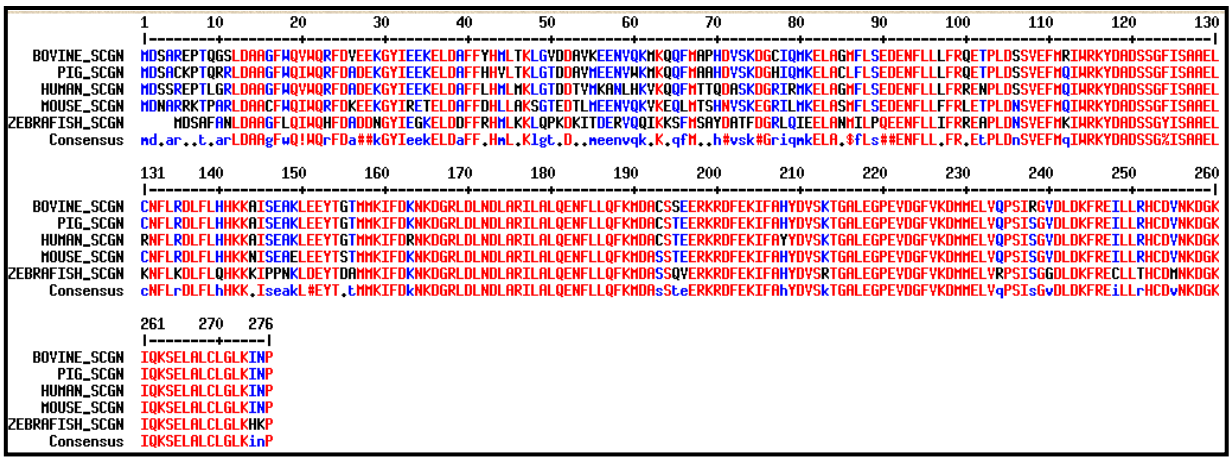

Figure 1.3: Multiple sequence alignment of Secretagogin of different animals (bovine, pig, human, mouse and zebrafish) using Multalin (F. CORPET, 1988, Nucl. Acids Res., 16 (22), 10881-10890)

MDSSREPTLGRLDAAGFWQVWQRFDADEKGYIEEKELDAFFLHMLMKLGTDDTVMKANLHKVKQQFM
TTQDASKDGRIRMKELAGMFLSEDENFLLLFRRENPLDSSVEFMQIWRKYDADSSGFISAAELRNFLRDLFL
HHKKAISEAKLEEYTGTMMKIFDRNKDGRLDLNDLARILALQENFLLQFKMDACSTEERKRDFEKIFAYYDV
SKTGALEGPEVDGFVKDMMELVQPSISGVDLDKFREILLRHCDVNKDGKIQKSELALCLGLKINP

Figure 1.4: Annotated sequence of human Secretagogin with six domains underlined, Calcium binding loop in green colour and site of mutation marked by red amino acids (Uniprot ID: O76038)

Human Secretagogin shows 73% identity with Secretagogin of Zebrafish, 85% identity with mouse Secretagogin, 90% identity with pig Secretagogin and 89% identity with bovine Secretagogin (NCBI blastp). Secretagogin of all the animals taken for alignment consists of 276 amino acids except that of Zebrafish which contains only 272 amino acids. Variation mostly lies in the first and second EF-hand motifs of the protein whereas the remaining EF-hands seems to be somewhat conserved.

The gene encoding secretagogin protein in located in chromosome 6 at the position 6p22.1-6p22.3 and possesses 10 exons with 5'-untranslated region containing 156bp and 3'-untranslated region containing 450bp (Y16752). The mRNA encoding secretagogin is 1492 bp and the gene itself is 831bp coding a 32kD protein with 276 amino acids (Wagner *et al*., 2000). Two variants of the protein has been identified, secretagogin Q22R and setagin. Secretagogin Q22R is formed by RNA editing such that glutamine is replaced by arginine at position 22 and shows calcium binding properties similar to normal secretagogin. Setagin, the second variant formed by alternative splicing is 49 amino acids long and has lost the calcium binding property and is exclusively found in pancreas. The function of setagin and its structural properties still remains a question mark. (Zierhut *et al*., 2005).

This protein functions in neurons to stimulate the exocytosis of neurotransmitters and in β- pancreatic cells stimulates the exocytosis of insulin in calcium dependent manner. It does so by binding with the protein Synaptosomal associated protein-25/SNAP-25 (which is the component of SNARE complex) which helps in fusion of the exocytotic

vesicles to the cell membrane (Rogstam *et al*., 2007). In β-pancreatic cells, secretagogin not only enhances the exocytosis of insulin but also significantly increases the expression of insulin by 5-10 folds. This protein is also involved in cell cycle control, cell differentiation or inhibition of replication (Wagner *et al*., 2000). The protein acts as a biomarker of different tumour and carcinoma. In the differentiated neuroendocrine cells, secretagogin is strongly expressed along with other neuroendocrinal markers. The protein is found to be localized both in cytoplasm and nucleus in normal neuroendocrine cells as well as differentiated NE cells and malignant carcinoma suggests its role in transcription (Adolf *et al*., 2007).

1.2 Missense mutation and its effect

Mutations can occur in any sequence of DNA due to error prone nature of DNA replication and failure of DNA machinery to correct it. The most common type mutation occurring in nature is Single Nucleotide Polymorphism (SNP) with the frequency of one per 1000 bases which occurs by missense mutation. Missense mutation is the mutation in DNA sequence that causes the conversion of a codon encoding one amino acid to the codon encoding some other amino acid. This mutation if occurs in the coding region might cause defect in protein. The effect of this mutation might be neutral with no alteration in the phenotype or may result in alteration of an individual's characters and phenotype which frequently occurs due to change in protein structure. These missense mutations are the root cause of almost half of the mutations causing genetic disease (Wang and Mount, 2001). The alteration in protein due to missense mutation can be beneficial that might cause gain of function or increase the fitness of the protein. Such mutations are positively selected by nature during evolution. But sometimes these mutations can lead to detrimental consequences by disrupting the protein's function. In this regard, the stability of protein might be affected by alteration of Gibb's free energy. Destabilization in protein structure might be caused by one or many of the following reasons, loss of hydrogen bonds, reduced hydrophobic interaction, removal of salt bridges, burying of charged residue, internal cavity formation, overcrowding, disruption of metal binding or loss of disulphide bonds. Some mutations might cause increment of Gibb's free energy and destabilize the folded state while other mutations might cause lowering of Gibb's free energy and make the protein structure too rigid, limiting the flexibility of protein structure as in case of enzymes. Others can affect protein-protein interaction, oligomerization, catalytic property, allosteric regulation as well as post translational modification (Wang and Moult, 2001) and (Studer, Dessailly, & Orengo *et al*., 2013).

1.3 Clinically important mutation in human secretagogin gene

Some missense mutations have also been reported in secretagogin gene and some are enlisted just in the database. The clinically important mutations in secretagogin are R77H, A216V, V108M, R135Q, Q22R and P276Q. Out of all the six mutations, R77H and A216V mutations are located in the calcium binding loop of EF-hand motif whereas the

remaining are positioned in the helix region of the EF- hand motif. The mutation R77H is reported to be involved in inflammatory bowel disorders including Cronh's disease and Ulcerative colitis (UC). These disorders might result as the consequence of R77H mutation in secretagogin gene in homozygous and recessive condition and first reported in consanguineous family of Mexican origin and is shown in fig. 1.5 (Llano *et al*., 2014). The mutation causes impaired secretion of Glucagon like peptide-1 (GLP-1) after fatty acid stimulation and affects the interaction of secretagogin with SNAP-25 and impairs the exocytosis as well as hormone release from enteroendocrine cells. The apo from of both proteins could not bind SNAP-25 whereas in holo form R77H showed insignificant binding with SNAP-25 (fig. 1.6). This could be considered as the sole cause of the disease (Norris *et al*., 2014). Other mutations in the gene related to cancer are listed in Human Cancer Proteome Variation Database. The mutations V108M and R135Q are associated with ovarian cancer and P276Q with pancreatic cancer (COSMIC). The variation A216V is non-cancer related mutation whose effect is not yet known.

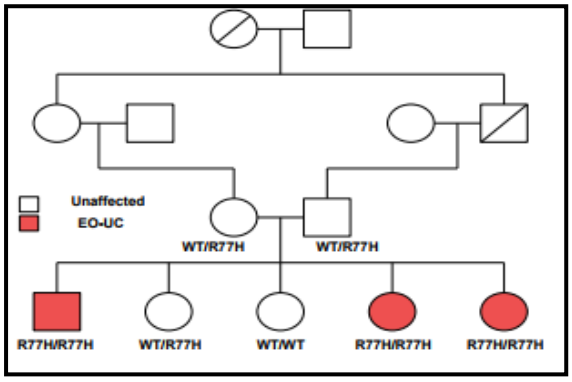

Figure 1.5: Pedigree analysis of three children diagnosed with early onset of UC showing homozygous mutation (R77H) in secretagogin (Norris *et al*., 2014)

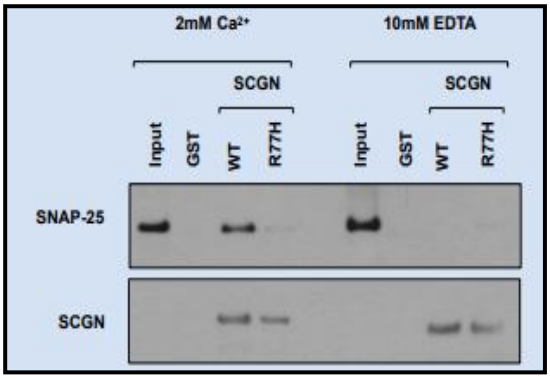

Figure 1.6: Western blot result showing R77H prevents binding with SNAP-25 (Norris *et al*., 2014)

Table 1: Cancer related variation in human secretagogin (Source: CanProVar)

NO.	csID	variation	change conservation+	Domain	cancer name	PubMed	data source++	interface
1	cs76235	V108M	1		Ovarian Cancer	18772890 21720365	TCGA, COSMIC	
2	cs63132	R135Q	1		Ovarian Cancer	18772890 21720365	TCGA, COSMIC	
3	cs47205	P276Q	-1		Pancreatic Cancer		COSMIC	

+Conservation of amino acid substitutions are defined here according to the BLOSUM62 matrix, conservative changes were those having a positive or neutral sign in the matrix, whereas non-conservative changes were those having a negative value (Cargill, et al. 1999).
++Data sources: HPI, COSMIC, OMIM, TCGA, BIOMART, Greenman2007, Sjoblom2006, Ding2008
Interface information was collected from Wang 2012

Table 2: Non-caner related variation in Secretagogin

Variant	UniProt ID	Mutation	Disease	Mutation type
VAR_042710	SEGN_HUMAN	A216V	-	Polymorphism

(Source: http://snpeffect.switchlab.org/uniprot/SEGN_HUMAN)

1.4 Rationale of the study

While new diseases and abnormalities are getting discovered day by day, the causes of many still remain unidentified. On average 3.3 millions of SNPs in human genome are identified whose consequences are yet to be studied. If correlation between these genetic variations and abnormalities could be studied, the causes of these abnormalities could be pointed out and their remedies and therapies could be established. Secretagogin, being a multifunctional protein, any defect in it can affect several systems in the cell. Many mutations in Secretagogin gene has been reported which are implicated in several abnormalities. These clinically important mutations are rare with very low frequency of occurrence in the population and thus are not well studied. Thus the study of these mutations can help to obtain clue about the abnormalities caused by such mutations and provide insights about how the abnormalities can be corrected or cured.

1.5 Research hypothesis

1. Single amino acid mutation in Secretagogin might or might not interfere with the structural integrity of the protein.
2. These mutations might or might not cause change in calcium binding properties of secretagogin protein.
3. These point mutations might or might not have any effect on the native function of secretagogin protein.

1.6 Research objectives

1.6.1 General objectives

1. To study the structural integrity of mutant human secretagogin.
2. To study the effect of mutations on calcium binding affinities and other thermodynamic parameter.
3. To understand the effects of mutation on the biological function of the Secretagogin protein (by protein-protein interaction).

1.6.2 Specific objectives

1. Cloning of wild type human secretagogin gene along with its mutants (A216V, R77H and V108M) in pET-21b vector system.
2. Protein overexpression and purification.
3. Characterization of mutants using different biophysical techniques.
4. Study of interaction of wild type and mutant Secretagogin with insulin
5. Cloning of the wild type and mutant *scgn* gene in mammalian vector, pEGFP-N3.
6. Transfection of SCGN knockout mouse pancreatic cell line (MIN6) with the constructs and establishment of stably transfected cell lines.

CHAPTER 2

LITERATURE REVIEW

2.1 Calcium binding proteins

Calcium, the third most abundant metal, is the most important metal ions involved in cell physiology. Calcium plays an important role from the birth of the cell, defence and cell immunity to its death (apoptosis). It acts as secondary messengers in a cell and has a critical role in cell signalling. The basal concentration of calcium in cytosol is maintained low i.e. about 100nM which is 20,000 times lower than the extracellular Calcium concentration (in millimolar range). This is necessary to prevent the precipitation of phosphates in the form of Calcium phosphate and hyperactivation of cell. Cell maintains this low concentration of calcium either by extrusion, buffering or compartmentation. Endoplasmic reticulum and mitochondria are the two most major storage bodies of calcium. Whenever required, calcium is either taken up from the extracellular matrix or from these calcium storages through specific channels. In electrically excitable cells like neurons and muscle cells, the cytosolic Ca^{2+} level rises to 400nM or above during membrane depolarization. The plasma membrane Ca^{2+} ATPase (PMCA) along with sarco-endoplasmic Ca^{2+} ATPase (SERCA) and other calcium channel helps in extruding Calcium from the cytosol and maintain basal Ca^{2+} level. Calcium binding proteins (CaBPs) are another mechanism through which the cell maintains low level of Ca^{2+}. The binding of these proteins with Calcium is coordinated by oxygen of carbonyl or carboxyl groups (sometimes neutral oxygen) forming pentagonal bipyramid. Usually the coordination of calcium occurs with 6 to 8 oxygens (Fig. 1.7) but coordination with upto 12 oxygens is also possible (Chapham, 2007). Specific properties of Calcium define why Calcium is preferred to other divalent cations like Magnesium. Unlike Ca, Mg has smaller size and lower polarizability which do not permit much flexibility in its geometry for the coordinating site (Brini *et al.*, 2013).

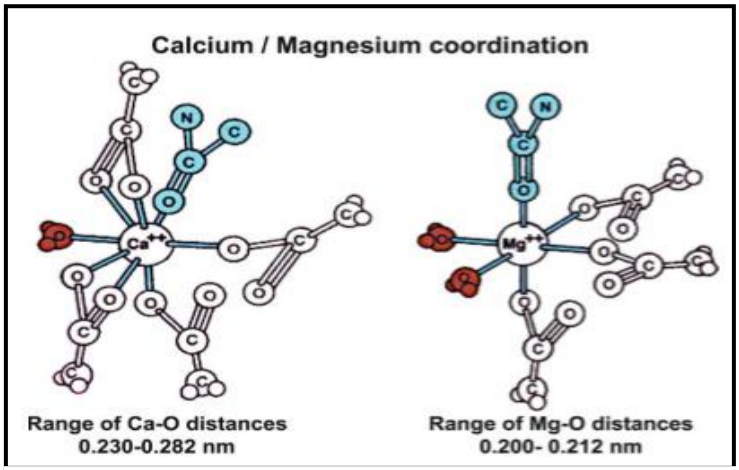

Figure 1.7: Hypothetical binding of Ca^{2+} and Mg^{2+} to EF-hand motif (Brini *et al.*, 2013)

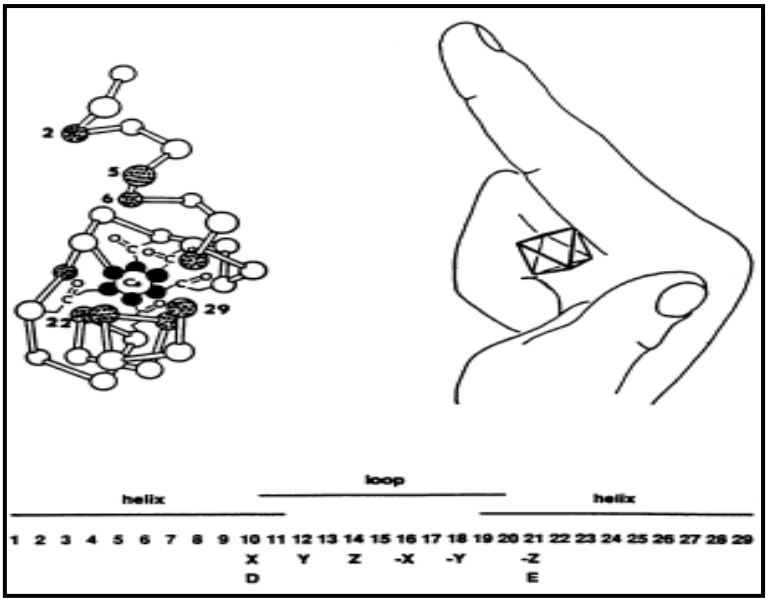

Figure 1.8: EF-hand Calcium binding domain

Several groups of CaBPs are identified which has distinct structure and diverse functions. The **EF hand** protein is a family of professional Calcium binding proteins bearing EF hand motifs with helix-loop-helix structure. The motif was discovered by Kretsingser and Knockholds in 1973 from crystal structure of of parvalbumin which contains six helices. The loop region contains 12 amino acids out of which residues at the position 1, 3, 5, 7, 9 and 12 are involved in calcium binding in the pattern X ● Y ● Z ● -Y ● -X ● ●- Z (Fig. 1.8). X, Y, Z, -X, -Y and –Z represent the residues that coordinate Calcium and ● represent the residues that are not involved in calcium coordination. The 6^{th} position in the loop is conserved for Glycine that provides flexibility to the structure. X and Y are usually Asp or Asn residues whereas at position Z, Asp, Asn or Ser are usually found contributing coordinating oxygen. At position –Y, a peptide carbonyl oxygen coordinates Ca^{2+} whereas a water oxygen coordinates Ca^{2+} at position –X. –Z position is conserved for Asp or Glu. EF hand motif usually occurs in pairs but sometimes single or odd number EF-hand motif is also observed (Brini *et al*, 2013). The motif consists of two perpendicularly oriented α-helices connected by flexible loop. The name was given from the E (5^{th}) and F (6^{th}) helices of parvalbumin which coordinates calcium and whose structure resembles that of hand. A protein can have one or multiple EF-hand motif among which all may not be functional. More than one EF-hand motif in same protein might have occurred by gene duplication during the process of evolution. The calcium binding residues in the loops if replaced by other residues results in the formation of non canonical EF-hand motif unable to coordinate calcium. Calmodulin is the most conserved EF-hand protein with 100% sequence identity in vertebrates. It consists of four EF-hands with different Calcium affinities. Thus it is taken as a model while studying the EF-hand proteins. The amino acid sequence of first EF-hand loop of Calmodulin is DKDGDGTITTKE. The large group of CaBPs that sequester calcium and acts as buffer maintaining its level in a cell like parvalbumin, calbindin and calbindin. Another group of protein called the sensor protein has additional function than just buffering calcium. The proteins having higher

affinity for calcium and undergoes huge conformational change upon calcium binding thus decoding the information for signal transduction. The binding of calcium exposes the hydrophobic patches in the protein, enabling the protein to interact with its binding partners. Calmodulin, troponin C and recoverin fall under this group (Carafoli and Krebs, 2016).

STIM1 (Stromal Interaction molecule-1) is another EF-hand protein present in the membrane of Endoplasmic reticulum that senses low calcium concentration in its lumen and activates Store operated Ca^{2+} Entry (SOCE) in non excitable cells. The low concentration of Ca^{2+} causes the release of Ca^{2+} from N-terminal low affinity EF-hand motif of STIM1 resulting in its change in conformation causing it to form aggregates just below the Orai protein in the plasma membrane which acts as a channel for Ca^{2+} entry (Brini *et al.*, 2013). S100 forms the largest family of EF-hand protein. Proteins from this family usually consist of 2 EF-hands and exist as homo- or heterodimer. The EF-hand motif at C-terminal is canonical whereas at N-terminal consists of pseudo-EF hand that consists of 14 residues long loop that coordinates Ca^{2+} with low affinity (Carafoli and Krebs, 2016).

Another Calcium binding structure is the C_2 domain that is involved mostly in signal transduction and membrane trafficking. Protein-kinase C, synaptogamins, Phosphoinositide 3-kinase (PI3K), phospholipases are few proteins containing C_2 domain. The protein has a β-sandwich structure with two four-stranded β-sheets connected by three loops at the top and four loops at the bottom. Ca^{2+} binding occurs at the three top loops in cluster. Five aspartate side chain, one serine side chain and three carbonyl groups form the calcium binding site. The binding of Calcium creates an electrostatic potential that induces the protein to associate with the membrane. The binding of these proteins with the phospholipids, fill the unsatisfied coordination sites on the bound Ca^{2+} ion thus resulting in 1000 fold increase in Ca^{2+} binding affinity of C_2 domain (Rizo and Sudhof, 1998).

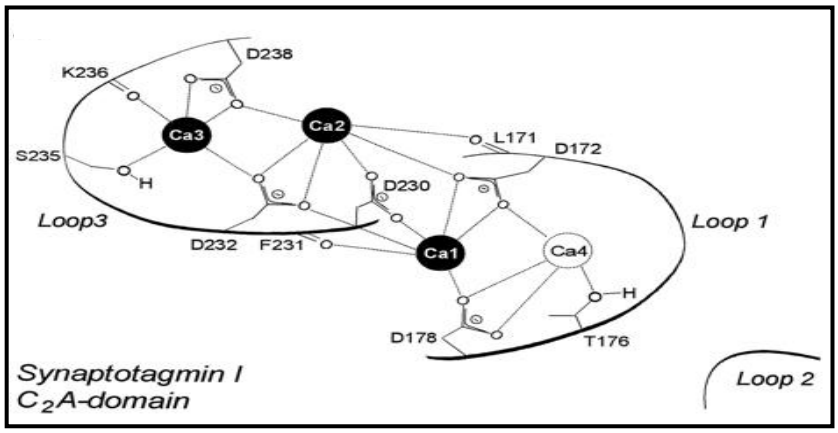

Figure 1.9: Calcium binding in C_2 domain (Rizo and Sudhof, 1998).

Annexins are diverse family of Calcium binding protein that binds to phospholipids present in the membrane in a Calcium dependent manner. These proteins serve in many

cellular processes including endo- and exocyotsis, anchorage of other proteins to the membrane, formation of Ca^{2+} channel, and inhibition of phospholipases. The protein consists of a divergent N-terminal head domain and a conserved C-terminal core. The core consists of four repeating segments with 5 α- helices. This helices forms tightly packed disc with slight curvature and two distinct sites. The convex side consists of loops that join the helices which forms Calcium binding site and faces the phospholipid bilayer when associated with the membrane. The N-terminal domain present in the concave side, points away from the membrane and is available for interaction with the cytoplasmic binding partners. Upto 12 Calcium binding sites may be present in the annexin convex side. Mutation, alteration in its structure or expression level in the cell might result in several pathological conditions including cardiovascular disease, physiological stress, heart disease, diabetes and cancer (Gerke and Moss, 2001).

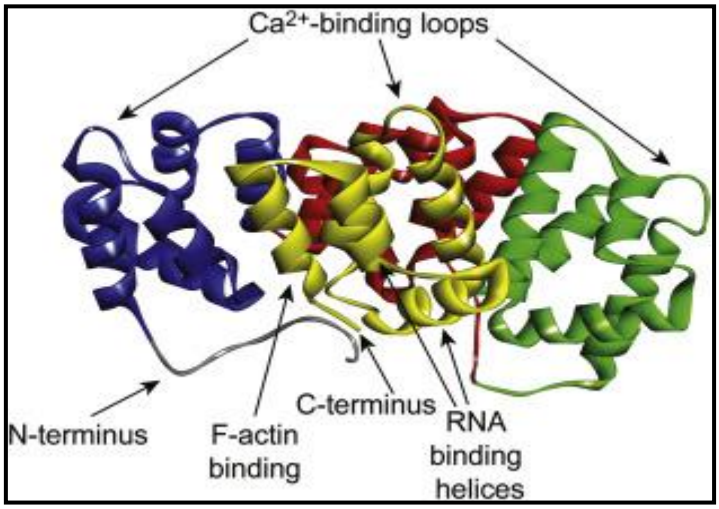

Figure 1.10: Crystal structure bovine AnxA2 Annexin A5 forming a curve disc. Source: ("Protein phosphorylation and its role in the regulation of Annexin A2 function," 2017)

2.2 Secretagogin

Secretagogin belonging to EF-hand family proteins binds four calciums with one site having very high affinity for calcium. Out of the four sites, the site with highest affinity for calcium acts as the sensor site whereas those with low affinity act as buffer site, which explains the dual nature of protein. Human secretagogin has three cysteine residues at the position 193, 253 and 269 however mouse secretagogin has four cysteine residues at position 16, 131, 253 and 269. Thus the protein is able to form disulphide bonds. The last two amino acids are able to form intrachain disulphide bond and the Cys 193 residue of human and Cys 131 and Cys 16 residues of mouse SCGN is involved in forming interchain disulphide bond. Thus this protein exists as the mixture of both monomer and cysteine dependent dimer or higher oligomer. The oligomerization is age and concentration dependent i.e. the protein tends to form oligomers at high concentration (3mg/ml) and after longer incubation even when the protein is freezed (Sharma *et al*., 2014). The protein as well as the gene is redox sensitive. The protein

shows higher affinity (of one site) towards the ligand in reduced condition such as cytosol and acts as sensor whereas in oxidizing condition such as in Endoplasmic reticulum, the protein shows lower affinity towards ligand acting as a buffer (Khandelwal *et al*., 2016).

As the protein possesses two set of binding sites, the binding with the first set of site is exothermic and the binding with other set of site is endothermic. At the physiological salt concentration the affinities of the four calcium binding sites are log k_1= 7.1±0.4, log k_2= 4.7±0.6, logk_3= 3.6±0.7 and log k_4= 4.6±0.6. The protein shows cooperative binding of calcium to lower affinity sites. The EF hand 1 and 2 do not bind calcium because the residues sequence in the loop does not match the EF-hand concensus sequence. The EF-hand 1 motif (DADEKGYIEEKE) has lysine residue at 5^{th} position where generally aspartic acid or arginine is present and the EF-hand 2 (DASKDGRIRMKE) has arginine where normally a negatively charged or hydrophilic residue forms hydrogen bond with Calcium cordinationg water molecule (Rogstam *et al*., 2007).

Secretagogin enhances glucose dependent insulin secretion (GSIS) in pancreatic β-cells as the amount of insulin released is directly proportional to the amount of Secretagogin present in the cell. There are two phases in GSIS, (i) rapid and transient pathway in which the previously formed pre-docked insulin granules are released (ii) gradually developed and sustained pathway in which newly recruited insulin granules are released. It has been found that Secretagogin affects second phase of GSIS and it does so by binding to actin and remodeling cytoskeleton. The change in actin dynamics helps in the recruitment and release of insulin granules. SCGN also facilitates focal adhesion and activates focal adhesion signaling by regulating actin cytoskeleton which is necessary for second phase of GSIS (Yang et al., 2016).

2.3 Site Directed Mutagenesis (SDM)

Site directed mutagenesis (SDM) is an indispensable technique for mutational studies at gene level or at protein level. SDM is an in vitro procedure that utilized custom designed oligonucleotide primers to introduce mutation at specific site in a double-stranded DNA plasmid. SDM helps to study the function of the whole gene or protein, or the specific region of the protein along with the study of protein structure/function relationship. Many protocols for SDM have been developed all of which involves the annealing of oligonucleotide primer containing the desired mutation/s with the target sequence. Deletion, Insertion or Substitution can be done using this technique in the whole plasmid or the gene or PCR product depending upon the requirement and type of technique followed. In order to simplify the process of transformation, SDM can be carried out in the plasmid containing the confirmed gene by PCR based method. This method helps to overcome the problem of digestion, ligation and self-annealing. There are three general techniques to induce SDM in whole plasmid.

a) Inverted PCR: In this method, the entire circular plasmid is amplified using two back to back primer out of which one contains the desired mutation (fig. 1.11). The PCR product needs to be treated with klenow fragment and must be phosphorylated. The efficiency of this method is 82% (Hemsley *et al*., 1989).

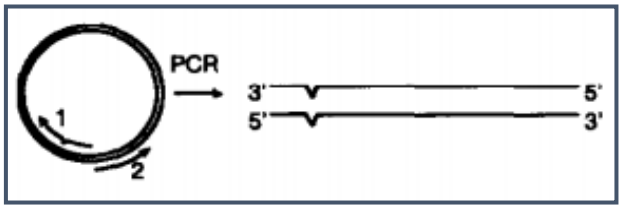

Figure 1.11: Inverted PCR to induce site directed mutation at desired site in the plasmid

b) Recombinant circle PCR: In this method, two PCR needs to be carried out in such a way that the primers directing mutation is kept in separate PCR reactions. The product of these PCR is then purified, combined, denatured and reannealed to recombine (fig:1.12). The product can be directly transfected into *E.coli*. The gaps in the plasmids can be repaired *in vivo*. The efficiency of this method is 82% to 100% (Jones *et al*., 1992).

c) Recombination PCR: This method requires two overlapping primers and a single PCR reaction. The single step PCR reaction gives double stranded nicked plasmid product which can be directly used for transfection (fig: 1.13). Since the DNA product consists of homologous segment, recombination can occur in vivo (Jones and Winistorfer, 1991).

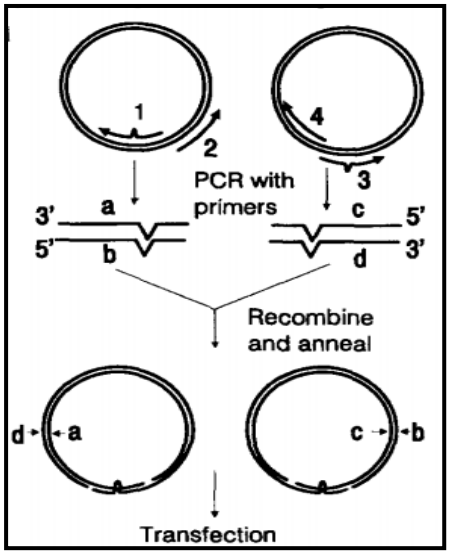

Figure 1.12: Recombinant Circle PCR to induce site directed mutation at desired site in the plasmid

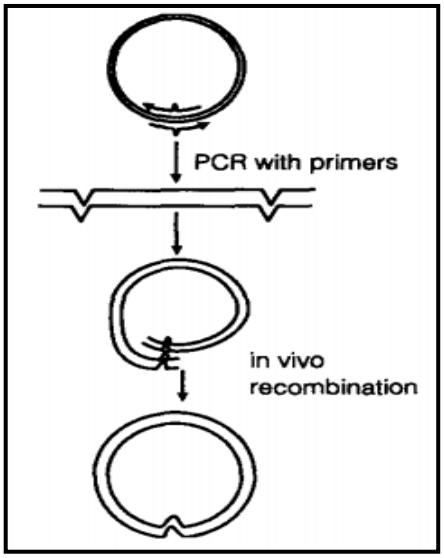

Figure 1.13: Recombination PCR to induce site directed mutation at desired site in the plasmid

2.4 Characterization of protein

Proteins are versatile biomolecules of living system. Many proteins are being identified and their structure is being studied. Many proteins are known to play important role as drugs and pharmaceuticals, thus are being produced with recombinant method. Many

proteins are found to be involved in pathologies. Thus the study of protein is the current need of time. Proteins have complex three dimensional structures and the structure of protein determines its function. Thus the study of protein structure is indispensable to understand its functions and properties. Structural and functional characterization of protein contributes to understanding the biological processes at molecular level. Many techniques have been developed in this regard to reveal the structure of protein including Nuclear magnetic resonance (NMR), X-ray crystallography, mass spectrometry and electrospray ionization. Each of these techniques has its own pros and cons. X-ray crystallography gives the static picture of protein structure as the crystal structure may not relate to the structure of protein in solution form. NMR spectroscopy though have high resolution, is limited for small protein. Mass spectrometry doesn't give direct information about the structure and needs highly pure compound. To overcome the drawbacks of these techniques, low resolution techniques can be used that provide some information about the structure of the molecule like tryptophan fluorescence, circular dichroism, Fourier Transform Infrared (Tiber *et al*., 2011). The choice of technique to be chosen entirely depends upon the type and intensity of information required.

2.5 Circular Dichroism (CD)

Circular dichroism is the difference in the absorption of left handed and right handed circularly polarized light that occurs in asymmetric molecules. CD can be used to study the secondary and tertiary structure of biomolecules, to compare the structure of mutants of same protein, to determine the conformational stability of proteins under different conditions or to study protein-ligand or protein-protein interaction. When a plane polarized light is passed through suitable plate or filter, it splits out into two circularly polarized lights rotating in opposite direction having equal amplitude but differing in phase by 90°. When these circularly polarized light passes through chiral molecules, the left and right circularly polarized light is absorbed at different extent. This results in rotation of plane of light wave such that the addition of two vectors results a vector that trace out an ellipse. Thus the resulting light wave is called as elliptically polarized. Ellipticity is defined as the angle whose tangent is the ratio of minor to the major axis of the ellipse (Greenfield, 2009)

$CD = A_L - A_R$

The polarimeter also follows Beer Lambert's law:

$A = AL - AR = \varepsilon L \times l \times C - \varepsilon R \times l \times C = \Delta\varepsilon \times l \times C$

Where L and R denotes left and right, ε denotes extinction coefficient, l denotes path length and C denotes concentration.

For proteins, the result is expressed as mean residual ellipticity (MRE).

$$[\theta] = \frac{\theta \times 100 \times M}{C \times l \times n}$$

Where θ is the ellipticity in degrees, *l* is the optical path length, *C* is the concentration in mg/ml, *M* is the molecular mass and *n* is the number of residues in the protein.

The secondary structure of the protein is determined in the wavelength range from 180-250nm i.e. in far UV region. The peptide bond act as chromophore at this wavelength and proper signal is only received when it is present in regular and folded environment. Each secondary structure has its unique signal. CD gives the average signal of the entire molecular population. α- helix gives two negative bands at 208nm and 222nm and a positive band at 190nm. β-sheet shows negative band at 218 and positive band at 196nm. Random coil gives positive band at 212nm and negative at 195nm (fig.1.14).

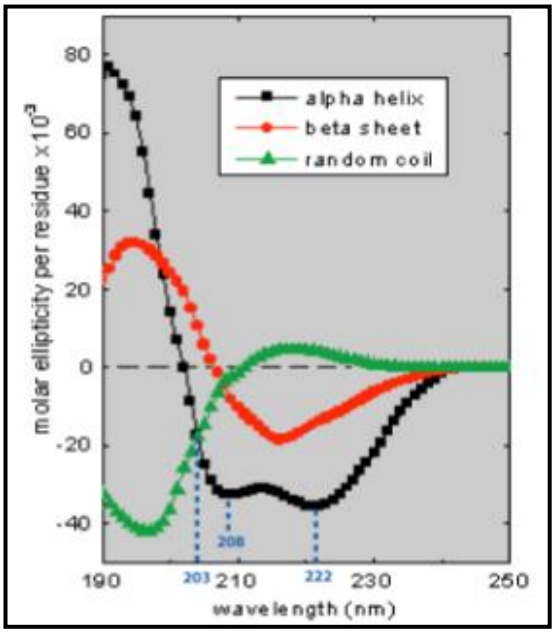

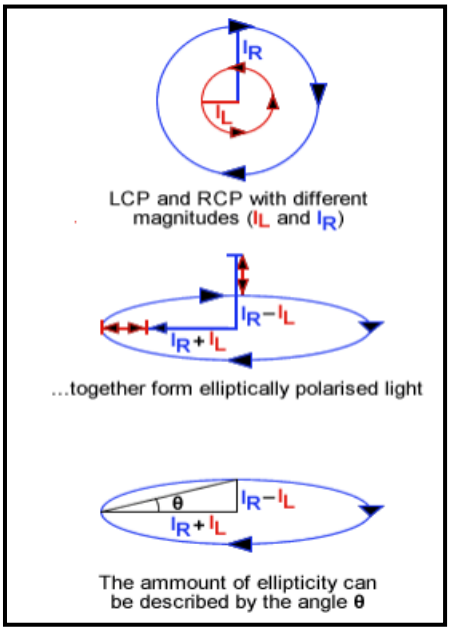

Figure 1.14: CD spectra for different secondary strucures **Figure 1.15**: Ellipticity

Tertiary fingerprint of a protein can be obtained in the far UV region i.e. 250-300nm where aromatic amino acids and disulphides have major contribution in CD signal. Signals in the region from 250-270nm is attributed to phenylalanine residues, 270-290 are attributed to tyrosine residues and from 280-305 are attributed to tryptophan residues. Disulphide bond give CD signal at around 260nm and has wider peak than aromatic residues (Correa and Ramos, 2009).

2.6 Fluorescence spectroscopy

Fluorescence spectroscopy can be used to study the structure of proteins and peptides. Unlike other biomolecules, proteins display intrinsic fluorescence which has been widely exploited in biophysical studies. The aromatic amino acids, tryptophan, tyrosine and phenylalanine act as intrinsic fluorescent probe to study the conformation, dynamics and intermolecular interaction of protein. The fluorophore absorb light of specific wavelength and emit light of specific and shorter wavelength which is called fluorescence. Phenylalanine has the lowest quantum yield and low absorptivity so its contribution in the intrinsic fluorescence of protein is very low. Tyrosine and tryptophan

has high quantum yield but tryptophan is considered as the major one as it is most dominant is protein and the indole group of tryptophan is very effective in UV absorption at 280nm and emission at 350nm in proteins. Moreover tryptophan fluorescence is highly sensitive upon the external environmental condition at the emission from 308nm to 355nm. Tyr emission is usually quenched in native protein by its interaction with the native peptide chain or via energy transfer to tryptophan. This high dependency of tryptophan on external surrounding is widely elucidated to study protein conformation changes, ligand binding and unfolding studies (Ghisaidoobe and Chung, 2014).

Table 3: Fluorescence property of aromatic amino acids in water at neutral p^{H}

	Lifetime (τ) (ns)	Absorption		Fluorescence	
		λ (nm)	Absorptivity (ϵ)	λ (nm)	Quantum Yield (Φ_F)
Tryptophan	3.1 (mean)	280	5600	348	0.2
Tyrosine	3.6	274	1400	303	0.14
Phenyl alanine	6.4	257	200	282	0.04

Phenylalanine consists of two symmetry-forbidden transitions L_a and L_b at 207nm and 255nm respectively and the first allowed π-π^* transition $B_{a,b}$ at 185nm. Greater perturbation of benzene electronic configuration occurs in tyrosine resulting in lowering of symmetry and introducing some allowed character in symmetry forbidden transition. L_a and L_b peaks are located at 222nm and 273nm respectively and shows larger red shift and intensity than that of Phenylalanine. There is further more structural perturbation in tryptophan with a strong $B_{a,b}$ at 218nm and overlapping L_a and L_b band at 277nm and 288nm respectively (Uversky, 2007). Trp fluorescence occurs from ^1L_a state except when the environment is non polar. In the polar environment, emission occurs due to ^1L_a state resulting in red shift. In hydrophobic environment, ^1L_b state has lower energy than ^1L_a state but dominate the emission of tryptophan resulting in blue shift. So during unfolding studies, as the protein gets unfolded, the tryptophan is exposed to hydrophilic environment resulting in red shift (Ghisaidoobe and Chung, 2014).

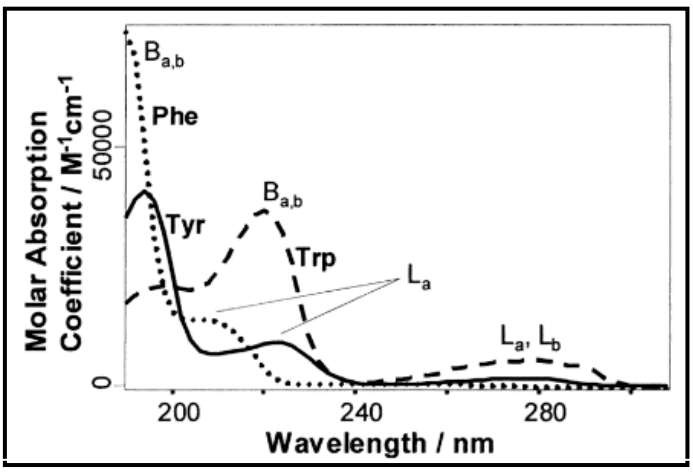

Figure 1.16: Transition state of aromatic amino acid during excitation

2.7 Isothermal titration calorimetry (ITC)

ITC is a very advanced and recent technique that is used to measure the energetic of a reaction. This is the only technique which helps to determine multiple thermodynamic parameters like enthalpy, entropy, free energy, binding constant and the stoichiometry of binding from the single experiment and also helps to elucidate the mechanism of binding. ITC is commonly used in biophysics to study the binding of ligand and macromolecule. ITC is often used in pharmaceutical research to identify the lead compounds for therapeutic invention and to optimize the affinity and selectivity of a drug candidate molecule. The ligand is continuously titrated in defined volume into the macromolecule till the macromolecule is fully saturated with the ligand. If binding occurs, heat is either absorbed or released depending upon whether the reaction mechanism is endothermic or exothermic. The amount of heat absorbed or evolved is directly proportional to the concentration of bound ligand. The reference cell is kept at constant temperature. After each injection, when the temperature of the system changes, the system is brought back to the defined temperature within certain seconds before the next injection is given. During initial injections, most of the ligand added is readily bound up by the macromolecule giving large endothermic or exothermic signal but later the concentration of free ligand is limited which causes lower heat change and less signal .

The result of ITC is obtained in the form of a graph called isotherm which is obtained from the enthalpy of the reaction. The data is fitted in order to minimize the Chi square value and error and the best fit is selected. Initial concentration of the macromolecule (protein) and ligand is the critical factor in an ITC experiment which is determined from the unitless constant called the c value. The shape of the isotherm depends upon the c value (Freire *et al*., 1990).

$c= n[M]/k_d$

where ‘n’ is the no of binding sites per protein molecule, [M] is the concentration of protein and k_d is the dissociation constant. The isotherm gives the value of heat of the reaction which can directly be used to calculate the enthalpy change along with the dissociation constant of the reaction. Hence the formula, $\Delta G= RTl_nk= \Delta H - T\Delta S$ can be used to calculate entropy change of the reaction.

The c value should be between 20 to 100 in order to obtain sigmoidal shape of isotherm in order to get good fit to estimate k_d, ΔH, ΔS and n. If the c value is very high, one can estimate ΔH and n but other parameters such as k_d cannot be determined since the transition would be very sharp and few points would be collected near equivalence i.e. protein may get saturated in single injection of ligand. If the c value is less (<5), very broad transition might be obtained and the equivalence point cannot be determined. The ligand concentration is taken n*30 times the concentration of protein concentration (Dutta, Rösgen, & Rajarathnam, 2015).

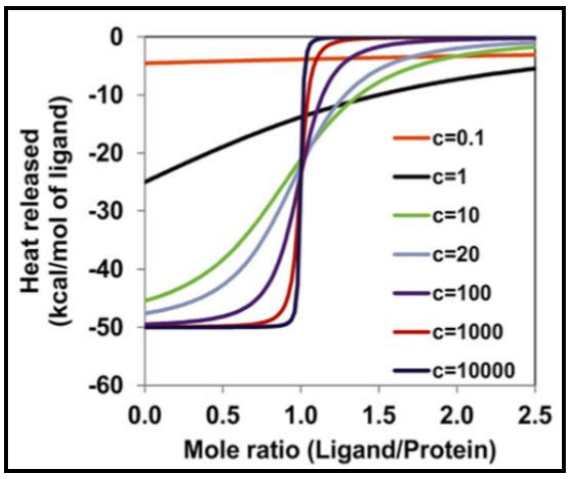

Figure 1.17: Isotherm for 1:1 binding system showing the affect of c value on the shape of isotherm

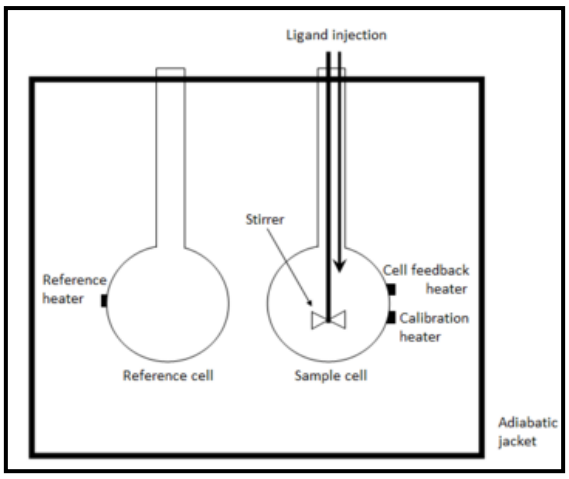

Figure 1.18: Schematic diagram of a isothermal calorimeter

2.8 Analytical gel filtration chromatography

Gel filtration chromatography often referred to as size exclusion chromatography is the method in which biomolecules are separated on the basis of their shape and molecular size forming a molecular sieve. The method employs a gel media suspended in aqueous medium which is packed into a chromatographic column. The gel media consists of porous particles which forms defined pore size through which biomolecules can diffuse to different extent depending upon their molecular sizes. Small molecules can easily enter through the pores of the gel particles and thus their movements is retarded and elute out later whereas larger molecules cannot pass through the pores and thus move along with the mobile aqueous phase in the void volume and are eluted early. Thus molecules are eluted out in the order descending molecular size. This chromatrography is either used for preparative purposes to purify protein, nucleic acids or other biomolecules or for analytical purposes for characterization of proteins. The type of column (gel) to be used depends on the purpose. For preparative purposes, the column with lower resolution like Sephadex can work fine but for analytical purposes, column with higher resolution like superdex must be used. The resolution depends upon pore size, column length as well as the rate of flow of the aqueous phase. Sepharose is the crosslinked dextran whereas Superdex is the highly porous cross linked agarose beads to which dextran is covalently bonded and thus provides greater resolution. Thus superdex is a composite gel in which the agarose matrix attributes high physical and chemical stability of the gel and the dextran chain determines the gel filtration properties (“Gel filtration Principles and Methods,” n.d.).

The result of chromatography is obtained in the form of a chromatogram which is analyzed for determining and comparing the molecular weight, oligomeric state, concentration of proteins. Proteins show high degree of heterogeneity in their oligomeric state. Along with monomer, dimer, higher oligomers as well as protein

aggregates of the same protein might also be present in the solution. In order to determine the concentration of these oligomeric state and to separate these oligomeric population from one another in order to obtain homogenous protein population for final purification, analytical gel filtration is carried out. The area under the peak gives the concentration of the protein fraction. The molecular weight and size of uncharacterized protein can also be determined at different conditions like pH, ionic strength, temperature, etc from this method by comparison with the marker of known molecular size (Agilent Technologies, 2015).

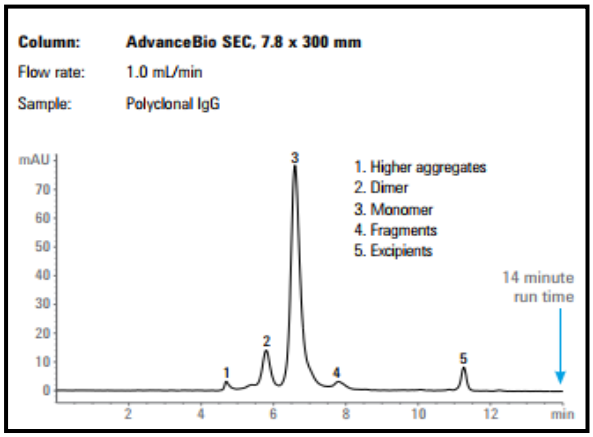

Figure 1.19: Elution of different oligomers of same protein at different time shown by different peaks in the chromatogram

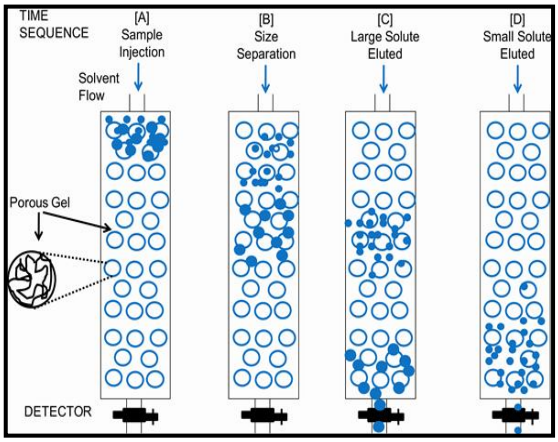

Figure 1.20: Elution pattern of small and large molecules. Larger molecules eluted earlier than the small molecules

2.9 Limited proteolysis: Partial trypsin digestion

Protein function not only depend upon the three dimensional structure of protein but also upon structural mobility. High resolution techniques may give idea about the position of the individual atoms but does not give much information about flexible and disordered regions in the protein and are not applicable for large scale processing. The flexibility of protein might be directly related with the protein function, ligand binding, and stability or might allosterically regulate these processes. Thus limited proteolysis can successfully probe such conformational features of protein. It is restricted only to those loops that show conformational flexibility whereas the protein core, remain rigid and are resistant to proteolysis. Studies have shown that proteolysis usually occurs at the region rather than specific site of protein. Digestion never occurs at the region of α-helices though target residues may be present but always occurs at the loop (Fontana *et al*., 2004). Limited proteolysis can also pinpoint the site of local unfolding of protein chain and are often used to isolate protein fragments that can fold autonomously, have some properties of the original protein and thus help in identification of functional domain (Aghajanian *et al*., 2003).

Single or multiple mutations may alter these loops and flexible region affecting the overall stability and function of protein. The eukaryotic system works in such a way that only stably folded protein reaches to maturity. Those proteins that are misfolded

undergo degradation by proteases or undergo aggregation. Some mutation can cause exposure of loops and flexible regions of protein to its surface while others can cause burial of these loops into the protein core. The pattern and intensity of digested bands thus gives idea about how the conformation of the protein might be altered due to mutation. Many enzymes like trypsin, thrombin, subtilisyn, chymotrypsin have been utilized in this context among which trypsin is the one most commonly used. Trypsin is a serine protease whose substrate specificity is based on positive charge of side chain of lysine and arginine residues. It cleaves protein at the carboxyl end of amino acids lysine and arginine except when either is bound to a C-terminal proline. Partial trypsin digestion followed by mass spectrometry is often carried out for characterization of protein which gives information about the complete amino acid sequence in the protein fragment (Aghajanian *et al*., 2003).

2.10 Glutaraldehyde crosslinking

Crosslinking is the process of chemically joining two or more molecules with covalent bond. Crosslinking is induced using cross linking reagents that contain two or more reactive ends that can attach themselves to certain functional groups (amines, carboxyl, sulfhydrls) in the protein. Most of the protein functions by forming protein assemblies. Therefore defining and mapping of the protein complex is essential for understanding the biological function. Because protein-protein interaction is transient event, crosslinking is an essential tool for capturing them and stabilizing for analysis. ("Crosslinking Applications," n.d.) It can also be utilized in studying the oligomerization state of a single protein. If two proteins interact with each other, they can be covalently crosslinked. This provides a strong evidence of close proximity between the two proteins. Not only the identity of the interacting proteins, but also the point of contact between them can be determined through this method (Kapoor, n.d.).

Glutaraldehyde is a strong carbonyl (-CHO) reagent that condenses amines via reductive amination. It is a 5 carbon containing dialdehyde with straw colour and pungent oily appearance and is soluble in water and alcohol at all proportions. It reacts rapidly with the amines at around neutral p^H and is more efficient than other aldehydes in forming stable crosslinks. However the results can be uninformative and ambiguous as the reagent is non-specific and can react with all the nitrogen of the protein mainly with lysines, tyrosines, arginines and histidines. Therefore intra- and inter-molecular links could be formed between neighbouring but not interacting molecules yielding artificial protein oligomers that have no biological significance. Therefore, it is necessary to optimize all the parameters including time, p^H, and concentration of glutaraldehyde as well as protein (Fadouloglou, Kokkinidis, & Glykos, 2008).

CHAPTER 3

MATERIALS AND METHODS

All the works carried out in the project was performed in CSIR-CCMB at Dr.Yogendra Sharma's lab. Total RNA extracted from human pancreas was provided by Mr.Sumit Paliwal.

3.1 Cloning of human secretagogin (hscgn)

3.1.1 Reverse transcription PCR using total RNA

Total pancreatic RNA of human was provided in the lab. The first reaction mix was prepared in the PCR tube by mixing 5µM of random hexamer, 1mM of dNTPs mixture and 1µg of pancreatic RNA in 10µl of nuclease free water. The mixture was incubated at 65°C for 5 minutes and cooled immediately on ice. This product was then used to prepare second reaction mix by adding Prime script buffe(1X), RNAse inhibitor (20units), Primescript RTase (200units) and RNAse free water in 20µl volume (Takara). This reaction mix was then incubated using the following conditions, 30°C for 10 minutes, 42°C for 60 minutes and then at 95°C for 5 minutes which was then cooled on ice. Rnase H was the added to the product, mixed well and incubated at 37°C for half an hour. The mixture was finally diluted to 40µl with autoclaved MilliQ water.

3.1.2 Second strand synthesis of Human Secretagogin using gene specific primers

The single strand prepared after reverse transcription was used as template. The PCR reaction mix was prepared by mixing Emerald 2X master mix (Takara), template DNA, primers and milliQ. The sequence of the primers used is forward: 5'-ATTCATATGGACAGCTCCCGGGAACC-3' and Reverse: 5'-TATCTCGAGTTATGGGTTGATTTTCAGCCCAAG-3'.

Then gradient PCR was carried out using the following conditions, 95°C for 5 mins, 95°C for 30secs, annealing was then carried out at 3 temperatures 56°C, 58°C and 60°C for 30 secs then extension was carried out at 72°C for 1 min. The cycle was then repeated for 35 times and final extension was carried out at 72°C for 10 minutes. The PCR product was then loaded in 1.2% agarose gel and gel elution was carried out to recover the amplicon using Gel extraction and PCR Cleanup kit (MN).

Second PCR was carried out taking the annealing temperature 60°C since maximum amplification was obtained at this temperature in gradient PCR. After PCR, the product was run on 1.2% agarose gel and gel extraction of DNA was carried out.

3.1.3 Restriction digestion of the insert and vector with *Nde*I and *Xho*I enzyme

Digestion mix was prepared by adding 2µg of pET-21b, 10units of *NdeI* (10,000 units/ml, NEB), 10 units of *Xho*I (10,000 units/ml, NEB), 1X cutsmart buffer (stock 5X) was taken in an eppendroff tube and the volume was adjusted to 50µl with autoclaved milliQ. The digestion mix was incubated at 37°C overnight. One hour before the incubation was over, Shrimp alkaline phosphatase (SIP) was added (10units) to it and incubation was continued for one more hour for 37°C.The digestion product was then loaded in agarose gel and electrophoresed. The gel was then observed in UV transilluminator and DNA band was cut. Then DNA was extracted from the gel using Gel extraction and PCR Cleanup kit (MN). The concentration of DNA obtained was then quantified using nanodrop (Thermo fischer).

Digestion mix was prepared by adding 1 µg of insert, 10 units of *NdeI* (10,000 units/ml, NEB), 10 units of *Xho*I (10,000 units/ml, NEB), 1X cutsmart buffer (5X) in an eppendroff and the volume was adjusted to 50 µl with autoclaved milliQ. The digestion mix was incubated at 37°C overnight. The digestion product was then loaded in agarose gel and electrophoresed. The gel was then observed in UV transilluminator and DNA band was cut. Then DNA was extracted from the gel using Gel extraction and PCR Cleanup kit (MN). The concentration of DNA obtained was then quantified using nanodrop (Thermofischer).

Ligation of the digested vector and insert: 40ng of digested pET-21b, 18ng of digested insert (as calculated from ligation calculator with vector: insert ration taken 1:4), 10 units T4 DNA ligase (10,000 units/ml,Takara) and 1X ligase buffer (10X, Takara) was added to prepare ligation mix. The mix was then incubated at 16°C overnight. Ligation control mix was also prepared by adding all the components except the insert to check the efficiency of digestion and ligation.

3.1.4 Transformation of the construct into *E.coli* DH5α by heat shock method

Two vials of competent *E.coli* DH5α cells was taken out from -80°C and kept in ice for thawing. The ligated product as well as ligation control was added into competent *E.coli* DH5α cells vial and incubated in ice for 20 minutes. Heat shock was given to the cells by placing them at 42°C for exactly 90 seconds. The vial was immediately kept in ice and incubated for 10 minutes. Then 900µl of LB media was added to it and incubated at 37°C for about an hour. After that the cells were pelleted down by centrifugation at 4,000 rpm for 5 minutes. Supernatant was discarded. The cell pellet was redissolved in 200µl of LB broth. After transformation, *E.coli* transfected with both the test and control DNA was plated on LB agar plate with 100µg/ml ampicillin. The plates were incubated at 37°C for 15 hrs and then observed for colonies. The number of colonies formed in the control and test plate was compared.

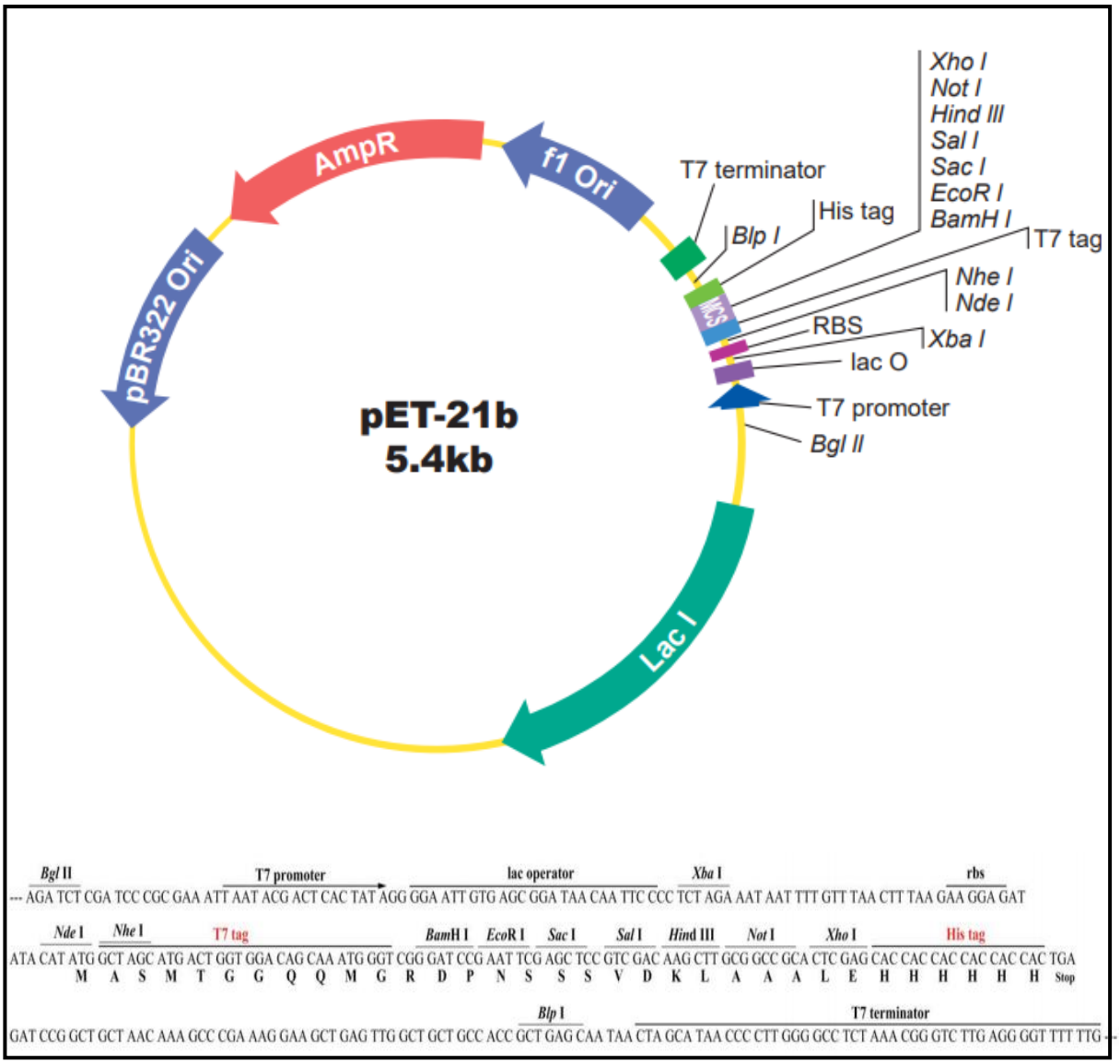

Figure 1.21: Vector map of pET-21b- Novagen (Source: https://www.genscript.com/gsfiles/vector-map/bacteria/pET-21b.pdf)

3.1.5 Colony PCR

PCR reaction mix was prepared by adding Emerald 2X Mastermix, gene specific forward and reverse primer and autoclaved MQ. 10µl of reaction mix was aliquoted in each well of multi-welled PCR plate. 20 colonies were randomly selected from the test plate, patched in new LB with ampicillin agar plate and added into the PCR plate wells. Then the plate was placed in thermocycler set to following conditions, 95°C for 10 minutes, 95°C for 30 seconds, 58°C for 30 secs, 72°C for 1 minute which is repeated for 25 cycles. Then final extension was kept for 72°C for 10 minutes. The product was then loaded on 1.2% agarose gel and the gel was visualized on UV transilluminator.

The colonies which give band at correct size (positive band) in colony PCR were selected and kept for primary culture in LB broth with 100µg/ml Ampicillin and incubated at 37°C for 15 hours. Plasmid was then isolated from the cultures using Nucleospin plasmid purification kit (MN) and quantified in nano drop.

3.1.6 Site directed mutagenesis and Cloning of Mutants

SDM primers were used to induce single point mutation. The mutants of h*scgn* were prepared using the following set of primers.

R77H

CGC to **CAC**

Forward: 5' -TAAAGATGGTCACATTCGGATGAAAG -3', 26 Bases, 38.5% GC content, 55.2°C Tm

Reverse: 5'- CTTTCATCCGAATGTGACCATCTTTA- 3', 26 Bases, 38.5% GC content, 55.2°C Tm

A216V

GCC to **GTC**

Forward: 5'-TAAAACAGGAGTCCTGGAAGGC-3', 22 bases, 50% GC Content, 56.8°C Tm

Reverse: 5'-GCCTTCCAGGACTCCTGTTTTA-3', 22 bases, 50% GC content, 56.8°C Tm

V108M

GTG to **ATG**

Forward: 5'- ACAGCAGC**ATG**GAGTTTATGCA- 3', 22 bases, 45.5 % GC Content, 57.3°C Tm

Reverse: 5' - TGCATAAACTC**CAT**GCTGCTGT - 3', 22 bases, 45.5 % GC Content, 56.6°C Tm

The first PCR reaction mix was made taking the WT gene in pET-21b vector as template (50ng) , forward and reverse SDM primers (5pM each) , 1X Q5 mastermix (stock-5X, New Englands Biolab) and the volume was maintained to 20µl using autoclaved milliQ. PCR was carried out using the following conditions, initial denaturation was carried out at 95°C for 3 minutes, denaturation at 95°C for 30 sec, annealing at 55°C for 30 seconds and extension for 5minutes. The cycle was repeated for 20 times and final extension was carried out at 72°C for 10 minutes. The 8µl of the amplicon was then added with DpN1 enzyme (5 units) along with 1X DpN1 buffer. The reaction mix was then incubated at 37°C for 3 hours. After DpN1 digestion, the product was used for transformation of competent *E.coli* DH5α cells. After transformation, the cells were plated in LB media with 100µM Ampicillin and incubated at 37°C for 15 hours. The colonies formed were patched in a new plate and sent for sequencing. The sequencing result obtained was opened using finch TV and protein sequence was analysed using expasy translate tool.

3.2 Protein overexpression analysis

The confirmed WT and mutant plasmid was transformed into competent *E.coli* BL21. Transformation was carried out in the manner similar to that of *E.coli* DH5α. Then two colonies from WT hSCGN in BL21 plate were selected and patched. They were cultured in 10ml LB broth with 100µg/ml Ampicillin for different time after induction, at different temperature and IPTG concentrations. Three time points, temperature (18°C, 25°C,

37°C) and IPTG concentrations were used. The culture was induced with IPTG after the O.D. had reached 0.6. And after desired time period, 1 ml and 2 ml aliquot of culture was taken out from each culture tube. The cells were pelleted down.

1ml pellet of every different condition was resuspended in 30µl of milliQ water and then mixed with 10µl of 4X loading dye. Samples were boiled for 5min minutes and then spinned at 14,000rpm for 20 minutes. Then 20µl of each sample was loaded on 12% SDS PAGE. Electrophoresis was then carried out at constant voltage of 200V and current was kept maximum i.e.400mA. After the dye was eluted out, the gel was removed and stained in freshly prepared staining solution for 30 minutes. Then the gel was destained and then visualized to analyze the conditions at which maximum overexpression of protein had occurred.

We wanted the protein in soluble fraction. So it was necessary to determine the condition at which protein was over expressed in soluble fraction rather than in inclusion bodies. For this purpose, the pellet from 2ml culture was taken and resuspended in 100µl of milliQ. It was then sonicated for 2 minutes (at 21% amplitude, 6 seconds on and 4 seconds off cycle with probe temperature set to 4°C) until the suspension becomes translucent. It was then spinned at 14,000 rpm for 30 minutes and the supernatant was immediately aspirated in another eppendroff tube, mixed with loading dye and boiled for 5 minutes. 20µl of it was loaded in the gel. The pellet was resuspended in 30µl of milliQ and mixed with loading dye. It was boiled and centrifuged at 14,000rpm for 1 minute. 15µl of it was loaded in the gel. Electrophoresis was carried out and the gel was analyzed to select the condition with maximum over expression in soluble fraction.

3.3 Purification of hSCGN

10ml Primary culture of BL21 hSCGN was made. 1ml of it was inoculated in 100ml LB media (1% primary culture) in 250ml conical flask. The flask was then incubated at 37°C for 3 or 4 hours. When the O.D. had reached 0.6, the culture was then induced with 800µl of 1M IPTG and then incubated at 25°C for 10 hours. The cells were then pelleted down in a 50ml falcon tube in chilling centrifuge at 4°C.

3.3.1 Anion exchange chromatography

The pellet was resuspended in 20ml of lysis buffer (50mM Tris, p^H 7.5). A pinch of Deoxycholic acid, phenylmethylsulfonyl chloride (PMSF) dissolved in isopropanol and 1µl DNase was added to it. The cell suspension was then sonicated at 21% amplitude with 6sec on and 5sec off cycles till the lysate became clear. The lysate was then transferred to special Beckman tube (Orchis tube). The Beckman coulter with JA25.50 rotar was kept was pre chilling. The tube was then placed in the Beckman coulter with suitable balance and then centrifuged at 18,000 rpm for 40 minutes at 4°C. After the centrifugation was over, the supernatant was immediately transferred to a new flask and kept in ice.

The Q sepharose column was regenerated was before use by washing it with 100ml of MilliQ then with 50ml of 0.5N NaOH and finally with 300 to 400ml of MilliQ (till the p^H of the flow-through reached 7.5). The column was then equilibrated with 100ml of lysis buffer. The supernantant was loaded into the column and flow-through was collected. The flow-through was passed twice through the column. The column was then washed with Wash buffer 1 (50mM Tris, p^H 7.5) then with Wash buffer 2 (50mM Tris, p^H 7.5 and 2% Triton X) and finally with wash buffer 3(50mM Tris, p^H 7.5). The tubes were arranged in fraction collector. Then elution of protein was carried out using NaCl gradient from 0M to 1M in Tris buffer with the help of gradient mixture. The eluate was collected in collection tubes with 3ml eluate in each tube. The fractions were the loaded in SDS gel and electrophoresed. The protein band was observed after staining and destaining of gel.

3.3.2 Hydrophobic interaction chromatography (HIC)

For optimization of purification, HIC was performed. Bacterial pellet form 100ml of bacterial culture was prepared as above. The pellet was resuspended in lysis buffer (50mM Tris, 100mM KCl, 1mM $CaCl_2$, 1mM $MgCl_2$). Deoxycholic acid, PMSF and DNase was added to it after which the cell suspension was sonicated. The cell lysate was then pelleted down in Beckman coulter and the supernatant was separated. 20µl of the supernatant was separated in an eppedroff tube. The Phenyl Sepharose column was regenerated as above and equilibrated with HIC lysis buffer.

The supernatant was then loaded in the column. The flow-through was collected, passed twice in the column and the column was washed with 300ml of the same lysis buffer. The wash buffer was also collected. Then elution was performed with elution buffer containing 50mM Tris and 0.5mM EDTA and the fractions were collected in the tubes. The sonicated pellet, supernatant, flow-through as well as the collected fractions were loaded in SDS gel. After electrophoresis, the gel was stained, destained and the proteins fractions were selected and pooled out for further purification by gel filtration chromatography. The fractions were selected on the basis of purity and pooled together for mutiple injections into Gel filtration (GF) column in order to further remove impurities.

The purification was optimized in order to obtain protein of highest purity for which hydrophobic interaction chromatography followed by anion exchange chromatography was followed. For large scale protein purification, 4l to 5l cultures was kept and pelleted down and then processed as above.

3.3.3 Gel filtration (GF)/Size exclusion chromatography

The fractions pooled out together was concentrated to 5ml in centricon(10KD cut off) in a chilling centrifuge. The sephadex 75 column was pre-equilibrated with running buffer (50mM Tris, 100mM KCl). The collection tubes were arranged in tube rack in fraction collection system. The concentrated protein was then taken in a syringe fitted with GF

needle. The protein was then injected in injection port in the gel filtration chromatography system. The program was made to inject the protein into the column and then collect the fraction after 40 ml of the void volume had passed. After the collection of fraction was completed, the fractions were selected on the basis of chromatogram obtained in program (fractions in which protein had eluted out is shown by the peaks in chromatogram). The selected fractions were then loaded in the SDS gel for checking the purity.

3.3.4 Decalcification and buffer exchange

The pure protein fractions (90% pure accepted) were selected from the gel and pooled together. Protein concentration was measured by urea method. EDTA was then added to the concentration 10 times greater than that of the concentration of calcium binding sites. After 30 minutes of incubation, the protein was concentrated to 1.5ml in centricon (10kD) and then chelex treated Tris-KCl buffer was added to it upto 15ml. The buffer exchange was continued till the EDTA concentration was reduced to picomolar quantity. Then the protein was diluted and contentration was measured by urea method using the following formula,

Concentration= A X D.F./ Molar Extinction coefficient (gives concentration in Molarity)

=A X D.F./ division factor (gives concentration in mg/ml)

Where A= Absrobance

D.F. = Dilution factor

The protein concentration was then adjusted to 2mg/ml, aliquoted in 1.5ml eppendroff tubes and freezed at -20°C.

For all the three mutants protein expression check, overexpression and purification was carried out using the same method.

3.4 Tryptophan fluorescence

One vial of each protein was thawed. The protein was diluted to 2µM concentration and incubated for a while. The spectrophotometer was turned on 20 minutes before use in order to allow the lamp to get heated up. Calcium chloride stock of 10µM, 100µM, 1mM, 10mM, and 100mM was prepared from 1M Calcium chloride solution (sigma). The parameters was set as follows, Excitation wavelength 295, X-axis scale: 300 to 400, EX slit: 2.5, EM slit: 5, PMT voltage: 700, Response: 2.

The spectrum of buffer was taken at first by taking 600µl of Tris-KCl buffer in cuvette. Then 600µl of protein was taken in the fluorescence cuvette and spectrum was measured and saved. The protein was titrated with different calcium concentration serially. Titration was carried out in such a way that minimum calcium solution (less than 10%) is to be added from the stock. The calcium titration was carried out as follows;

Table 4: Titration of 600µl of 2µM protein with different concentration of Calcium to study the Tryptophan Fluorescence spectra

Final calcium concentration	Stock concentration	Volume to be added
100nM	100µM	0.6µl
500nM	1mM	0.24µl
1µM	1mM	0.3µl
10µM	10mM	0.54µl
100µM	100mM	0.54µl
500µM	1M	0.24µl
1mM	1M	0.3µl
2mM	1M	0.6 µl

The calcium titration spectra for each protein was recorded and saved. The file was then converted to text format. The data was then imported in origin and buffer subtraction was carried out. The graph was plotted for each protein and compared.
In order to study the behaviour of protein in reduced condition, the protein was incubated with 1mM of DTT and then calcium titration and spectra measurement was performed in similar manner to that in oxidized condition.

3.5 8-Anilinonapthalene-1-sulfonic acid (ANS) fluorescence

10mM stock of ANS was prepared in Methanol. 10µM of ANS was then added to 2µM of protein at different condition (Protein + 100µM EGTA, Protein + 2mM Calcium, Protein+ 1mM DTT+ 100µM EGTA and Protein+ 1mM DTT+ 2mM Calcium) and incubated for 30 minutes in dark (as ANS is light sensitive). For ANS fluorescence, the excitation wavelength was kept at 365nm and emission was measured in the range of 400nm to 600nm. The excitation and emission slit, both were kept 5. The spectra of ANS in all four conditions were taken as blank. The spectra was then taken for protein and plotted in origin.

3.6 Circular Dichroism (CD)

i) UV CD (Tertiary CD)

For Near UV CD 1ml of 1mg/ml protein is required. Quartz cuvette of 1cm path length was taken. The nitrogen flow was turned on and the valve was opened. The flowmeter on the left hand side of spectropolarimeter was set to 5. After 5 minutes the spectropolarimeter was turned on and spectra manager software was opened. The machine was allowed to get purged with nitrogen gas and then measurement was started 10-15 minutes after the lamp was turned on. The parameters were set as follows; Sensitivity Standard (100mdeg), Start 350nm, End 250nm, Data pitch 0.2, Scanning mode continuous, Scanning speed 100nm/min, Response 2sec, Band width 2 and Accumulation 5
The Calcium titration was carried out in the following manner as shown in table 4;

Table5: Titration of 1ml of 1mg/ml protein with different concentration of Calcium to study the tertiary CD spectra

Final concentration of Calcium	Stock Calcium concentration	Volume to be added
100µM	100mM	1µl
500µM	1M	0.4µl
1mM	1M	0.5µl
2mM	1M	1µl
5mM	1M	3µl

For maintaining reduced condition, protein was incubated with 4mM DTT for 2 hours and spectra measurement and calcium titration was performed in similar manner. The data was then converted to text format, imported in origin and plotted into graph.

ii) Far UV CD (Secondary CD)

For taking the far UV CD spectrum, sandwich cuvette of pathlength, 0.01 cm was used. The protein concentration of 1mg/ml and 60µl volume was required. All the four proteins were taken at six different conditions (protein alone, protein+ 100µM EGTA, Protein+ 2mM Ca, Protein+ 1mM TCEP, Protein+ 1mM TCEP+ 100µM EGTA, Protein+ 1mM TCEP+ 2mM Ca) and incubated for 2 hours. The parameters were set on CD as follows; Sensitivity Standard (100mdeg), Start 250nm, End 195nm, Data pitch 0.2, Scanning mode continuous, Scanning speed 100nm/min, Response 2sec, Band width 2, Accumulation 3. The samples were then kept in sandwich cuvette one by one and spectra were taken.

3.7 Analytical Gel Filtration

For analytical gel filtration, superdex 75 column was used for high resolution. Analytical gel filtration was carried out in four different conditions, apo form (500µM EDTA), holo form (2mM Ca), reduced apo form (1mM DTT+ 500µM EDTA) and reduced holo form (1mM DTT+ 2mM Ca). 1mg/ml of WT hSCGN and its three mutant proteins were prepared in all the four conditions and incubated for one hour. For protein in reduced condition, DTT was added first and after incubation for one hour Calcium or EDTA was added. The column was equilibrated with 25ml of the buffer which was in same condition as that of the protein. After equilibration, 250µl of protein was injected into the injection valve with the help of hammilton syringe and 25ml of buffer was passed into the column. The eluted protein was detected by the detector which was displayed in the form of chromatogram. After injection of all four protein in same set of condition, the column was washed with one column volumn of filterd MilliQ water and equilibrated with buffer in another condition. Then injection of proteins in the same condition was carried out one by one. The data was then converted into text format and then imported in origin and plotted into graph.

3.8 Isothermal titration calorimetry (ITC)

ITC was carried out by titrating wild type and mutant proteins with calcium (ligand) in both oxidized and reduced condition. 1.8ml of 75µM WT and mutant proteins and 2ml of 5mM Calcium chloride in Tris-KCl were prepared separately in eppendroff tube and spinned at high speed. ITC machine was washed with 2 litres of milliQ water. Both the protein and calcium solutions were kept for degassing. Then the ligand was filled into ITC syringe and the macromolecule was injected into ITC sample cell with the help of 5ml Hammilton syringe. The sample was injected with continuous stirring in order to remove any air bubbles. Isothermal temperature was set to 25°C and other parameters were set as follows;Experiment parameters were set as Total injections 50, Cell temperature 25, Reference power (gCal/sec) 15,Initial delay (sec) 60, Syringe concentration (mM) 5,Cell concentration (mM) 0.075, Stirring speed 387. Injection parameters were set as Volume (µl) 6, Duration (sec) 12 , Spacing (sec) 220, Filter period (sec) 3.

For reduced condition, 1mM TCEP was added both in the ligand solution and protein solution and incubated for at least an hour. The experiment was then performed in the similar manner. For both condition, the titration of respective blank solution was also carried out in same conditions. Then data fitting was carried out in Microcal origin software. For data fitting the data was imported in the software, buffer substraction was carried out, ligand and macromolecule concentration was provided and then fitting was performed to reduce the Chi square to the lowest possible value.

3.9 Trypsin digestion

Trypsin digestion for all the four proteins was performed at four different conditions, oxidized apo form (100µM EDTA), oxidized holo form (2mM Ca), reduced apo form (1mM DTT+100µM EDTA) and reduced holo form (1mM DTT+ 2mM Ca). 20µg of protein was taken in all the four conditions. Trypsin was then added with trypsin and protein at the ratio of 1:50, 1:100 and 1:200. The sample was incubated at 37°C for 30 minutes at 37°C. Then SDS loading dye and PMSF was added immediately. The samples were boiled for 5 minutes and loaded on 15% SDS gel. Electrophoresis, staining and destaining of gel was performed and bands were analysed.

3.10 Glutaraldehyde crosslinking

Glutaraldehyde crosslinking for all the four proteins was performed at four different conditions, oxidized apo form (100µM EDTA), oxidized holo form (2mM Ca), reduced apo form (1mM DTT+100µM EDTA) and reduced holo form (1mM DTT+ 2mM Ca). For this experiment, protein was buffer exchanged to bring it into Hepes-KCl buffer (p^H 7.5). 30µg of protein was taken in 30µl of buffer. 0.012% of glutaraldehyde was then added to all the protein. Then it was incubated at 37°C for 10 minutes. Then 3µl of 1M Tris, pH 8 was added to stop the reaction. Laemmli buffer was then added and the samples were boiled and loaded on 10% SDS gel. Electrophoresis, staining and destaining of gel was performed and bands were visualized.

3.11 Guanidium hydrochloride (GdmCl) unfolding assay

8M GdmCl was prepared in chelex water and filtered. Concentration on GdmCl solution was checked using refractrometer taking the refractive index of chelex water and GdmCl solution and calculating as follows,

Concentration= 57.147 (ΔN) + 38.62 $(\Delta N)^2$+ 91.6 $(\Delta N)^3$

10 X Tris-KCl buffer (1000mM Tris and 500mM KCl) was prepared separately with 1mM EDTA and 20mM Ca. Each protein brought to the concentration of 2mg/ml. Tubes were labeled properly with the concentration of GdmCl.Then protein was subjected to increasing concentration of GdmCl by mixing the components as shown in table 5;

Table 6: Preparation of protein solution in different concentration of Guanidium hydrochloride for GdmCl unfolding assay

GdmCl concentration(in M)	Chelex water (in ml)	GdmCl (in ml)	Buffer (In ml)	Protein (2mg/ml stock in ml)	Total
0	510	0	60	30	600
0.01	509.25	0.75	60	30	600
0.02	508.5	1.5	60	30	600
0.03	507.75	2.25	60	30	600
0.04	507	3	60	30	600
0.05	506.25	3.75	60	30	600
0.06	505.5	4.5	60	30	600
0.07	504.75	5.25	60	30	600
0.08	504	6	60	30	600
0.09	503.25	6.75	60	30	600
0.1	502.5	7.5	60	30	600
0.2	495	15	60	30	600
0.3	487.5	22.5	60	30	600
0.4	480	30	60	30	600
0.5	472.5	37.5	60	30	600
0.6	465	45	60	30	600
0.7	457.5	52.5	60	30	600
0.8	450	60	60	30	600
0.9	442.5	67.5	60	30	600
1	435	75	60	30	600
1.1	427.5	82.5	60	30	600
1.2	420	90	60	30	600
1.3	412.5	97.5	60	30	600
1.4	405	105	60	30	600
1.5	397.5	112.5	60	30	600
1.6	390	120	60	30	600
1.7	382.5	127.5	60	30	600
1.8	375	135	60	30	600
1.9	367.5	142.5	60	30	600

2	360	150	60	30	600
2.1	352.5	157.5	60	30	600
2.2	345	165	60	30	600
2.3	337.5	172.5	60	30	600
2.4	330	180	60	30	600
2.5	322.5	187.5	60	30	600
2.6	315	195	60	30	600
2.7	307.5	202.5	60	30	600
2.8	300	210	60	30	600
2.9	292.5	217.5	60	30	600
3	285	225	60	30	600
3.1	277.5	232.5	60	30	600
3.2	270	240	60	30	600
3.3	262.5	247.5	60	30	600
3.4	255	255	60	30	600
3.5	247.5	262.5	60	30	600
3.6	240	270	60	30	600
3.7	232.5	277.5	60	30	600
3.8	225	285	60	30	600
3.9	217.5	292.5	60	30	600
4	210	300	60	30	600
4.2	195	315	60	30	600
4.4	180	330	60	30	600
4.6	165	345	60	30	600
4.8	150	360	60	30	600
5	135	375	60	30	600
5.2	120	390	60	30	600
5.4	105	405	60	30	600
5.6	90	420	60	30	600
5.8	75	435	60	30	600
6	60	450	60	30	600
6.2	45	465	60	30	600
6.4	30	480	60	30	600
6.6	15	495	60	30	600
6.8	0	510	60	30	600

Blank was also prepared by mixing the entire component except protein. To study unfolding in apo from, buffer with EDTA was used whereas for holo from buffer with Calcium was used. For reduced condition 10X TCEP (10mM) was mixed with the respective buffer. The tubes were incubated overnight. Next day the tryptophan fluorescence of each sample was recorded in fluorescence spectrophotometer. The spectrum of blank was substracted from each spectra of sample. Then λmax and F.I. max was recorded for each sample. GdmCl unfolding was performed for each of the four proteins in four different condtions, oxidized apo and holo, reduced apo and holo. Graph was plotted for FI 360/320 vs. GdmCl concentration and λmax vs. GdmCl.

3.12 Study of Interation of WT hscgn and its mutants with Insulin using

i) Tryptophan fluorescence

Study of interaction of WT hSCGN and its mutants with insulin was carried out in both apo (100µM EGTA) and holo (2mM Ca) condition. 2uM all four proteins in apo and holo condition were titrated with different concentration of insulin and the spectra was recorded. Titration was carried out in following manner;

Table 7: Titration of protein with different concentration of insulin for studying tryptophan fluorescence spectra

Final concentration of Insulin	Stock concentration	Volume to be added
0.5µM	170µM	1.8µl
1µM	170µM	1.8µl
5µM	1.7mM	1.4µl
10µM	1.7mM	1.76µl
20µM	1.7mM	3.5µl
40µM	1.7mM	7.06µl
60µM	1.7mM	7.06µl

In the similar manner, respective buffer was also titrated with insulin and later subtracted from the respective protein spectra to cut out the fluorescence due to insulin.

ii) Near UV CD spectra

The parameters in spectropolarimeter were set same as the normal near UV CD spectra. 1mg/ml concentration of all four proteins was prepared in both apo (100µM EGTA) and holo (2mM Ca) form. Insulin was titrated to it in the following manner,

Table 8: Titration of protein with different concentration of insulin for studying CD spectra

Final concentration of Insulin	Stock concentration	Volume to be added
0.5µM	1.7mM	0.29µl
1µM	1.7mM	0.29µl
10µM	1.7mM	5.29µl
20µM	1.7mM	5.89µl
40µM	1.7mM	11.76µl
60µM	1.7mM	11.76µl

Buffer was also titrated with insulin in similar manner and later subtracted from the respective protein spectra. Graph was then plotted in origin. The insulin titration spectra of WT hSCGN was then compared with the spectra of mutants.

iii) Far western blotting

a) Native PAGE: 10% native gel was prepared by adding all the components except SDS in the polyacrylamide gel. 80µg each of WT hSCGN and mutant proteins was prepared in 40µl volume. In the same way, 80µg of mouse wild type secretagogin, BSA, negative control protein (Xanthinollin) and Insulin were also prepared.500µM EGTA was added to prepare the apo form of the proteins whereas 2mM Ca was added to the proteins to prepare the holo form. The proteins were mixed with native PAGE dye (without SDS and β-mercaptoethanol) and then loaded in the gel along with the prestained marker and electrophoresis was carried out. After the dye had moved an inch below the stacking gel, the gel was removed and then washed with MilliQ water.
b) Transfer: 1 litre of transfer buffer was prepared. The gel as well as the Poly vinylidene difluoride (PVDF) membrane was cut into desired size. The transfer cassette was set such that the gel was placed towards the cathode (black) and the membrane towards the anode (red) and the cassette was placed in the transfer apparatus. Transfer was carried out at 120V at 200-250mA current for three hours.
c) Blocking: The membrane was placed in 5% BSA overnight with continuous shaking in rocker in cold room.
d) Incubation with insulin: 100µM Insulin solution was prepared in Tris Buffer Saline Tween (TBST, 0.1%) and 0.5% BSA. The membrane was then incubated with insulin overnight at cold room with continuous shaking at low speed.
e) Washing: The membrane was washed with TBST (0.1%) at high speed at room temperature for 4 times.
f) Incubation with primary antibody: Rabbit anti-insulin antibody was diluted in 2% BSA in TBST at the dilution of 1:10,000. The membrane was incubated with primary antibody overnight in cold room with continuous shaking at low speed.
g) Washing: The membrane was washed 4 times with TBST (0.1%) at high speed at room temperature.
h) Incubation with secondary antibody: Anti rabbit antibody was prepared in 5% BSA at the dilution of 1:10,000. The membrane was then incubated with secondary antibody at room temperature with continuously shaking at low speed.
i) Washing and blot development: The blot was then washed four times at high speed with TBST. Then the blot was flooded with 3,3',5,5'-tetramethylbenzidine (TMB) substrate and the chemiluminescence was measured in chemidoc.

3.13 Cloning of WT and mutant hscgn gene in mammalian vector, eGFP N3 by restriction free cloning method

Primers were designed in such a way that it targeted half of the segment from the pEGFP-N3 vector and the other half from the desired gene. The same primer worked for cloning of WT and mutant gene but the template was taken different. The primer used were 5'-GAGCTGGTTTAGTGAACCGTCAGATCATGGACAGCTCCCGGGAA-3' as forward primer with plasmid annealing temperature 61°C , Target annealing temperature 59°C and Length 44 and 5'-ACAGCTCCTCGCCCTTGCTCACTGGGTTGATTTTCAGCCCA-3'as

Reverse primer with plasmid annealing temperature 64°C, Target annealing temperature 55°C and Length 44. For restriction free cloning, two PCR was carried out.
First PCR was carried out with high fidelity phusion mastermix and the PCR mix was prepared by mixing 10pM each of forward and reverse primer, 500ng of template (WT h*scgn* in pET-21b vector), 1X Phusion mastermix (Thermo scientific, stock-2X) and autoclaved MilliQ water to maintain the volume to 50µl. First PCR was carried out using the following conditions; initial denaturation at 95°C for 5 minutes, denaturation at 95°C for 30 seconds, annealing at 55°C for 30 seconds and extension at 72°C for 1 minute. The step from denaturation to extension was repeated for 34 cycles after which final extension was carried out at 72°C for 10 minutes. For mutants, the respective confirmed mutant gene in pET-21b vector was taken as template in first PCR.

The amplicon was the loaded on agarose gel, electrophoresis was carried out, after which the DNA was eluted out from the gel using DNA extraction and purification kit (MN). Then second PCR was carried out using the first PCR product as template using Pfu DNA polymerase (G-Biosciences). PCR mix was prepared by mixing the following components, 100ng of template DNA, 1.25unit Pfu enzyme (stock 5unit/µl), 1X Pfu buffer (G-Biosciences), 1mM dNTPs and autoclaved MilliQ to bring the volume to 20µl.PCR was conducted using the following conditions; initial denaturation at 95°C for 5 minutes, denaturation at 95°C for 30 seconds, annealing at 59°C for 30 seconds and extension at 72°C for 25 minutes. The step from denaturation and extension was repeated for 18 cycles after which final extension was carried out at 72°C for 50 minutes. After second PCR, 8µl of the amplicon was treated with DpN1 enzyme (5 units) and incubated at 37°C for 3 hours. The product was used for transformation into *E.coli* DH5α cells and the cells were plated in Kanamycin(50µg/ml) plate and incubated at 37°C overnight. Colony PCR was carried out to select the positive clones. For colony PCR gene specific primers were used. Two of the positive colonies were selected from the Kanamycin plate and cultured in LB broth. Plasmid was extracted from the culture using DNA, RNA and protein purification kit (MN). The plasmids were then given for sequencing.

3.14 Mediprep of plasmid from confirmed colonies

The confirmed *E.coli* colonies were cultured in 250ml culture and then harvested in a 50ml falcon tube by centrifugation at 5000rpm for 10 minutes at 4°C. The pellet was resuspended in 8ml of resuspension buffer. 8ml of cell lysis buffer was added to it and the mixed 5 times by inverting gently and incubated for 5 minutes at room temperature. 8ml of neutralization buffer was added to the suspension and mixed till the blue colour was changed to white. The lysate was then clarified by centrifugation at 5000rpm for 10 minutes. The column provided was fitted with the filter and it was equilibrated with 12ml of the equilibration buffer. The lysate was loaded into the column through the rim of the filter. The column filter and column were washed with 5ml of the equilibration buffer. The filter was then removed from the column and the column was given second wash with 8ml of buffer wash. The plasmid DNA was then eluted with 5ml of elution

buffer in a sterile Orchis tube. 3.5ml of isopropanol at room temperature was added to the eluate and vortexed. DNA was then precipitated by centrifugation at 15,000g for 30 minutes at 4°C in Beckman coulter. The supernatant was gently discarded. The pellet was washed with 70% ethanol and the pellet was reconstituted by centrifugation at 15,000g for 5 minutes at room temperature. The pellet was then air dried and resuspended in autoclaved MilliQ water and mixed properly by pipetting. The quantity of DNA was measured by nanodrop.

3.15 Culture of MIN6 cell line

The cryopreserved MIN6 cell vial was taken out from liquid nitrogen and thawed. After thawing, it was dispensed in a 15ml falcon 4ml Dulbecco's Modified Eagle's Media (DMEM) at 37°C. The cell suspension was centrifuged at 1500rpm for 5 minutes. Supernatant was discarded and the cell pellet was resuspended in 1ml of DMEM complete media. A T-25 flask was taken and the cell suspension was added to it along with 4ml of additional DMEM complete media. The suspension was swirled for mixing, observed under dissection microscope after which the flask was incubated in a CO_2 incubator at 37°C. After about 18 hours, the flask was observed under inverted microscope and the cell the density was observed. If the cell confluency is less than 70-80%, further incubation is required. The media was removed from the flask and the cells were washed twice with PBS. 5ml of DMEM was again added into the flask and the cells were further incubated to obtain a monolayer with 70-80% confluency.

3.16 Trypsinization

Trypsin-EDTA solution (0.05% Trypsin and 0.53mM EDTA) was brought to room temperature. After a confluent monolayer was obtained, the media was removed and the cell was once washed with PBS. Then 1ml of Trysin-EDTA solution was added into the culture flask and the solution was vigorously pipetted through the wall of the flask. Then the flask was tapped from one side. The detachment to cells from the vessel was observed under dissection microscope after about 2 minutes. The 4 ml of DMEM complete media was added into the flask and the suspension was mixed well. It was taken in a 15ml falcon tube and the cells were pelleted down by spinning at 1500rpm for 3 minutes. The supernatant was gently discarded and the pellet was dissolved in 1ml of DMEM complete media. The cell was then counted in haemocytometer and the concentration of cells was determined.

3.17 Transfection of the construct in MIN6 cell line

The cells were diluted in 1.5ml DMEM complete media to bring the concentration to 0.2 million. 2.5µg of the plasmid DNA (construct) was mixed with 5µl of Plus reagent (**Lipofectamine® LTX with Plus™ Reagent**, Invitrogen) dissolved in 125µl of Incomplete media (IM) and mixed 25 times. Then 5µl of lipofectamine reagent was diluted in 125µl of IM and mixed 25 times. The two mixtures were then mixed together and inverted 25 times for mixing. This final mixture was added to the diluted MIN6 cells and properly mixed. The cells were then pippetted into 6 welled plates. The process was carried out

for WT hSCGN and the three mutants separately and incubated in CO_2 incubator for 24 hours. The cells were washed each day with PBS and then incubated with Complete media (CM) containing Gentamicin to select the stably transfected cells. The concentration of Gentamicin was increased from 200µg/ml to 1000µg/ml. The cells were incubated for 21 days until strong green fluorescent signal was observed in fluorescent microscope.

CHAPTER 4

RESULTS

4.1 Cloning of Secretagogin gene in PET-21b vector

4.1.1 Amplification, digestion and confirmation of h*scgn* clones by colony PCR

After gradient PCR, amplicon of 830bp was obtained at all the temperature used but the most suitable condition for the amplification of h*scgn* gene was found to be 60°C as maximum amplification occurred at this temperature in gradient PCR. The amplicon as well as pET-21b vector was digested using *Nde*I and *Xho*I and run on gel (Fig. 1B). The digested pET-21b vector gave a single band in the gel. Restriction digested insert and vector were then subjected to ligation in the presence of T4 DNA ligase keeping a control (digested vector without insert). The ligated mixture was used for transformation into competent *E.coli* DH5α cells.

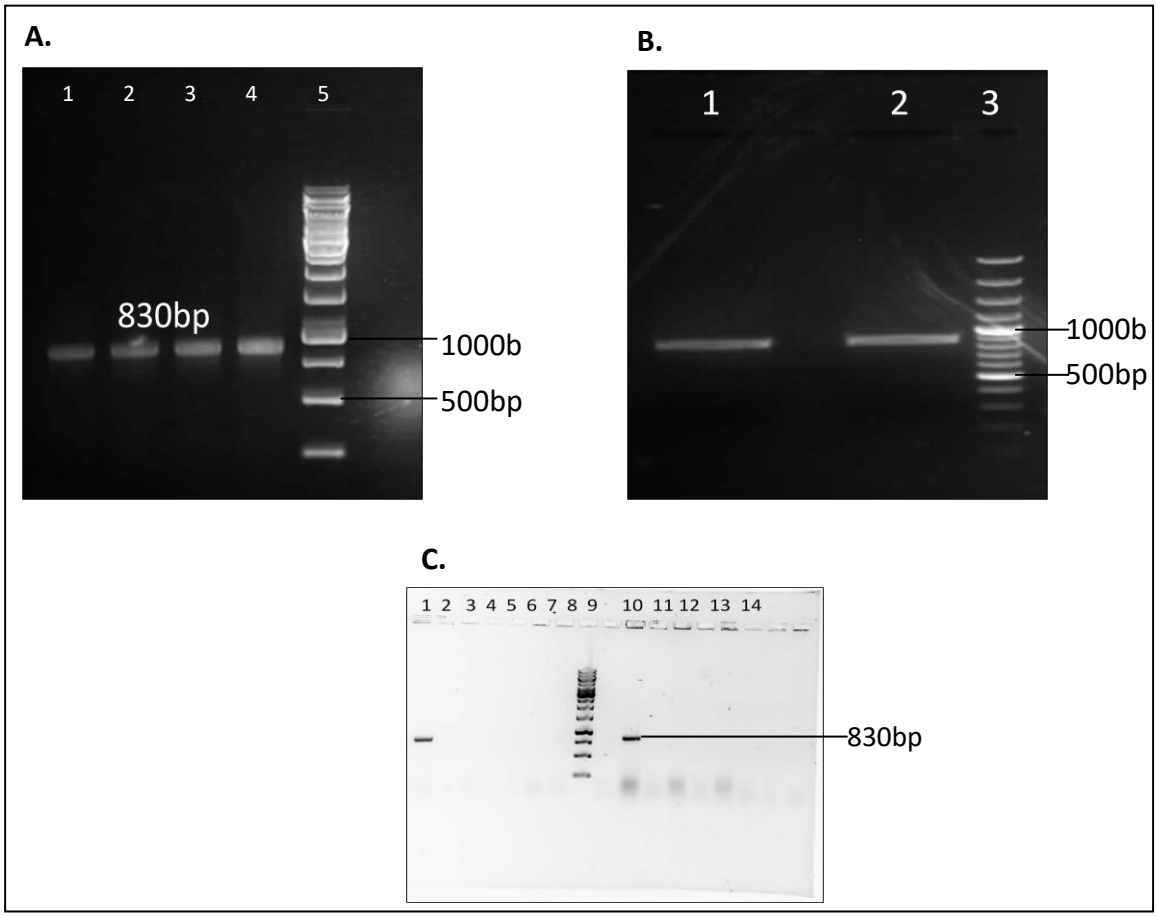

Figure 1: Cloning of WT h*scgn* gene in pET-21b vector, **Figure 1A**: PCR amplification of hSCGN using gene specific primers with *Nde*I and *Xho*I site (Lane 1 to 4), Lane 5: 1000bp DNA ladder (Thermo scientific). **Figure 1B**: Restriction digestion of insert with *Nde*I and *Xho*I (Lane 1 and 2). Lane 3: 100bp DNA ladder (Thermo scientific). **Figure 1C**: Colony PCR of wild type SCGN in pET-21b vector after transformation into *E.coli* DH5α, Lane 1 and 10 showing positive clones, Lane 9: 1000bp DNA ladder (Thermo scientific).

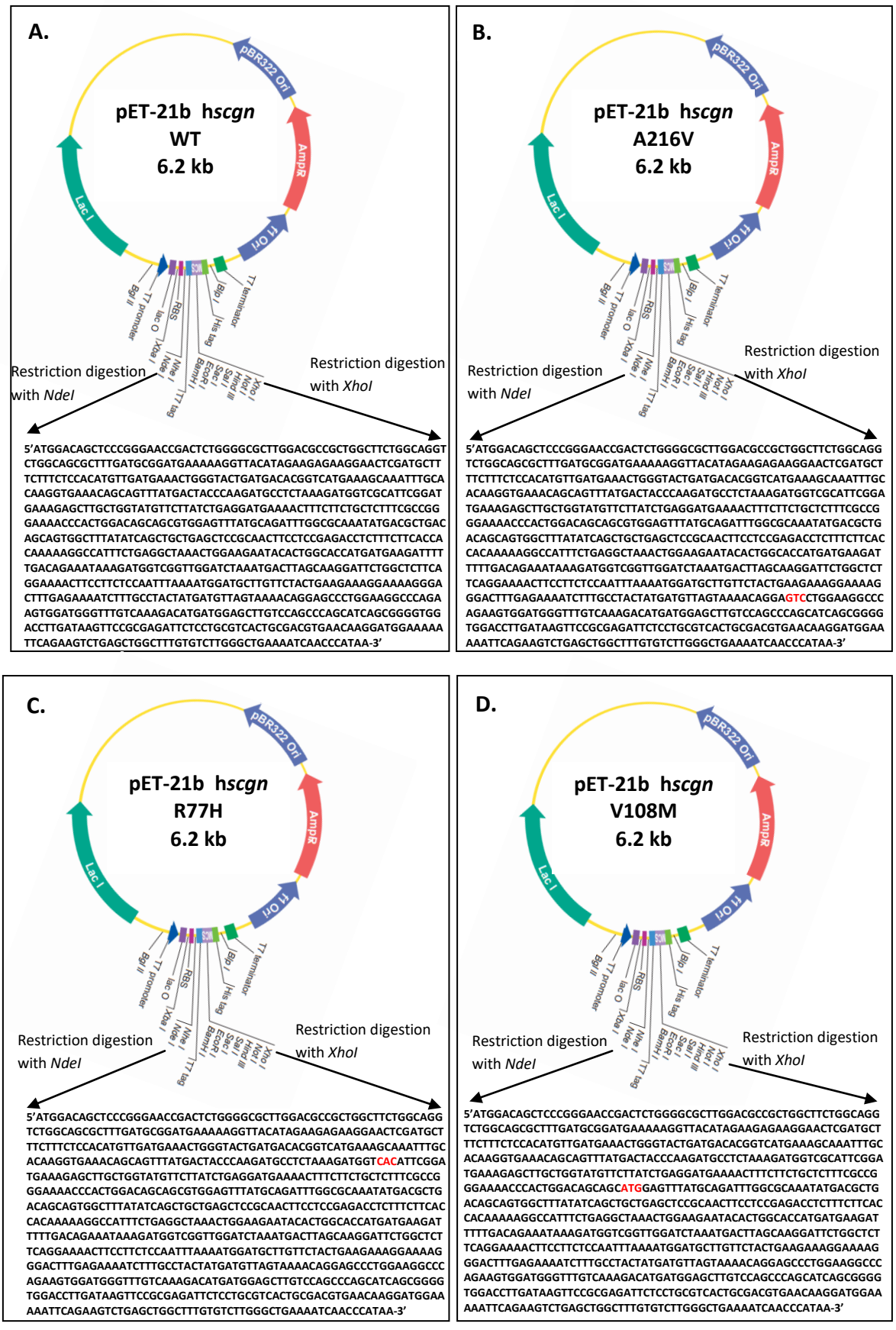

Figure 2: hscgn WT and its mutants inserted in pET-21b vector between *Nde*I and *Xho*I site. The site of mutation is marked as red nucleotides. **Fig A:** pET-21b hscgn WT, **Fig B:** pET-21b hscgn A216V, **Fig C:** pET-21b hscgn R77H and **Fig D:** pET-21b hscgn V108M

After overnight incubation at 37°C, the control plates gave very few colonies (7 colonies) indicating that digestion and ligation had occurred efficiently and the chances of self ligation was minimum. The plate with pET-21b hscgn gave greater than 100 colonies. Among them 13 colonies were selected for colony PCR. Two colonies (colony 1 and 9) gave band of 830bp size in the gel (Fig. 1C).

The insert i.e. h*scgn* was inserted in the multiple cloning site in pET-21b between the *Nde*I and *Xho*I sites. After digestion with *Nde*I and *Xho*I enzymes, the insert would have two sticky ends which ligates with the complementary sticky ends of the restriction digested vector. The insert would be placed under T7 promoter.

4.1.2 Confirmation of pET-21b hscgn by sequencing

Plasmid was extracted from the two colonies and given for sequencing using T7 forward and reverse primer. The sequencing result was analysed by snapgene viewer. The plasmid was confirmed to be pET-21b from NCBI blast tool as it showed 100% identity to pET-21b. The insert was also confirmed by the same method. For further confirmation, expasy translate tool was used to obtain the sequence of the protein encoded by the insert. The amino acid sequence encoded by the insert matched exactly with the amino acid sequence of human Secretagogin. Thus colony1 (Fig 2) was confirmed to be positive for pET-21b h*scgn*.

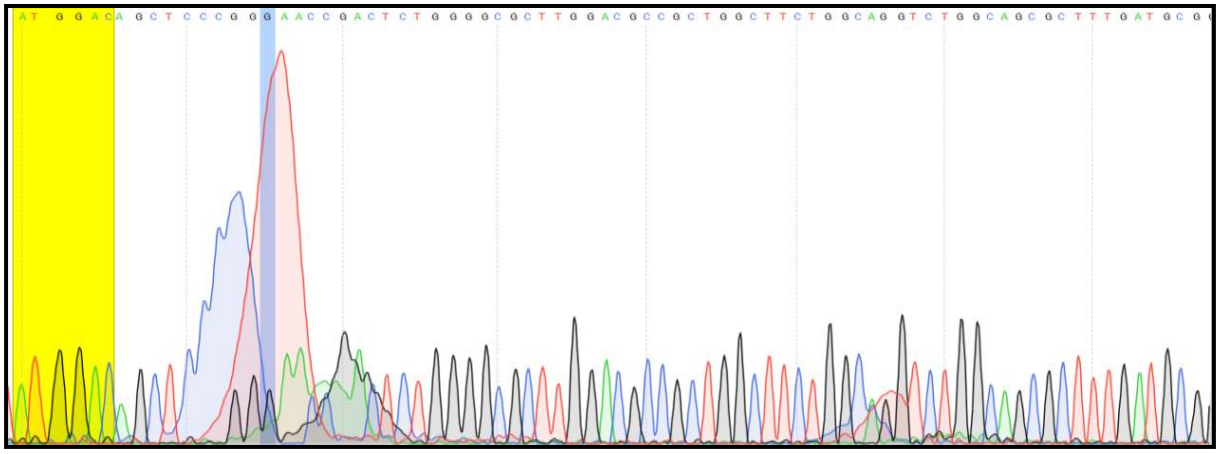

Figure 2D: Confirmation of pET-21b h*scgn* WT by sequencing showing the first codon methionine (ATG- highlited) viewed using snapgene viewer

4.2 Cloning of mutants of human Secretagogin

4.2.1 Confirmation of pET-21b A216V, pET-21b R77H and pET-21b V108M mutants by colony PCR

After PCR using SDM inducing primers and DpN1 digestion, the DpN1 digested product of respective mutant was transformed into *E.coli* DH5α cells. pET-21b vector alone was also kept for DpN1 digestion as digestion control to check the efficiency of DpN1 digestion. After incubation at 37°C colonies were formed in LB Amp plates where pET-

21b mutants were used for transformation. Very few colonies were formed in the control plates which indicate that DpN1 digestion was efficient.

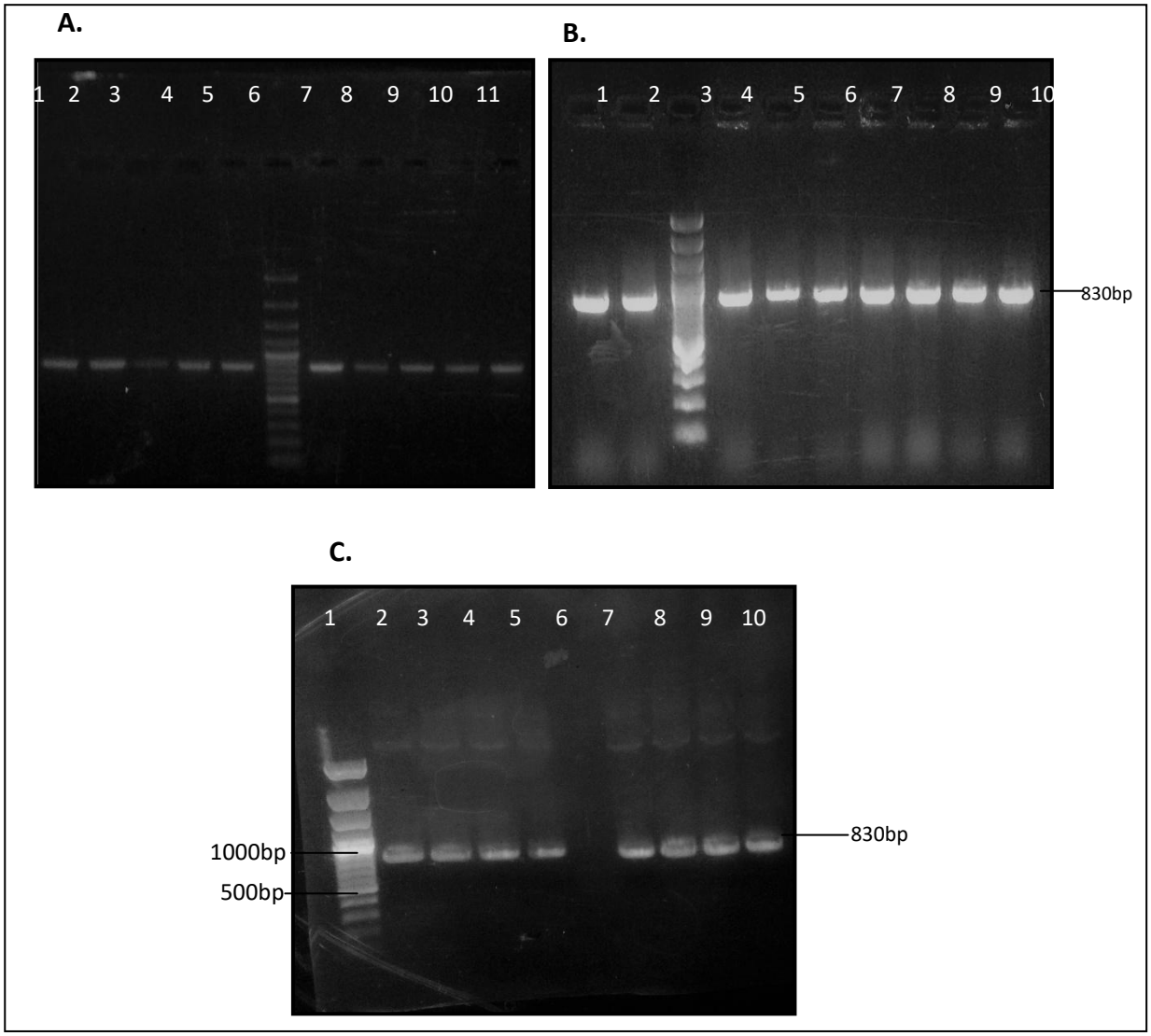

Figure 3: Confirmation of mutant clones by colony PCR. **Figure 3A:** Colony PCR for confirmation of pET-21b A216V hscgn clones, **Lane 6:** 100bp DNA ladder (Thermoscientific), all the lanes showing positive clones. **Figure 3B:** Colony PCR for confirmation of pET-21b R77H hscgn clones, **Lane 3:** 100bp DNA ladder (Thermoscientific), all the lanes showing positive clones. **Figure 3C:** Colony PCR for confirmation of pET-21b A216V hscgn clones, **Lane 6:** 100bp DNA ladder (Thermoscientific), all the lanes except lane 6 showing positive clones.

From pET-21b A216V plates, 10 colonies were selected for colony PCR whereas from pET-21b R77H and pET-21b V108M plates, 9 colonies each were selected. Positive clone gave DNA band of 830kb size. All the colonies selected, gave positive result in colony PCR in case of pET-21b A216V and R77H (Fig. 3A and 3B) whereas in case of pET-21b V108M (Fig. 3C), all the conolies selected except one gave positive result.

4.2.1 Confirmation of pET-21b A216V, pET-21b R77H and pET-21b V108M mutants by sequencing

Two colonies were selected for each mutant and given for sequencing. The sequencing result was viewed using snapgene viewer and observed for Site directed mutation. In case of A216V mutant, GCC is replaced by GTC at position 646 from the first nucleotide (Fig. 4A). In case of R77H and V108M mutants CTC is replaced by CAC and GTG is replaced by ATG at position 229 and 322 respectively form first nucleotide (Fig. 4C and 4D). For further confirmation, the nucleotide sequence was translated into amino acid sequence using expasy translate tool. The mutation was then confirmed from amino acid sequence.

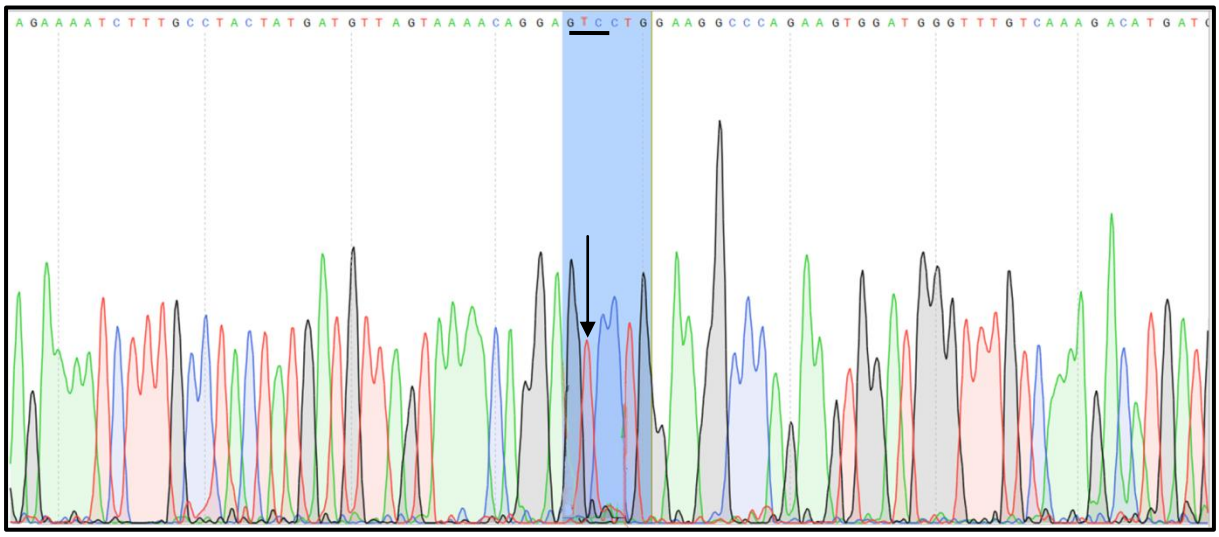

Figure 4A: Confirmation of pET-21b h*scgn* A216V mutant by sequencing where GCC is replaced by GTC in mutant

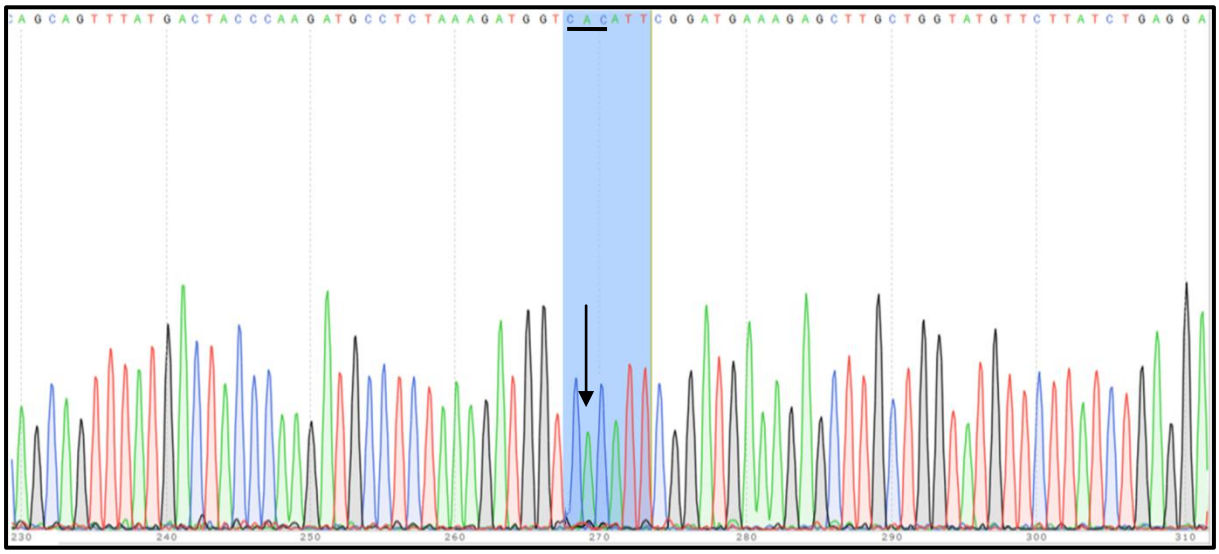

Figure 4B: Confirmation of h*scgn* R77H mutant by sequencing where CTG is replaced by CAC in mutant

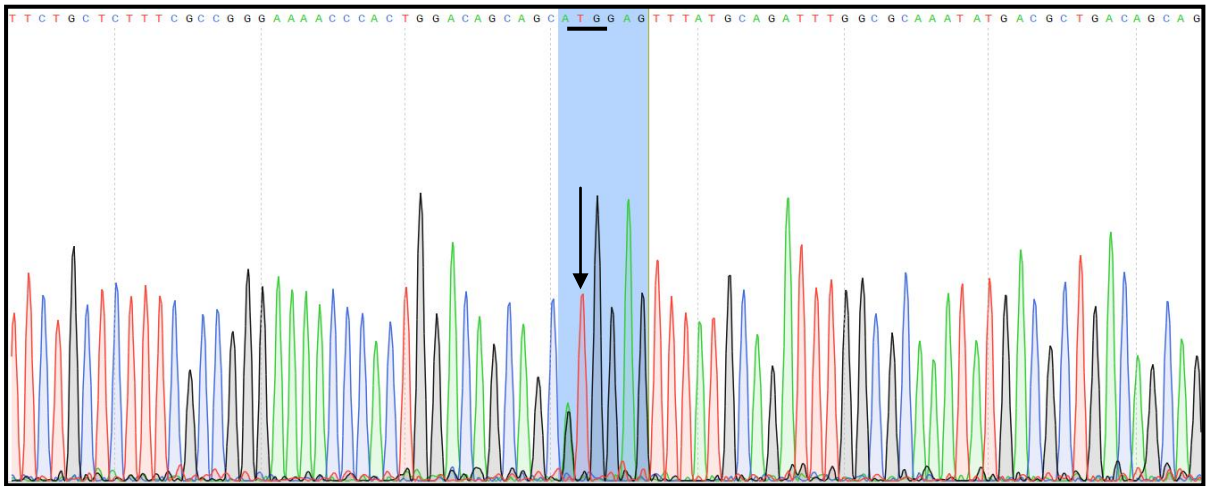

Figure 4C: Confirmation of h*scgn* V108M mutant by sequencing where GTG is replaced by ATG in mutant

4.3 Expression analysis of hSCGN wild type

As the information obtained from the review of literature of published work, expression check of hSCGN was carried out at 37°C for 4 hours and at 0.4mM concentration of IPTG. Protein band at 32kD was observed in all the lanes (Fig. 5). It was observed that there was large amount of leaky expression of protein even in the uninduced culture denoted by the presence of bands in lane 1 and 6 (Fig. 5). At 37°C, a large fraction of protein was found to be lost in insoluble fraction i.e. the protein formed inclusion bodies. Thus the condition for expression of the protein needed to be optimized.

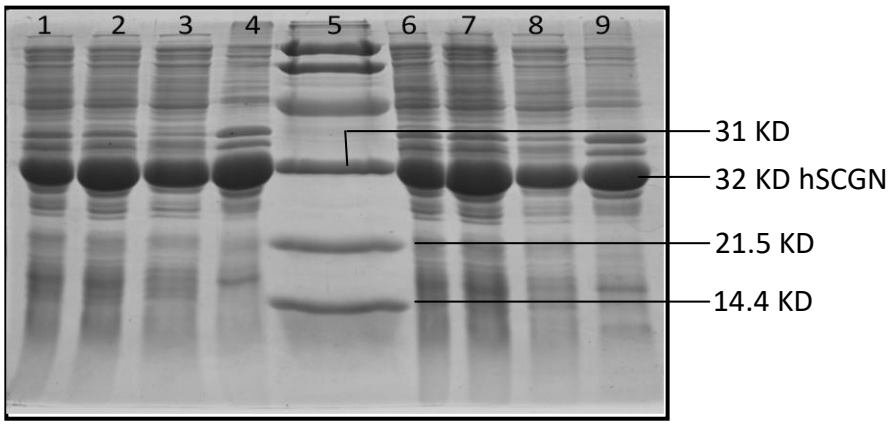

Figure 5: Expression analysis of two confirmed colonies of hSCGN by induction at 37°C for 4hour at 0.4mM IPTG concentration. **Lane 1 to 4**: Uinduced, total cell lysate, supernatant and pellet respectively of colony 1, **Lane 5**: Low range marker (Bio-rad), **Lane 6 to 9:** Uinduced, total cell lysate, supernatant and pellet respectively of colony 2

The expression of protein at 37°C and 25°C (Fig. 6A and 6B) was high whereas at 18°C the expression was found to be very low (Fig. 6C). After careful observation of the band, the condition in which there was highest overexpression was selected for each

temperature. Maximum expression was observed in the following conditions, 37°C, 4hrs at 0.4mM IPTG, 37°C 6hrs at 0.6mM IPTG (Fig. 6A), 25°C, 8hrs at 0.8mM IPTG, 25°C, 10hrs at 0.6mM IPTG, 18°C (Fig. 6B), 8hrs at 0.4mM IPTG, 18°C, 10hrs at 0.6mM IPTG and 18°C, 12hrs 0.6mM IPTG (Fig. 6C) which were then processed further for sonication. At 37°C, in both the conditions, large fraction of protein had gone to inclusion bodies (Fig. 7). At 18°C, though all the protein was expressed in soluble fraction but the yield was lower. Even at 25°C, all the protein was found to be expressed in soluble fraction but maximum yield of protein was observed at 0.8mM concentration of IPTG (Fig. 7A). Thus the most favourable condition for overexpression of hSCGN WT was found to be at 25°C, at 0.8mM concentration of IPTG and incubation for 8 hours.

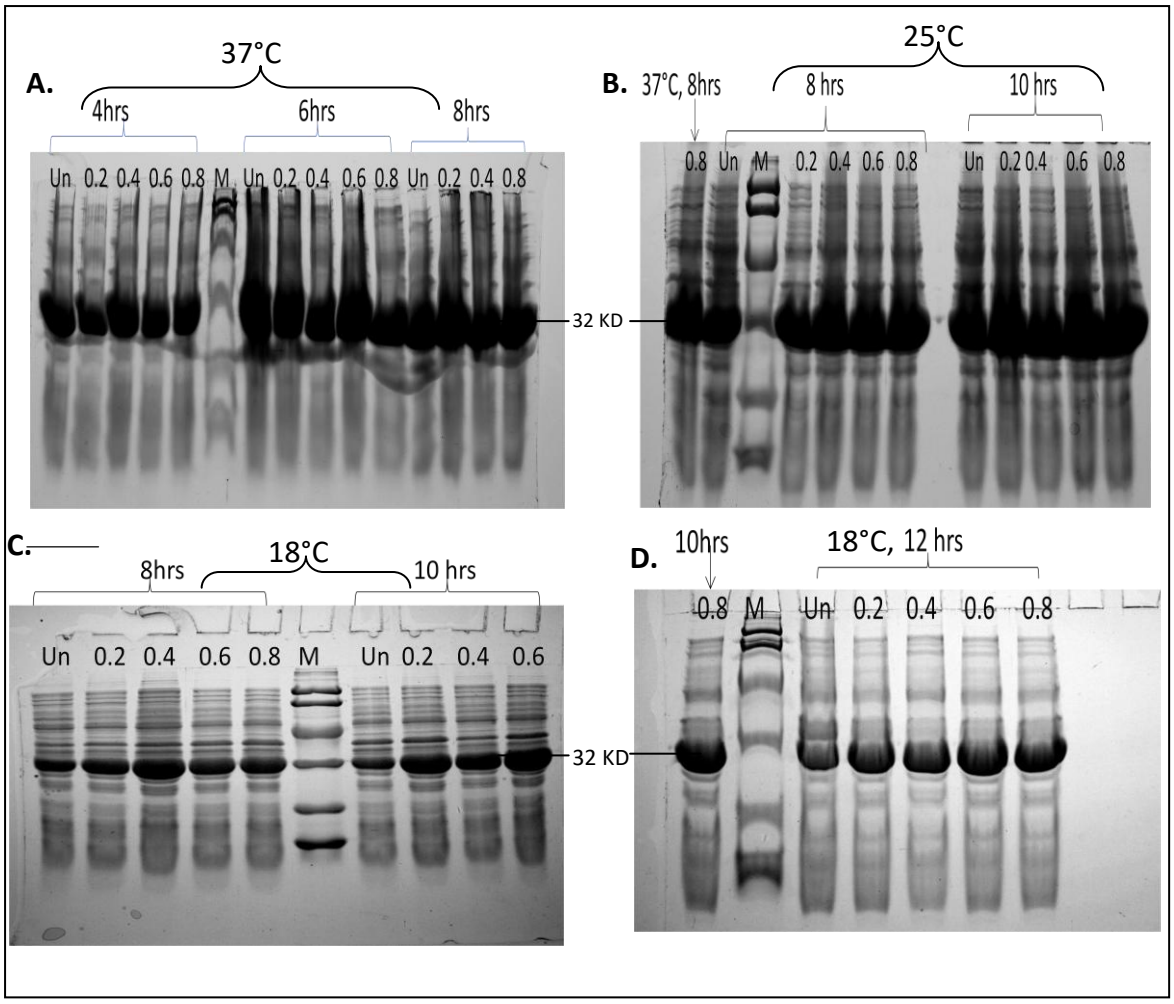

Figure 6: Expression check of hSCGN at different time, temperature and concentration of IPTG. **6A:** Expression check at 37°C induced at different concentration of IPTG (labeled above each lanes in mM) for 4hrs, 6hrs and 8hrs. **6B:** Expression check at 25°C induced at different concentration of IPTG (labeled above each lanes in mM) for 8hrs and 10hrs. **6C and 6D:** Expression check at 18°C induced at different concentration of IPTG (labeled above each lanes in mM) for 8hrs, 10hrs and 12hrs. M stands for low range protein marker (Bio-rad)

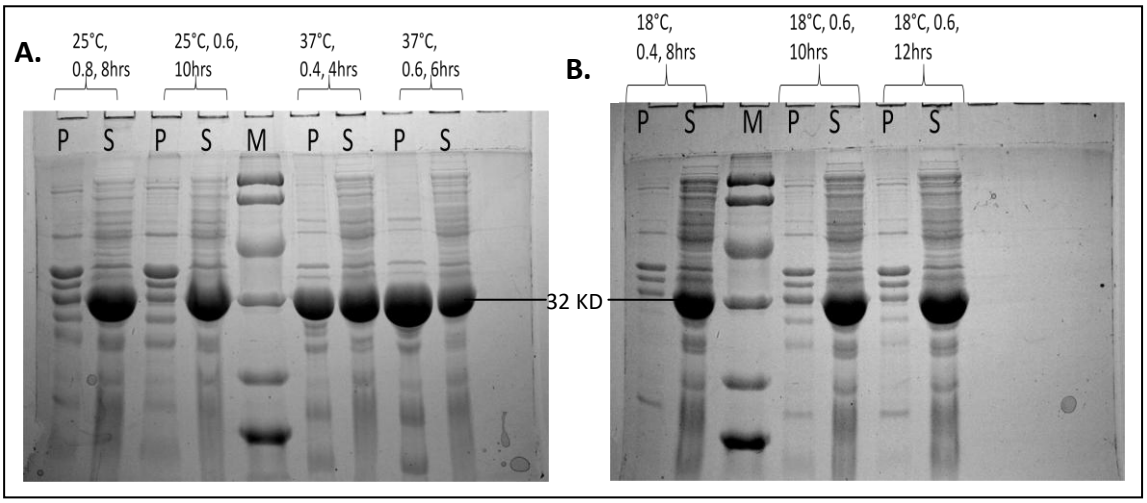

Figure 7: Checking whether the protein is expressed in soluble fraction or insoluble fraction after sonication by SDS PAGE. **Figure 7A**: Expression check in pellet and supernatant fraction at 25°C and 37°C. **Figure 7B:** Expression check in pellet and supernatant fraction at 18°C. M stands for low range protein marker (Bio-rad)

4.3 Expression analysis of hSCGN mutants

The expression of mutants was carried out directly at 25°C incubated with 0.8mM IPTG for 8 hours taking the wild type protein as reference. On analysis of mutant protein expression profile, it was observed that all the mutant proteins over expressed in soluble fraction at 25°C with 0.8mM IPTG under incubation for 8 hours. Two colonies were taken for expression analysis of A216V and V108M. The best performing colony was selected for each mutant i.e. Colony 2 for A216V hSCGN mutant (Fig. 8A) and Colony 1 for V108M mutant (Fig. 8C) and subcultured for protein production in large scale. For R77H, single colony was selected and expression analysis was carried out at 25°C and 37°C at 0.5mM and 0.8mM concentration of IPTG (Fig. 8B). At 37°C, most of the protein was lost in pellet as inclusion bodies whereas at 25°C, the protein came to the soluble fraction (Fig. 8B). Even in the case of R77H mutant, maximum overexpression was seen at 25°C with 0.8mM IPTG under incubation for 8 hours (Fig. 8B). Comparing the quantity of protein expressed, R77H seemed to be highest expressing protein as its protein bands were thickest among all the other proteins' band.

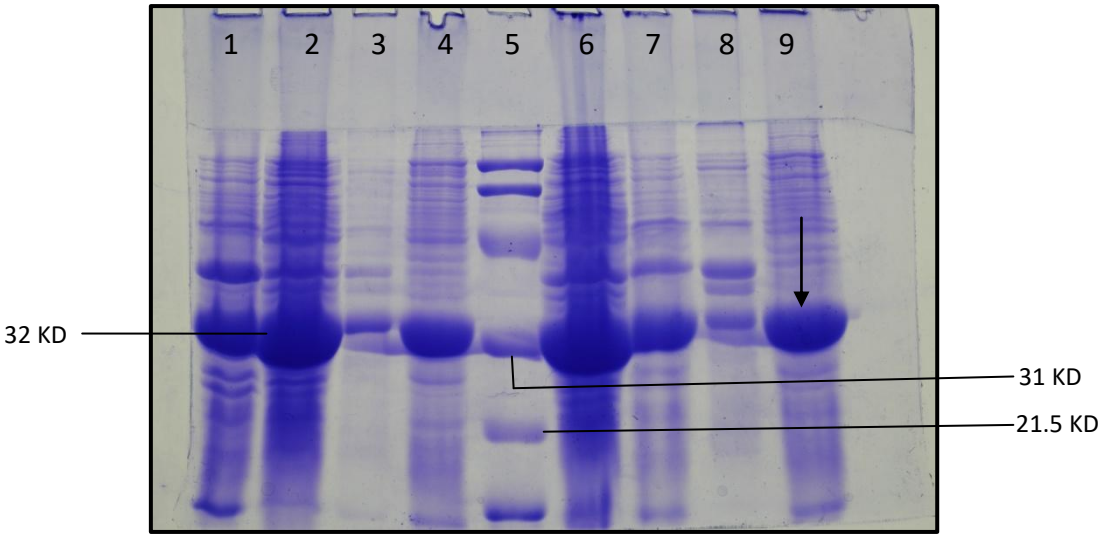

Figure 8A: Expression check of hSCGN A216V mutant induced at 25°C at 0.8mM concentration of IPTG for 8 hours, **Lane 1, 2, 3 and 4:** Uninduced, total cell lysate, pellet and supernatant respectively for first colony, **Lane 5:** Low range marker(Bio-rad), **Lane 6,7,8 and 9:** Uninduced, total cell lysate, pellet and supernatant respectively of second colony.

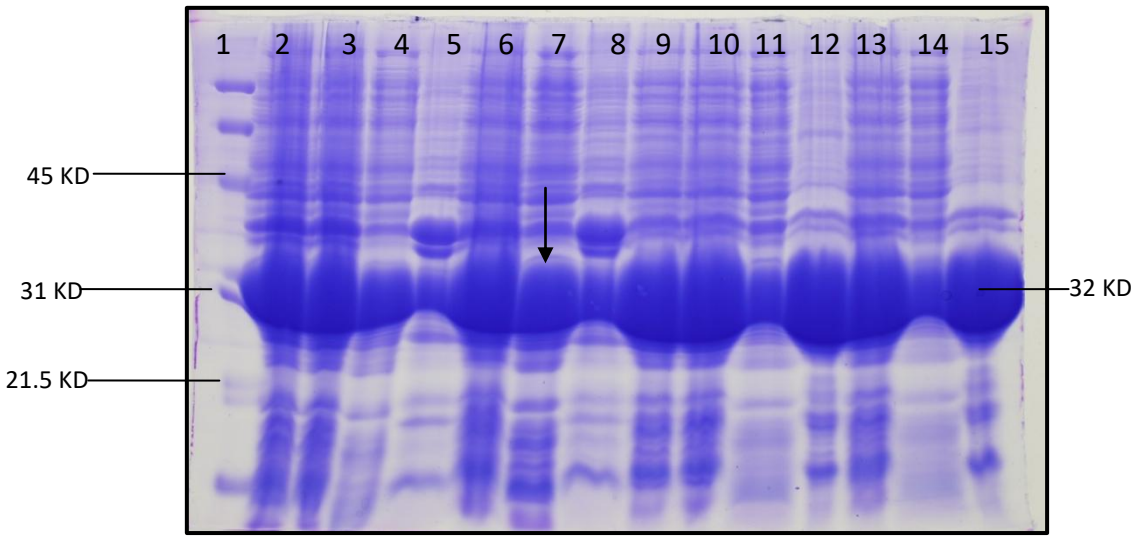

Figure 8B: Expression check for R77H hSCGN mutant, Lane 1: Low range marker (Bio-rad), **Lane 2, 3, 4 and 5:** Uninduced, Cell lysate, supernatant and pellet at 25°C, 0.5mM IPTG for 8hrs respectively, **Lane 6, 7 and 8:** Cell lysate, supernatant and pellet at 25°C, 0.8mM IPTG for 8hrs respectively, **Lane 9, 10, 11 and 12:** Uninduced, Cell lysate, supernatant and pellet at 37°C, 0.5mM IPTG for 8hrs respectively, **Lane 13, 14 and 15:** Cell lysate, supernatant and pellet at 37°C, 0.8mM IPTG for 8hrs respectively.

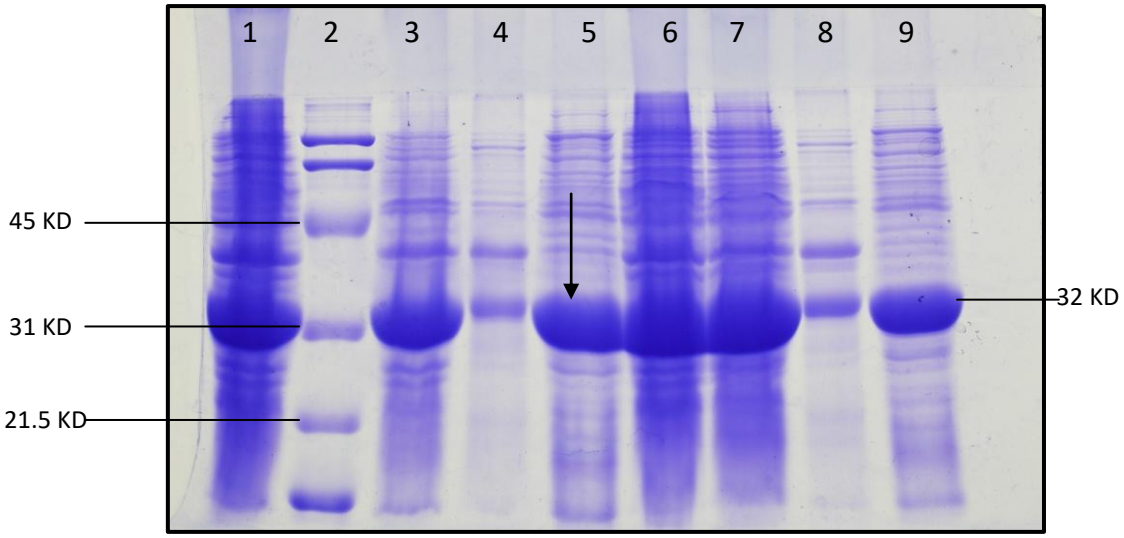

Figure 8C: Expression check for V108M hSCGN mutant induced at 25°C at 0.8mM concentration of IPTG, **Lane 1, 3, 4 and 5:** Uninduced, total cell lysate, pellet and supernatant respectively for first colony, **Lane 2:** Low range marker (Bio-rad), **Lane 6,7,8 and 9:** Uninduced, total cell lysate, pellet and supernatant respectively of second colony.

4.4 Purification of hSCGN using Hydrophobic interaction chromatography followed by Anion exchange chromatography and Gel filtration chromatography

Very less amount of protein was observed to be lost in pellet which might have occurred due to inefficient sonication. The eluate of HIC (Lane 5) contained some impurities, so it was further passed through anion exchange chromatography. Some protein was found to be lost in wash buffer of anion exchange chromatography but the loss was less and thus could be neglected. The elution of protein in anion exchange chromatography started from first fraction and was found to be maximum at fractions 7 and 9 (Fig. 9)

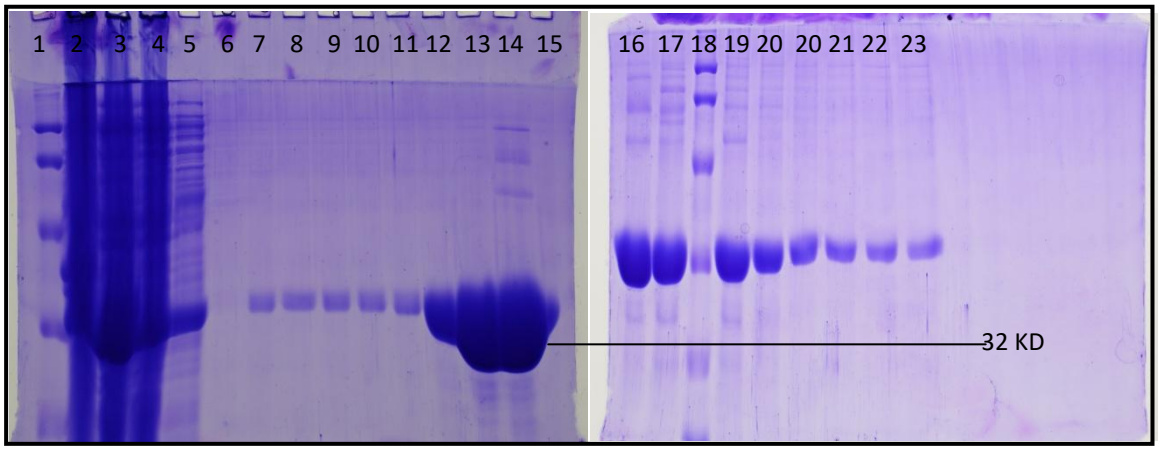

Figure 9: Purification of hSCGN WT by hydrophobic interaction chromatography followed by anion exchange chromatography, Lane **1 and 18**: Low range marker (Bio-rad), Lane **2, 3, 4, 5 and 6:** pellet, supernatant, flowthrough, eluate and wash of hydrophobic interaction chromatography, Lane **7,8 and 9:** Wash **1,2 and 3** of anion exchange chromatography, **Lane 10 to 23**: Alteranative Eluate fraction of anion exchange chromatography 1, 3, 5, 7 to 27 .

The protein eluted out after anion exchange was not pure. So further purification was needed to be done using Gel Filtration chromatography. The fractions were pooled out together for three gel filtration injection. Fractions 1 to 7 were pooled out and concentrated for first GF (Fig. 10A), 8 to 17 for second GF injection (Fig. 10B) and 18 to 27 for third GF injection (Fig. 10C). It as observed in the gel that, the concentration of protein was highest in the second GF fractions.

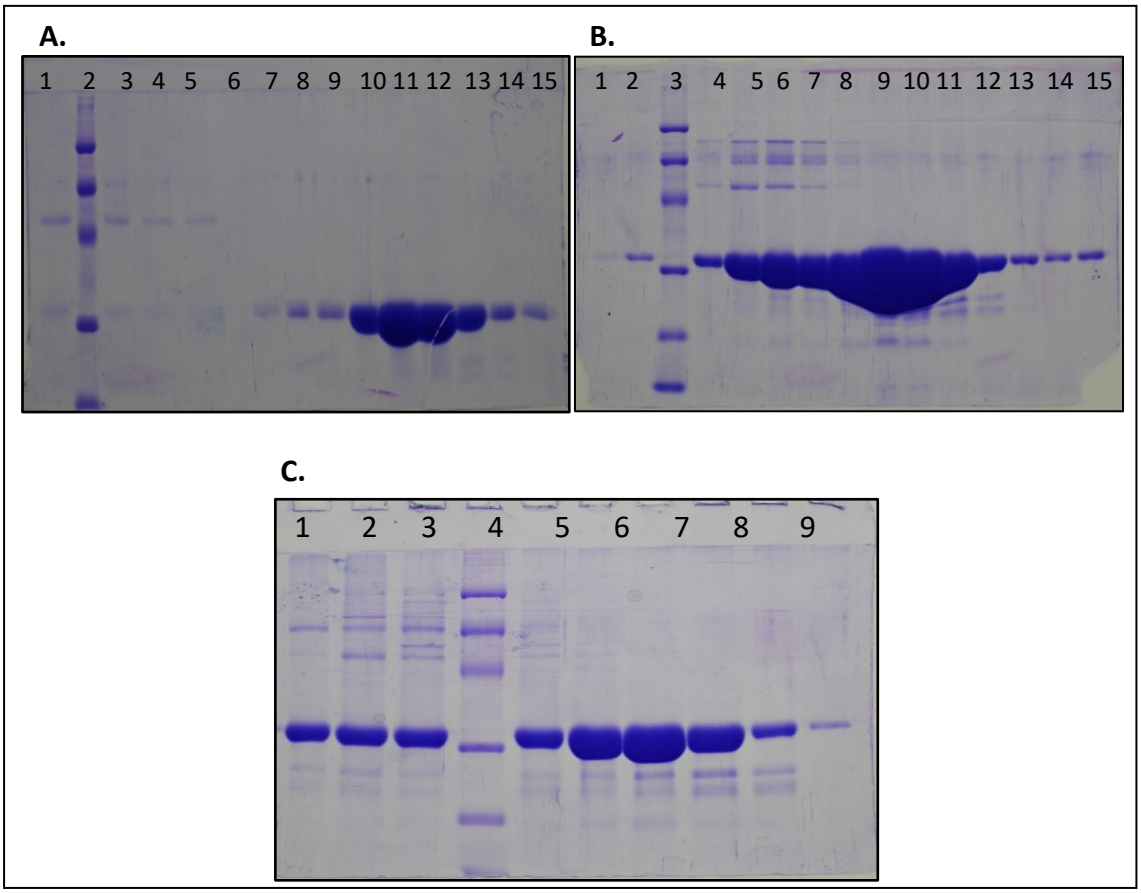

Figure 10: Protein fractions of hSCGN WT after gel filtration (3 injections), **10A, 10B and 10C**: GF 1, 2 and 3 respectively of hSCGN WT.

4.5 Tryptophan fluorescence

4.5.1 Tryptophan fluorescence of freshly prepared protein in oxidizing condition

The binding of protein with calcium is indicated by increase in fluorescence along with blue shift (>2nm). The freshly prepared WT protein, on addition of calcium showed 29% increase in fluorescence along with blue shift of ~4nm (Fig. 11A). A216V and R77H (Fig 11C and 11D) hSCGN showed lesser increase in fluorescence intensity (5.33% and 0.44%) but the blue shift was comparable with WT protein (Table 8). V108M (Fig. 11D) showed distinct character in that there was small decrease in fluorescence intensity on addition of calcium and blue shift was comparatively lower than WT and other mutants (Table 8). The initial decrease in F.I. upon titration with small concentration of calcium (Fig. 11) might have occurred due to structural rearrangement in the presence of low

concentration of calcium. This also indicated that the protein has two types of calcium binding sites.

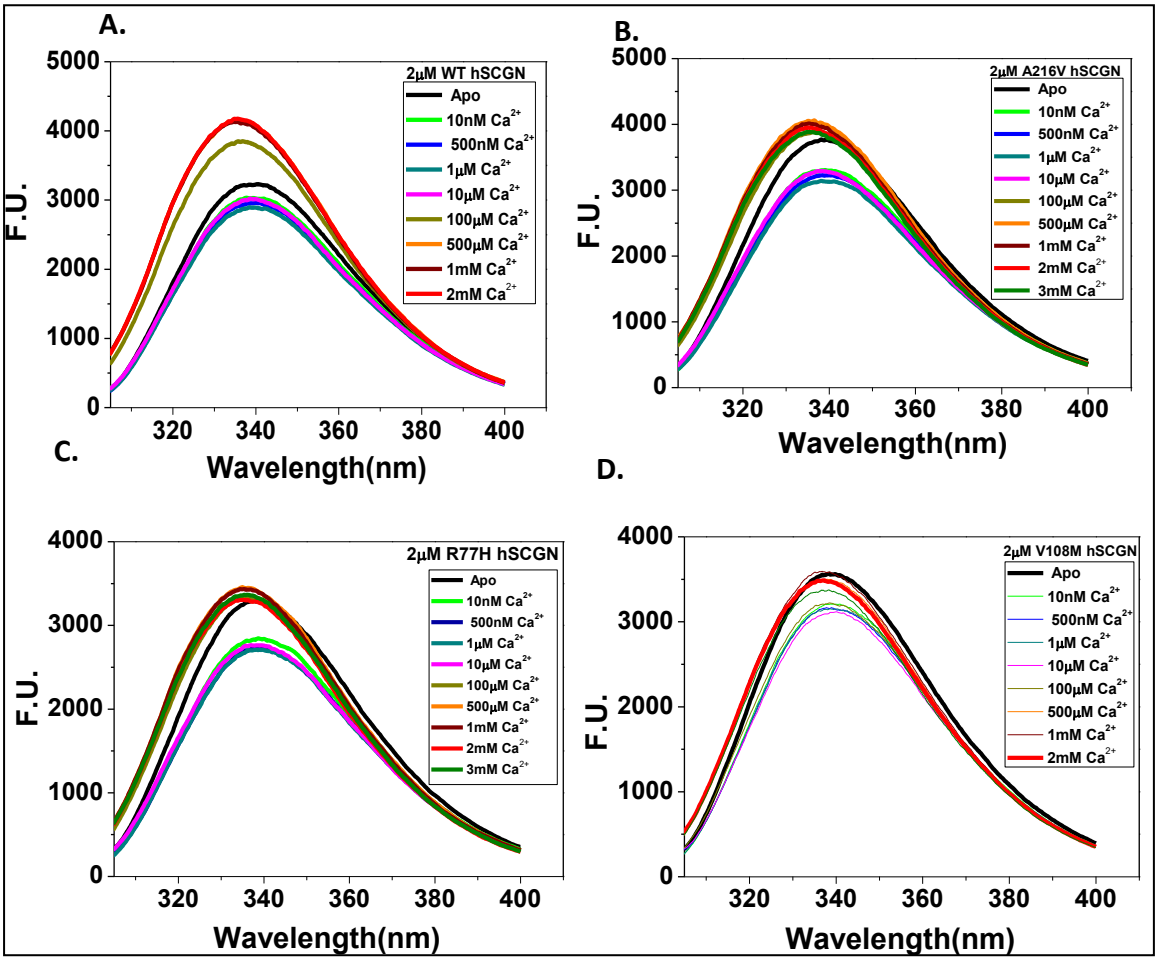

Figure 11: Tryptophan fluorescence spectra of fresh hSCGN WT and mutant proteins on titration with different concentration of Calcium in oxidizing condition denoted by different coloured lines. **Figure 11A:** WT hSCGN, **Figure 11B:** A216V hSCGN , **Figure 11C:** R77H hSCGN and **Figure 11D:** V108M hSCGN

Table 9: Change in λmax and F.I.max of WT and mutants hSCGN (freshly prepared) upon calcium titration in oxidizing condition

Protein	λmax	Fluorescence intensity max	% change in F.I.max	Decrease in λmax
WT hSCGN i) Apo ii) Holo form	 339.1 335.43	 3229.9 4169	29.07	3.67
A216V hSCGN i) Apo form ii) Holo form	 338.8 335.05	 3756.3 3956.8	5.33	3.75
R77H i) Apo form ii) Holo form	 338.3 335.06	 3309.4 3324	0.44	3.24

V108M i) Apo form ii)Holo form	 338.8 337.3	 3572 3499	-2.04	1.5

4.5.2 Tryptophan fluorescence of one week old protein in oxidizing condition

After the storage of protein for one more week, the change in fluorescence intensity of wild type protein was significantly decreased (Fig. 12A) and that of mutants A216V and R77H (Fig. 12B and 12C) remained similar whereas the blue shift was similar to freshly prepared protein (Table 7). In case of V108M, the percentage decrease in F.I. max was raised whereas the blue shift remained similar (Fig. 12D).

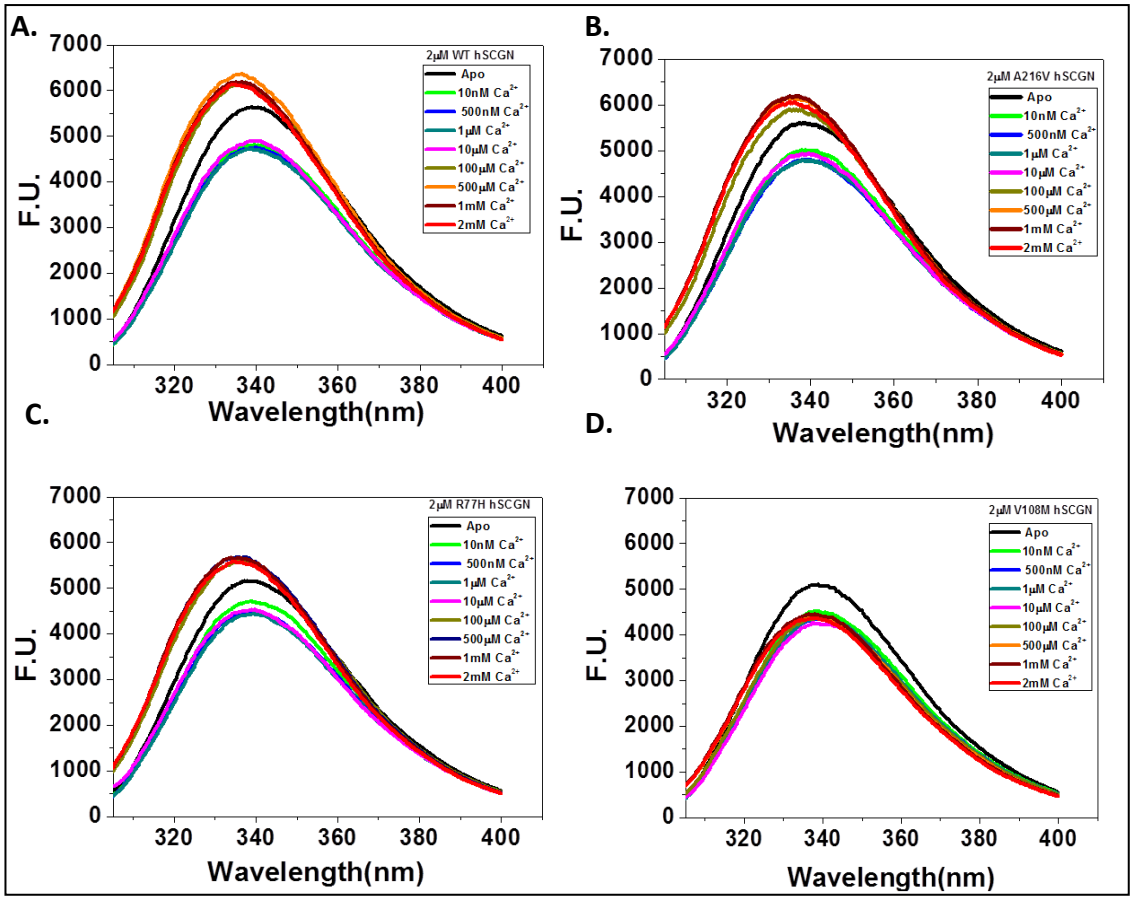

Figure 12: Tryptophan fluorescence spectra of one week old hSCGN WT and mutant proteins on titration with different concentration of Calcium in oxidizing condition represented by different coloured lines. **Figure 12A:** WT hSCGN, **Figure 12B:** A216V hSCGN , **Figure 12C:** R77H hSCGN and **Figure 12D:** V108M hSCGN. **F.U.:** Fluorescence unit

Table 10: Change in λmax and F.I.max of WT and mutants hSCGN (one week old) upon calcium titration in oxidizing condition

Protein	λmax	Fluorescence intensity max	% change in F.I.max	Decrease in λmax
WT hSCGN i) Apo ii) Holo form	 339.1 335.2	 5644 6141.2	8.8	3.9
A216V hSCGN i) Apo form ii) Holo form	 338 335.5	 5598.8 6042.9	7.9	2.5
R77H i) Apo form ii) Holo form	 338.5 335.3	 5165.9 5578.8	8	3.2
V108M i) Apo form ii)Holo form	 338.6 337.5	 5114.9 4389.49	-14.2	1.1

4.5.3 Tryptophan fluorescence of one week old protein in reduced condition

On calcium titration of WT protein in reduced condition, the change in F.I. max was 25.5 %, which was equivalent to the change in freshly prepared protein and the blue shift was 4nm (Fig. 13A). In reducing condition, A216V and R77H (Fig. 13B and 13C) showed increase in F.I. and blue shift equivalent to the wild type protein. In case of WT and the two mutants A216V and R77H, the change in F.I. max was drastically increased from 8.8%, 7.9% and 8% in oxidized state (Table 7) to 25.5%, 33.9% and 25.4% in reduced condition (Table 8) whereas the blue shift was constant. V108M in reduced condition showed 3.56% increase in F.I. max and the blue shift was also increased to 2.8 (Table 8).

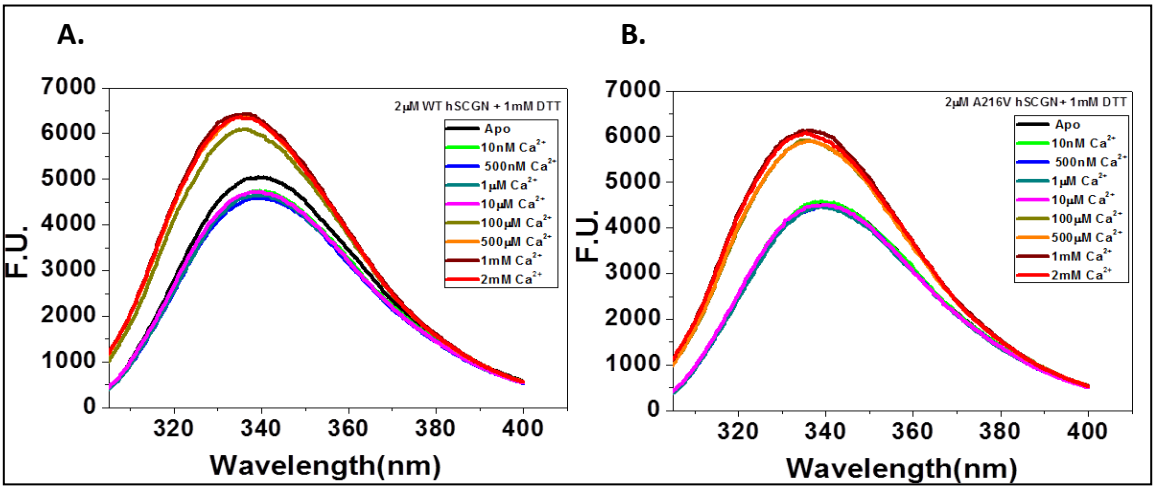

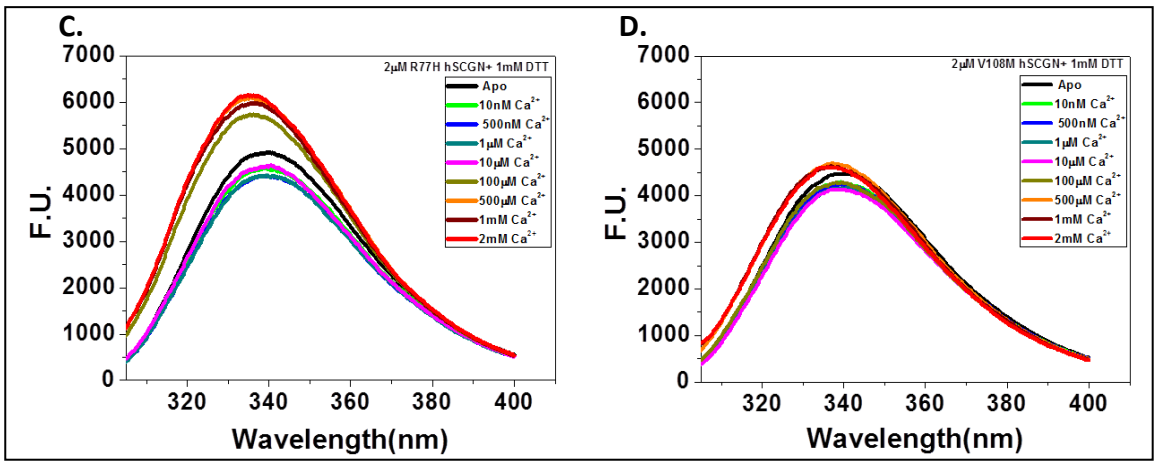

Figure 13: Tryptophan fluorescence spectra of one week old hSCGN WT and mutant proteins on titration with different concentration of Calcium in reducing condition (1mM DTT). **Figure 13A:** WT hSCGN, **Figure13B:** A216V hSCGN , **Figure 13C:** R77H hSCGN and **Figure 13D:** V108M hSCGN. **F.U.:** Fluorescence unit

Table 11: Change in λmax and F.I.max of WT and mutants hSCGN (one week old) upon calcium titration in reduced condition

Protein	λmax	Fluorescence intensity max	% change in F.I. max	Decrease in λmax
WT hSCGN i) Apo ii) Holo form	 339.1 335.1	 5065.7 6357.2	25.5	4
A216V hSCGN i) Apo form ii) Holo form	 339.3 335.3	 4523.2 6058.4	33.9	4
R77H i) Apo form ii) Holo form	 338.9 335.3	 4926.1 6178.3	25.4	3.6
V108M i) Apo form ii)Holo form	 339.5 336.7	 4468.1 4627.4	3.56	2.8

4.6 Measurement of extrinsic fluorescence of protein using ANS as fluorophore

The protein is hydrophobic if its ANS fluorescence spectra is blue shifted and has higher quantum yield (F.I.) than of the ANS fluorophore alone. The λmax of ANS fluorophore alone in Tris-KCl buffer was found to be 538nm. All the proteins taken at different conditions showed blue shift and quantum yield greater than ANS alone suggesting that they have hydrophobic surface in the presence or absence of Calcium. The apo from of hSCGN WT, A216V, R77H and V108M showed blue shift of 63nm, 61nm, 61nm and 65nm respectively (14A,B and C) i.e similar blue shift but different fluorescence intensity indicating that the confirmation of protein is different. V108M was found to be most hydrophobic among all with highest quantum yield (800 units) and blue shift. The addition of calcium caused blue shift (~2nm) along with increase in fluorescence

intensity in all the cases expect V108M mutant that did not show blue shift (14D) but the change in F.I. in presence of calcium in oxidizing condition is different for different protein (Fig. 14). In reducing condition, the hydrophobicity of apo form of hSCGN WT and V108M (black and grey line in Fig.14A and D) was slightly decreased than in oxidizing condition (red shifted spectra) while that of A216V and R77H remained similar(Fig.14B and C). In reducing condition, holo form of hSCGN WT and R77H (Fig14A and C) mutant did not show significant change in surface hydrophobicity compared to their apo form but holo form of V108M showed significant increase in hydrophobicity accompanied by increase in fluorescence intensity and blue shift of about 3nm. A216V mutant however displayed decrease in F.I. at this condition (Fig 14B).

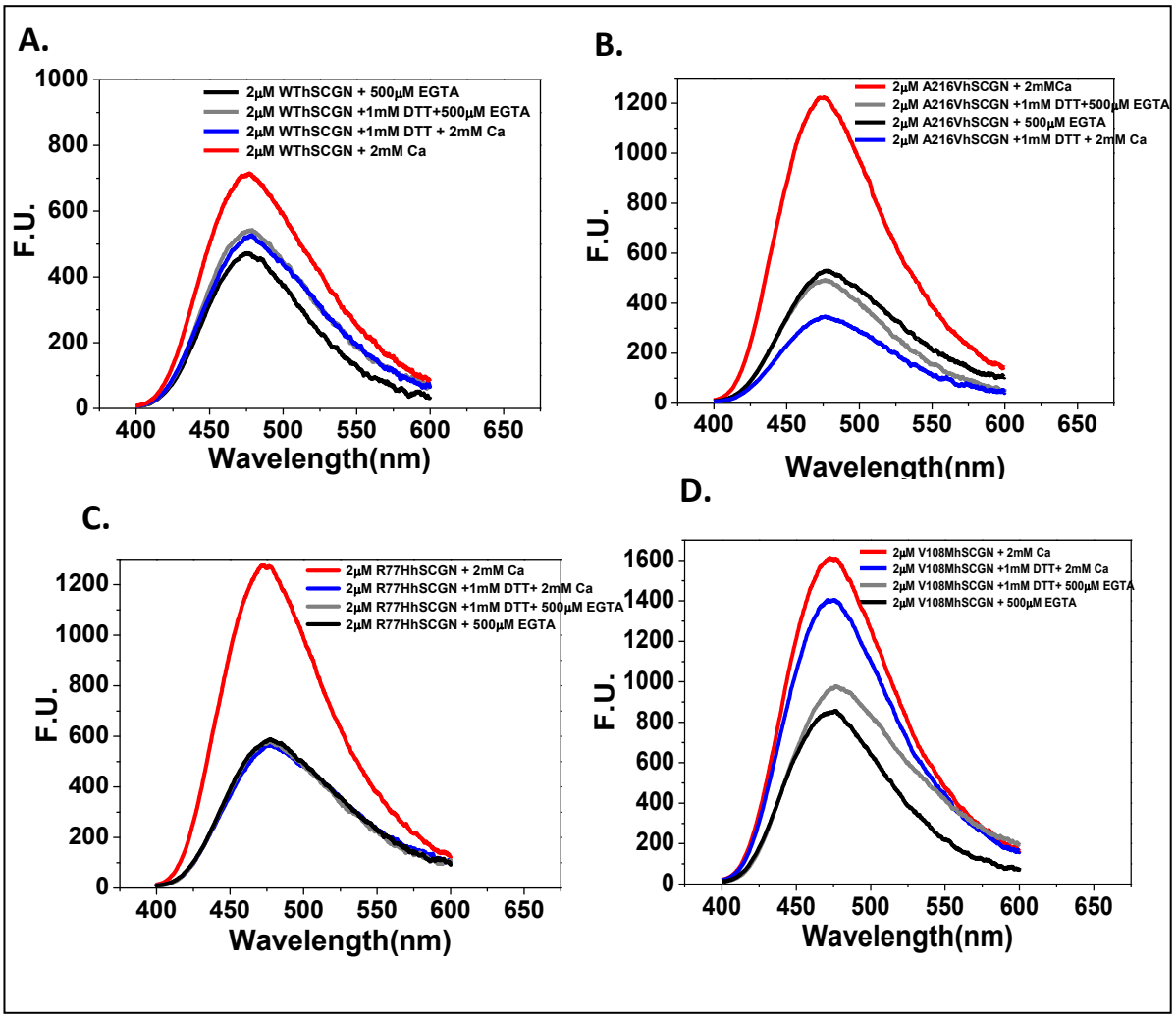

Figure 14: ANS fluorescence spectra of hSCGN WT and mutants at different conditions represented by different coloured lines. **Figure A:** hSCGN WT, **Figure B:** hSCGN A216V, **Figure C:** hSCGN R77H and **Figure D:** hSCGN V108M **F.U.:** Fluorescence unit

4.7 Circular Dichroism (CD)

4.7.1 Tertiary CD (Near UV CD)

4.7.1.1 In oxidizing condition

In the plot (Fig. 15), apo from of protein is represented by black coloured spectra and holo form is represented by red coloured spectra. The tertiary fingerprint of WT and the three mutant proteins were similar in apo form. On titration with calcium in oxidizing condition, the WT hSCGN and the two mutants A216V and R77H, did not show striking change in the tertiary spectra (Fig. 15A, B and C) whereas V108M mutant displayed evident change (increase in positive signal from -9.5 to -6) in tertiary spectra. hSCGN WT showed 1.5 unit increase in ellepticity (Fig. 15A), R77H showed 1 unit increase in ellepticity (Fig. 15C) and A216V showed less than 0.5 unit change in ellepticity upon calcium titratuin in oxidizing condition (Fig. 15B).

A.

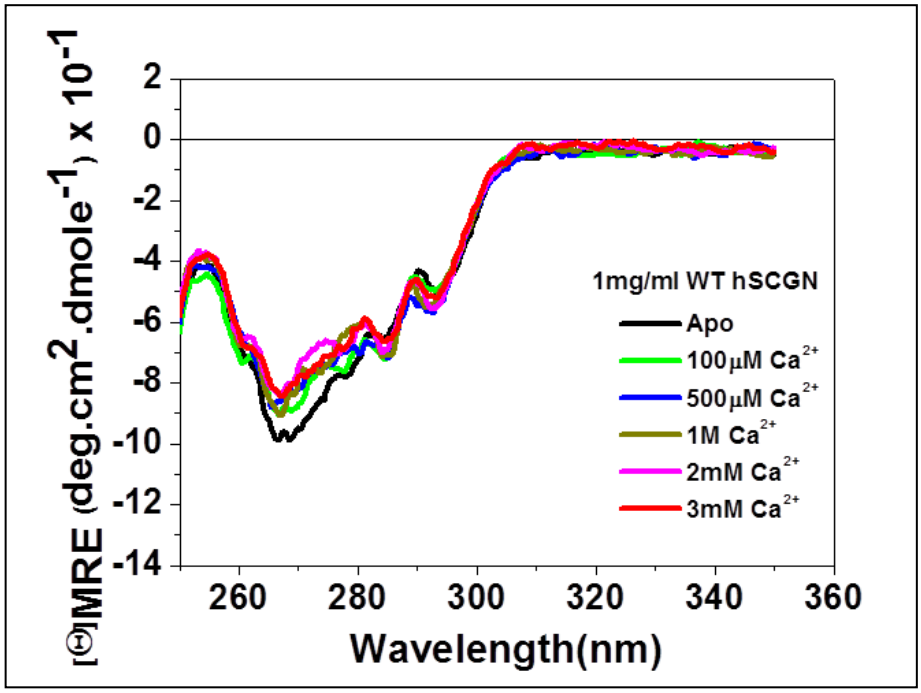

B.

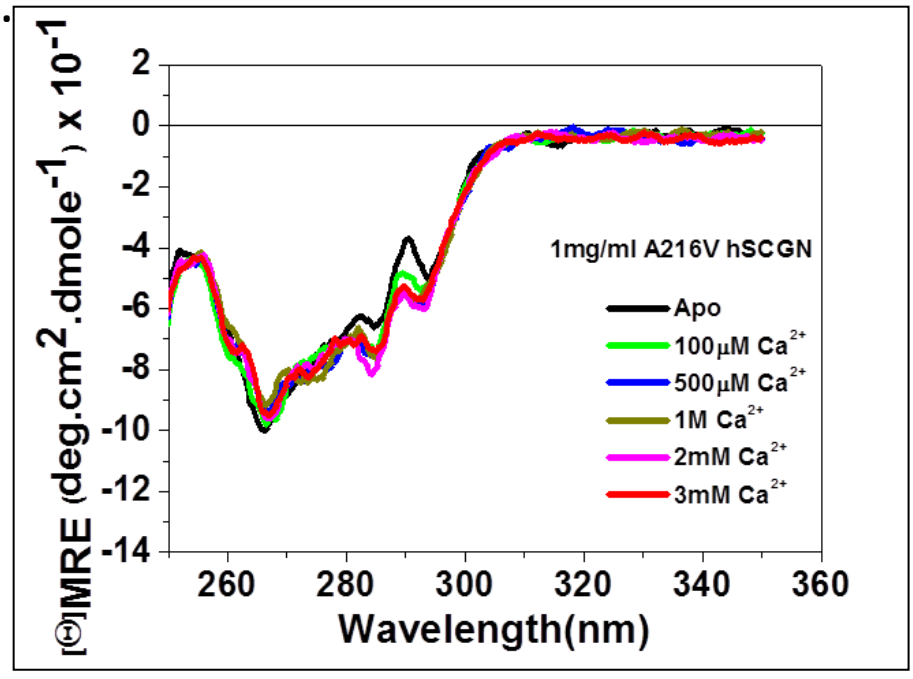

C.

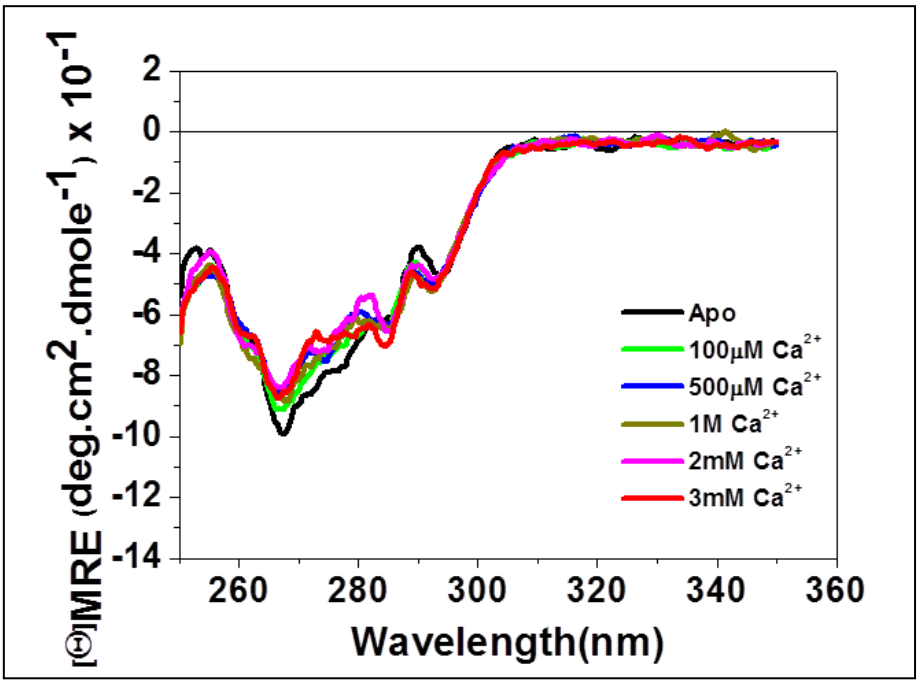

D.

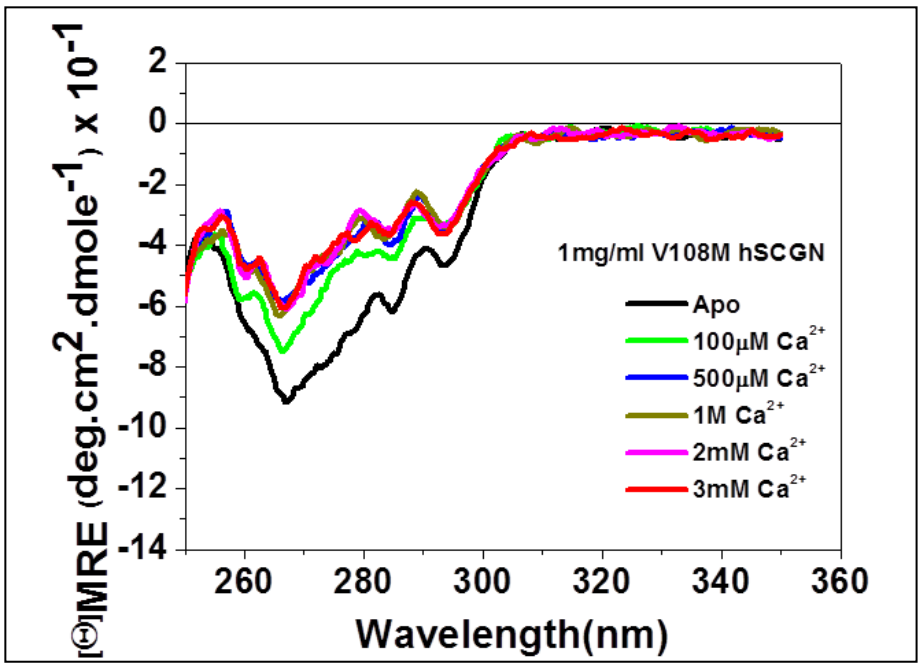

Figure 15: Tertiary CD spectra of hSCGN WT and mutants on titration with different concentration of calcium in oxidizing condition, **Figure 15A:** WT hSCGN, **Figure 15B:** A216V hSCGN , **Figure 15C:** R77H hSCGN and **Figure 15D:** V108M hSCGN

4.7.1.2 In reducing condition

Upon titration with Calcium in reduced condition, the WT hSCGN (Fig. 16A) protein showed prominent change in tertiary signal (5 units increase in positive signal) which was absent in oxidized condition. The two mutants A216V and R77H also displayed

increase in MRE by 2 units (Fig. 16B and 16C). But reverse was the case in V108M mutant which showed lesser change of only 2.5 units in spectra in reduced condition (Fig. 16D). The fingerprint of this mutant protein in apo-reduced form, as a whole was somehow different then the apo-oxidized form. V108M showed lowered response to calcium in reduced form.

A.

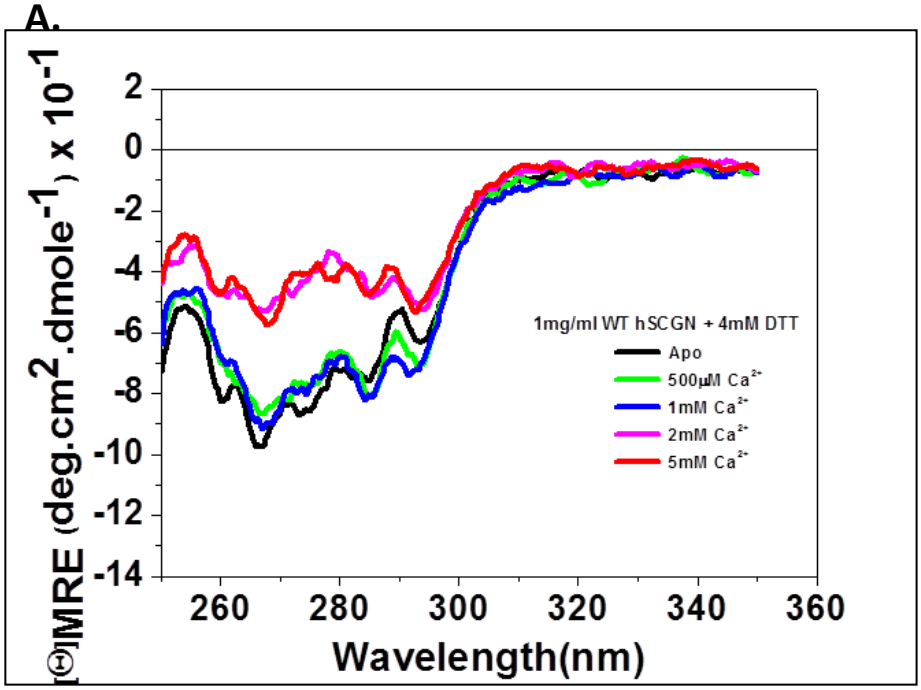

B.

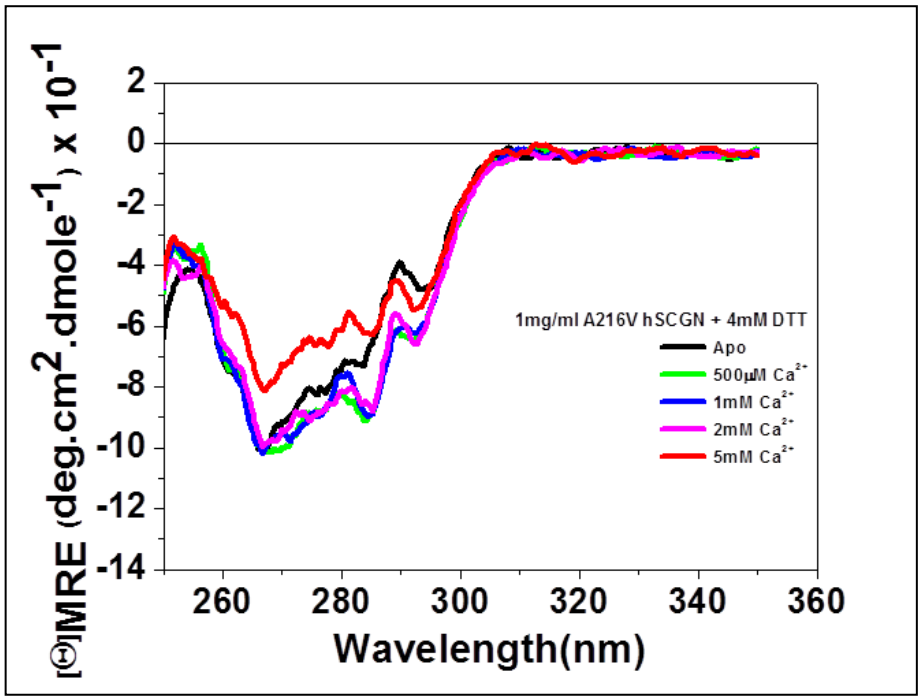

C.

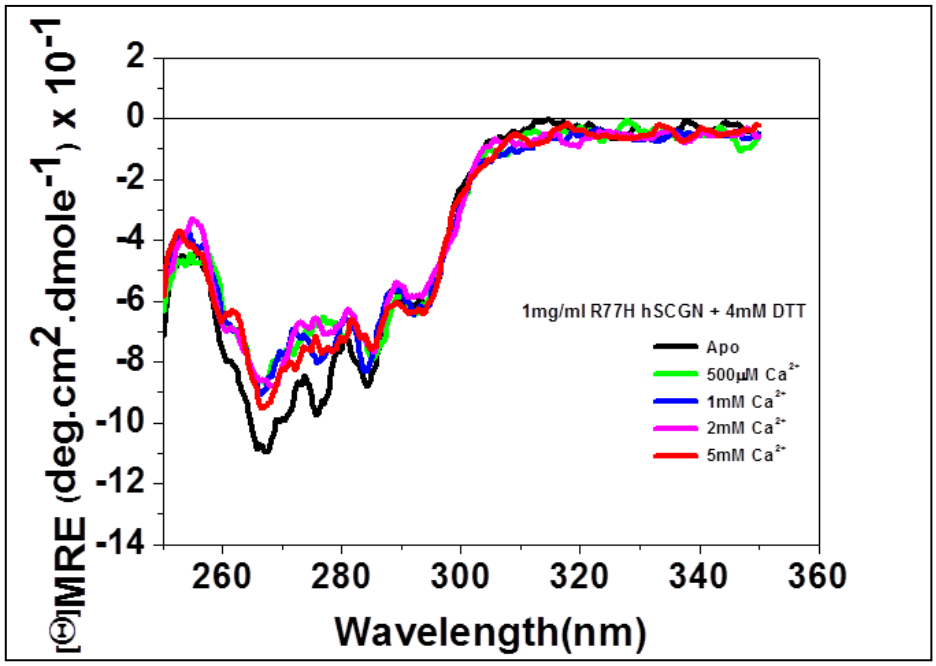

D.

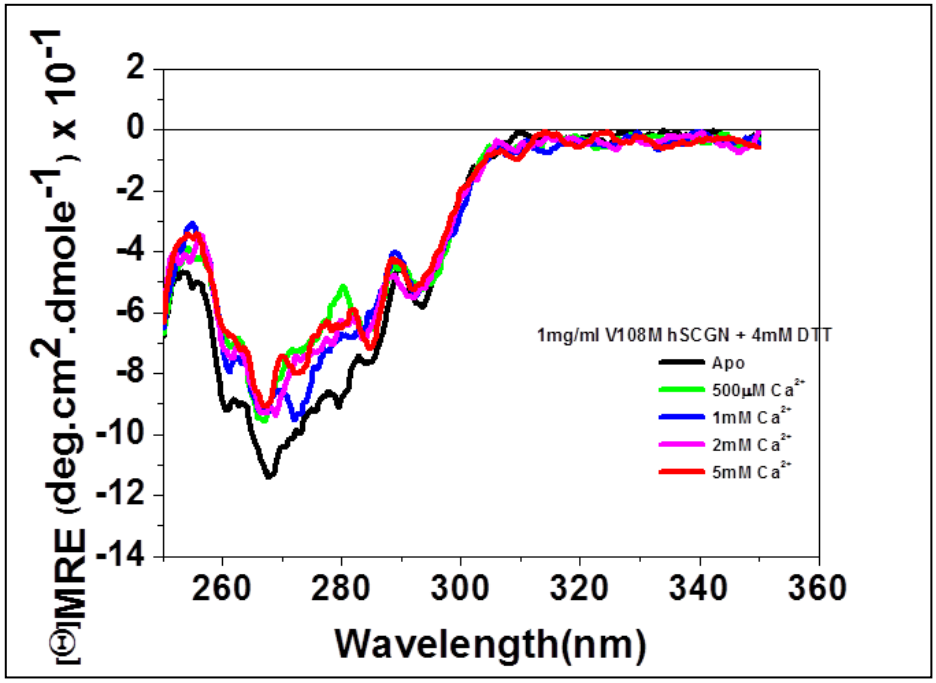

Figure 16: Tertiary CD spectra of hSCGN WT and mutants on titration with different concentration of calcium in reducing condition. **Figure 15A:** WT hSCGN, **Figure 15B:** A216V hSCGN , **Figure 15C:** R77H hSCGN and **Figure 15D:** V108M hSCGN

4.7.2 Secondary CD (Far UV CD)

The secondary CD of all the proteins showed α-helical structure signal with two negative bands at 208nm and 222m (Fig. 17). In all the proteins, the secondary CD spectra remained same at all conditions i.e oxidized apo and holo form and reduced apo and

holo form, with some minor changes. This signifies that all the protein remains majorly as α-helix at all the conditions.

A.

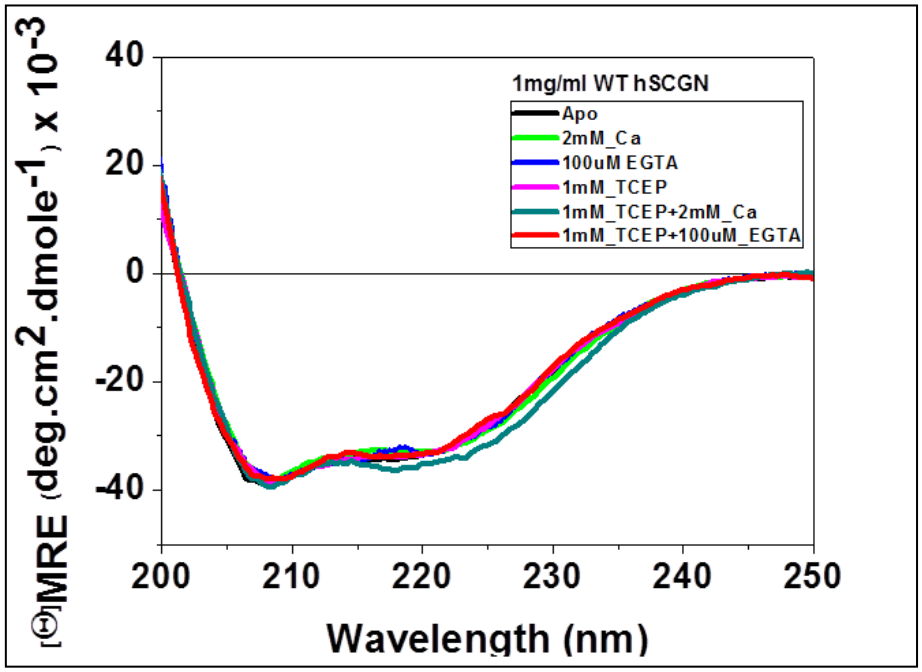

B.

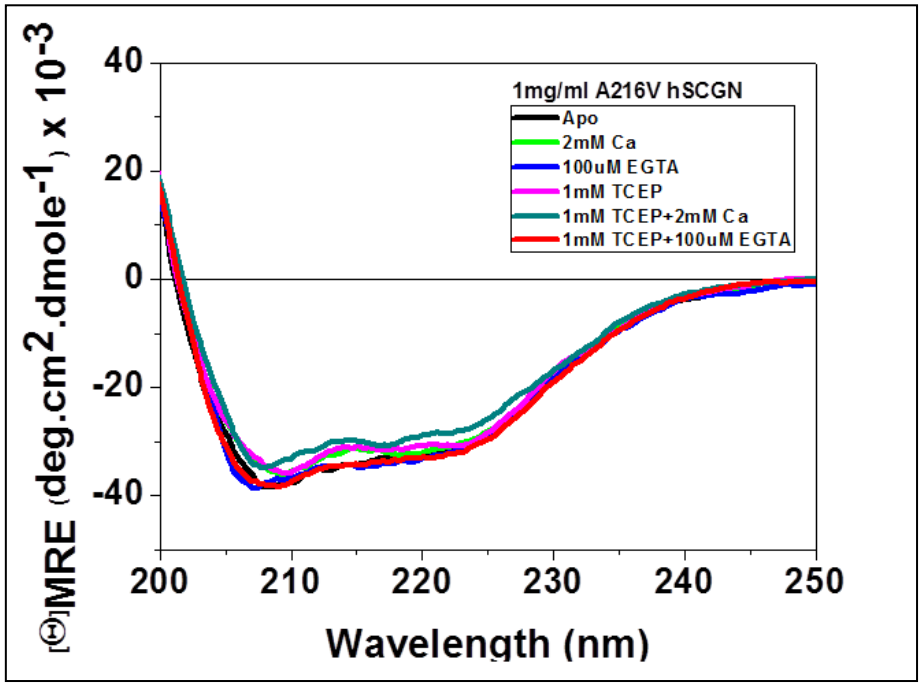

C.

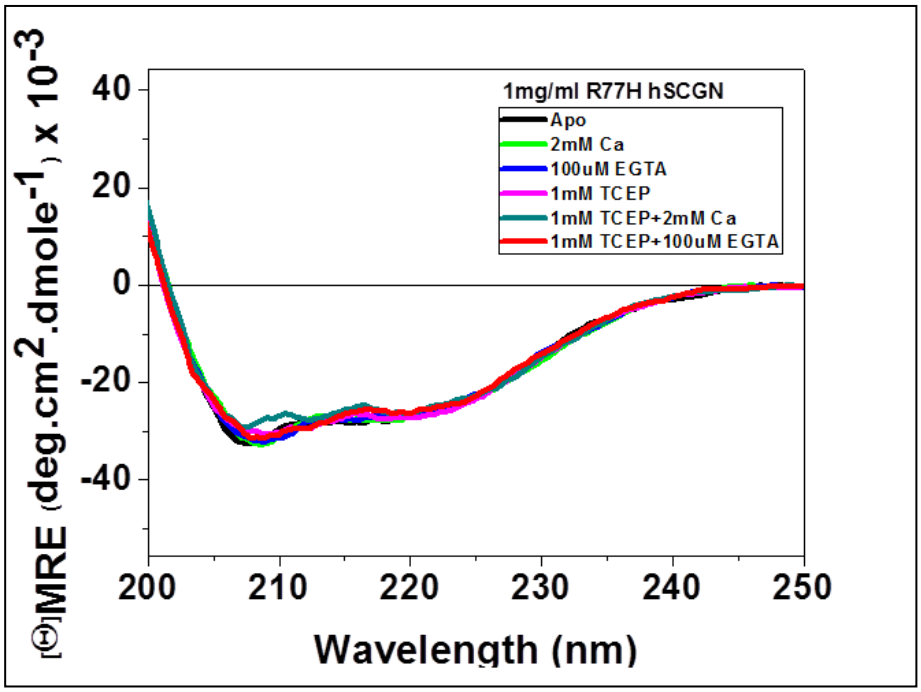

D.

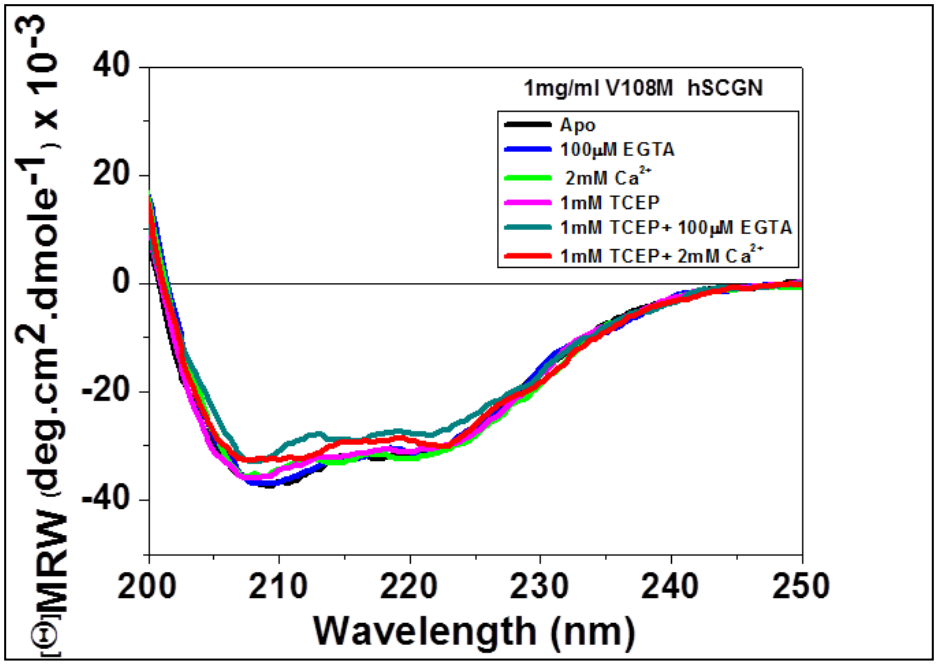

Figure 17: Secondary CD spectra of hSCGN WT and mutant at different conditions denoted by different coloured lines. **Figure 17A:** WT hSCGN, **Figure 17B:** A216V hSCGN , **Figure 17C:** R77H hSCGN and **Figure 17D:** V108M hSCGN

4.8 Analytical Gel Filtration Chromatography

The apo form of WT hSCGN showed higher monomeric population. The monomeric fraction elute at 33.5 minutes and dimeric fraction at 30minutes. The monomeric and dimeric fractions were present in the proportion of 60% and 40% respectively (in Fig.18A as black line). In all the mutants, A216V, R77H and V108M, the dimeric population was

highly dominant though small quantity of monomeric population was also observed (in Fig.18A as red, blue and magenta coloured line). Upon saturation with Calcium, oxidized holo form of WT hscgn showed equal monomeric and dimeric population which gives the clue that calcium induces dimerization in WT protein respectively (in Fig.18B as black line). In oxidized holo state, all the mutants displayed increased population of dimers with simultaneous decrease in monomeric fractions observed (in Fig. 18B). In presence of DTT, the disulphide bonds were broken reducing all the dimeric population to their monomer with elution occurring at around 33.5 minutes (Fig. 18C). In presence of calcium in reduced state, the proteins were eluted much later i.e. around 45 to 50 minutes (18D). This indicates that the proteins had become more compact upon Calcium binding due to which the size of the protein was reduced. The response of all proteins towards calcium is more intense in reduced form than in oxidized form. When we see the plot of apo form of all the proteins both in oxidized and reduced state, the peaks were coinciding with each other but in holo form, the peaks were not found to coincide with each other. This gives us the idea that the hydrodynamic radii of the proteins were altered in when the proteins bound calcium.

A.

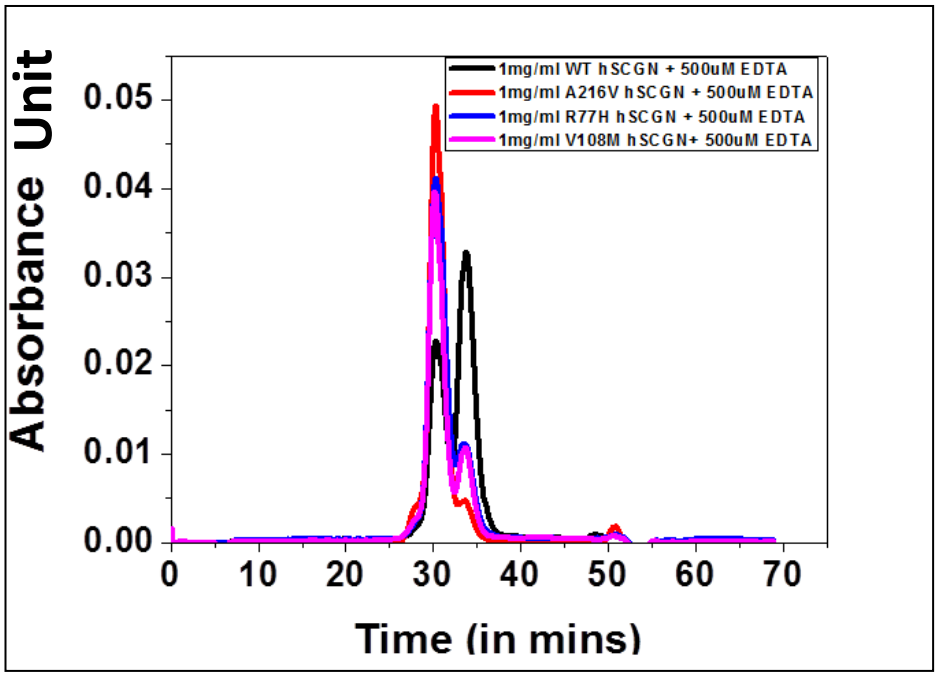

Figure 18A: Analytical gel filtration of hSCGN WT, A216V, R77H and V108M in the presence of 500µM EDTA (apo form) denoted by different coloured chromatogram

B.

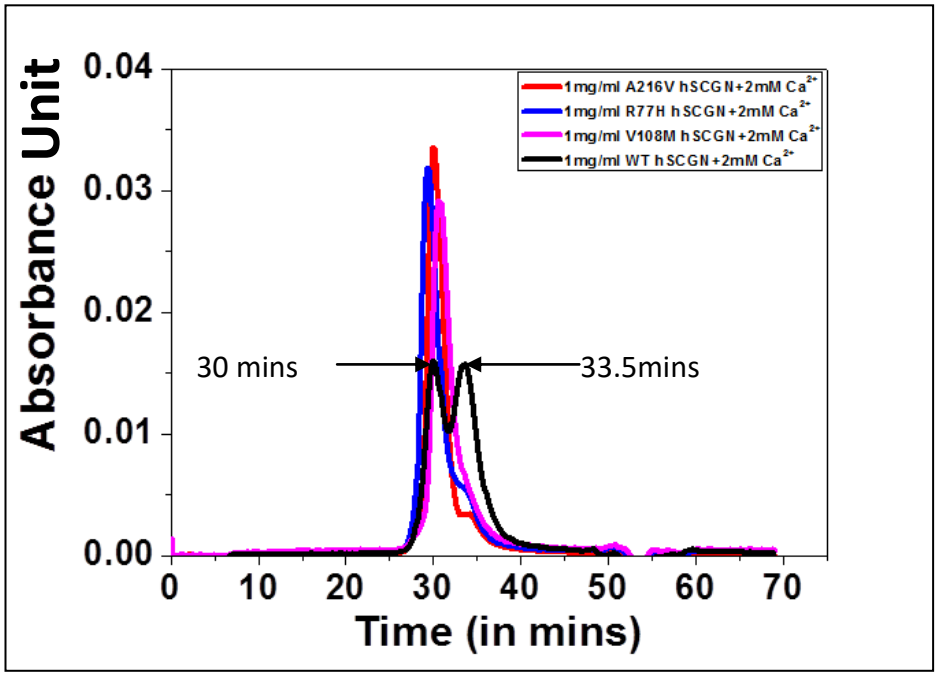

Figure 18B: Analytical gel filtration of hSCGN WT, A216V, R77H and V108M in the presence of 2mM Ca^{2+} (holo form) denoted by different coloured lines

C.

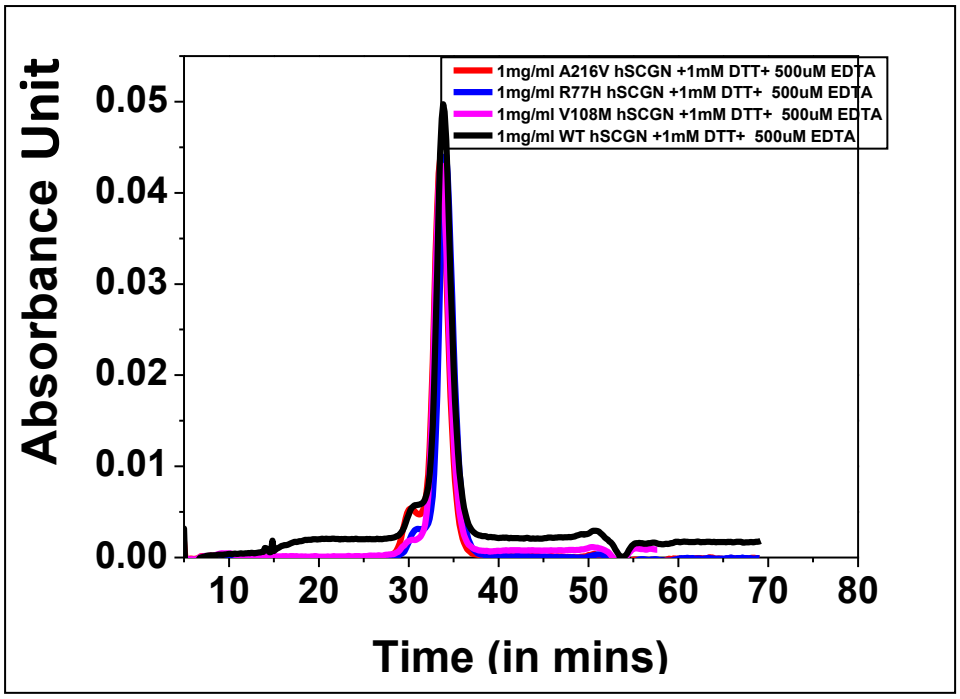

Figure 18C: Analytical gel filtration of hSCGN WT, A216V, R77H and V108M in the presence of 1mM DTT and 500µM EDTA (reduced apo form) denoted by different coloured chromatogram

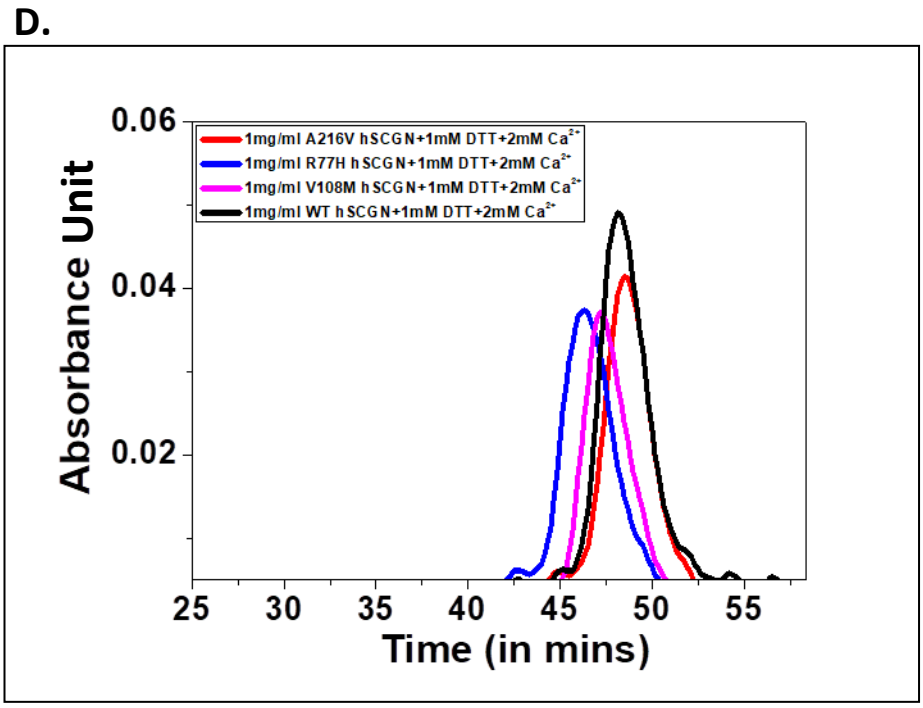

Figure 18D: Analytical gel filtration of hSCGN WT, A216V, R77H and V108M in the presence of 1mM DTT and 2mM Ca^{2+} (reduced holo form) denoted by different coloured chromatogram

4.9 Isothermal Titration Calorimetry (ITC)

The binding of Calcium with the protein was represented by heat gain or loss in the thermogram. The gain of heat indicated that the reaction mechanism was endothermic and was represented by positive enthalpy change in the thermogram whereas the release of heat indicating the reaction mechanism was exothermic was represented by negative heat change in the thermogram. As the protein molecules bound Calcium, the heat change was larger in the beginning because large number of unbound protein molecules would be present in the beginning but as the injection of ligand continued, the heat change decreased and finally became saturated. Saturation point was reached when there was no heat change upon addition of ligand (Fig. 19 and 20).

The data best fitted to sequential binding in four sites. In oxidizing condition, the WT hSCGN and R77H mutants (Fig. 19 A and C) show nearly equal binding constant for calcium (two binding sites with Ka in the range of $10^5 M^{-1}$and two in the range of $10^4 M^{-1}$). In A216V mutant one site has binding constant in the range of $10^5 M^{-1}$ and remaining sites in $10^4 M^{-1}$ range (Fig. 19 B). V108M mutant has least affinity for binding calcium with ka in the range of $10^4 M^{-1}$ and 10^3 M^{-1} for two sites each (Fig. 19D). Calcium binding of hSCGN WT and V108M protein showed endothermic reaction mechanism whereas A216V and R77H protein showed exothermic profile.

In reducing condition however the overall affinity of binding of proteins seems to be reduced. WT hSCGN showed highest binding for calcium than other mutants. One site showed higher affinity (Ka 10^5) than the other (10^4) (Fig.20A). In A216V, two sites showed Ka of 10^4M^{-1} and the other two 10^3M^{-1} (Fig 20B) whereas in R77H mutant, all the sites have Ka around 10^4 and one with 10^3(Fig 20C). V108M mutant has similar Ka in both oxidized and reduced condition (Ka of two sites 10^4 and other two 10^3). In reducing condition, hSCGN WT, A216V and R77H protein showed exothermic profile while V108M showed endothermic profile (Fig. 20 A, B, C and D).

4.9.1 In oxidizing condition

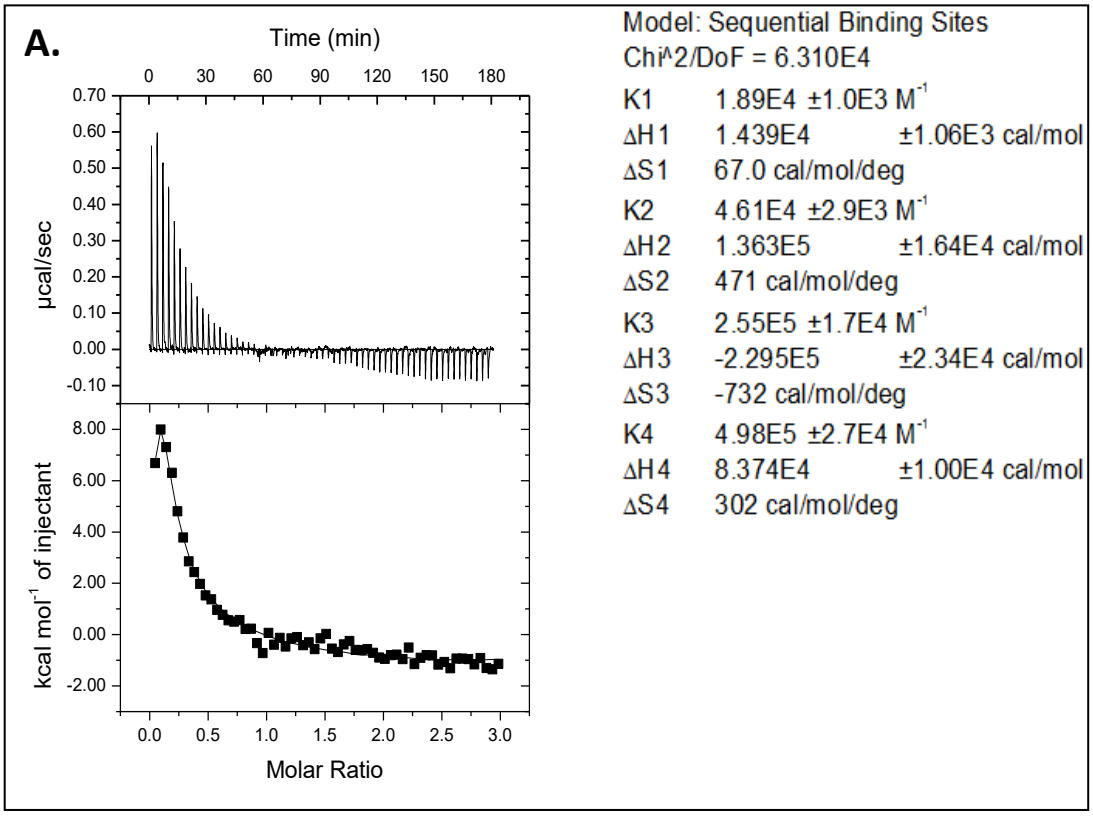

Figure 19A: Titration 75µM hSCGN WT with 5mM Calcium

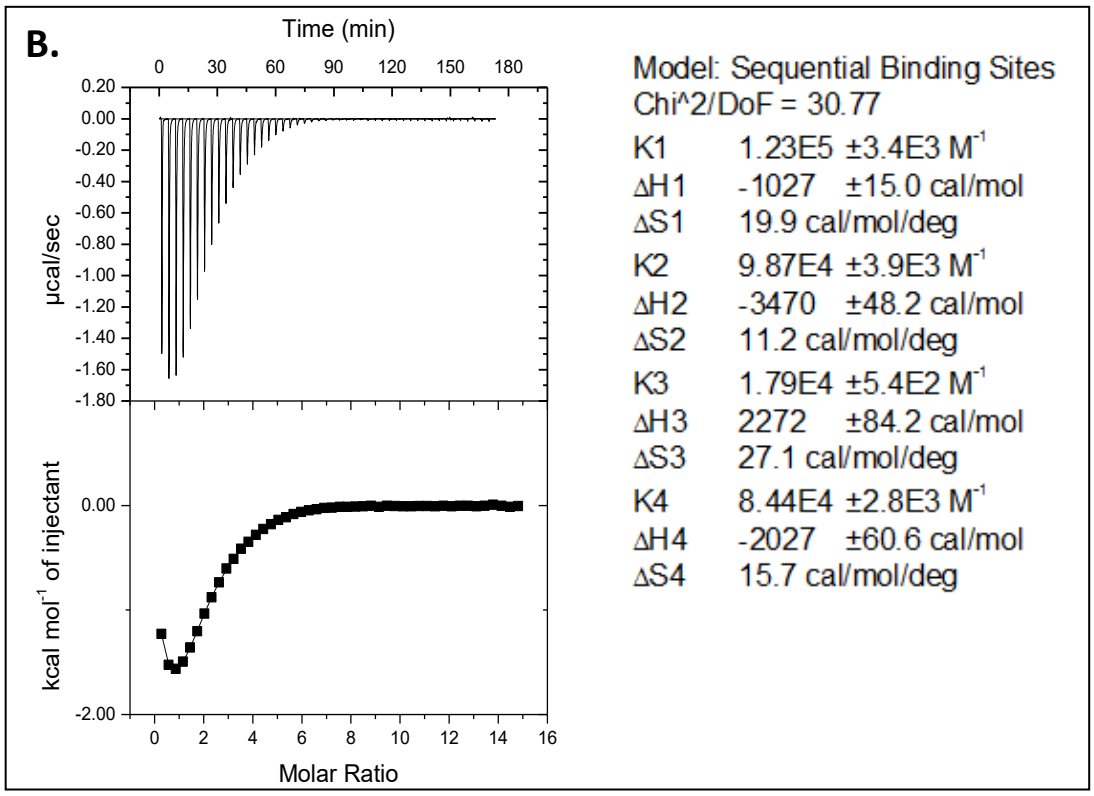

Figure 19B: Titration 75µM hSCGN A216V with 5mM Calcium

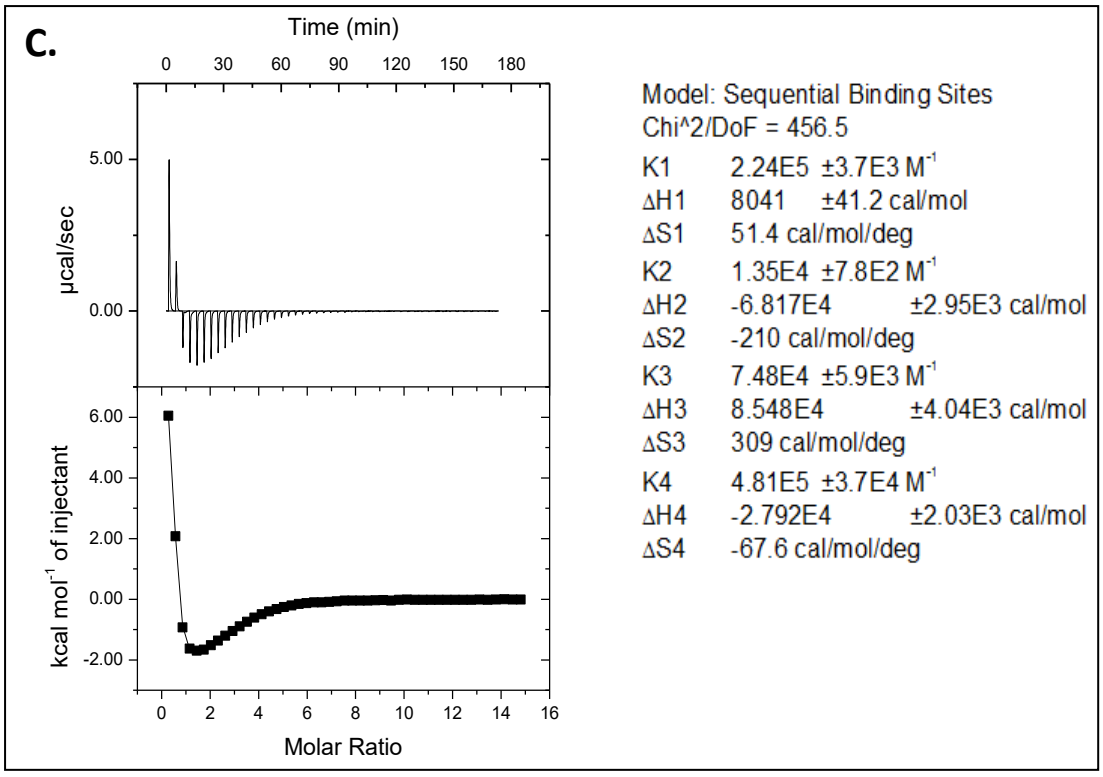

Figure 19C: Titration 75µM hSCGN R77H with 5mM Calcium

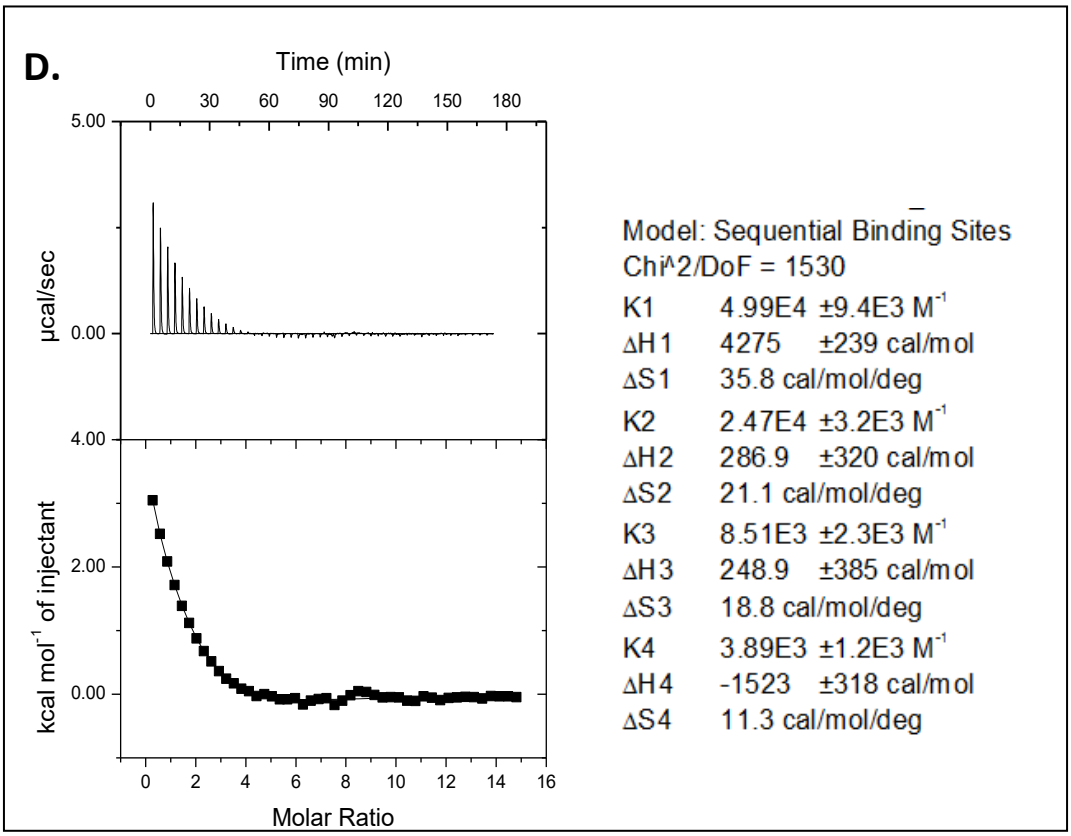

Figure 19D: Titration 75µM V108M hSCGN with 5mM Calcium

4.9.2 In reducing condition

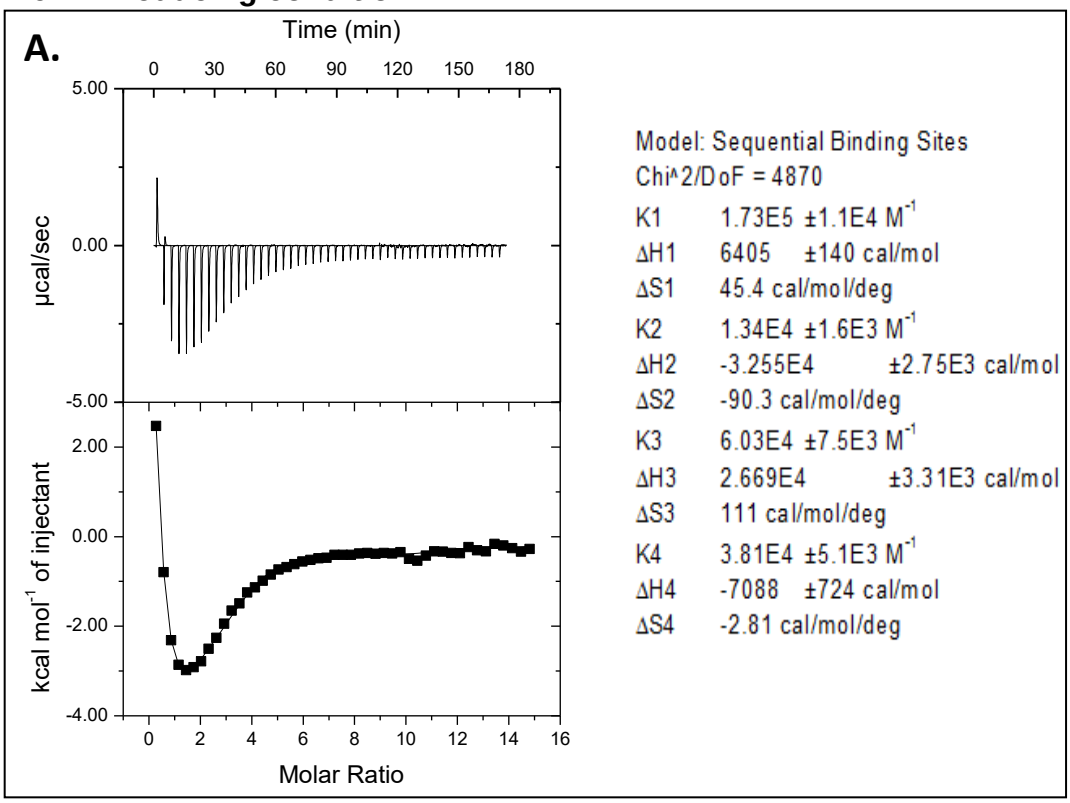

Figure 20A: Titration of 75µM hSCGN WT with 5mM Calcium in the presence of 1mM TCEP

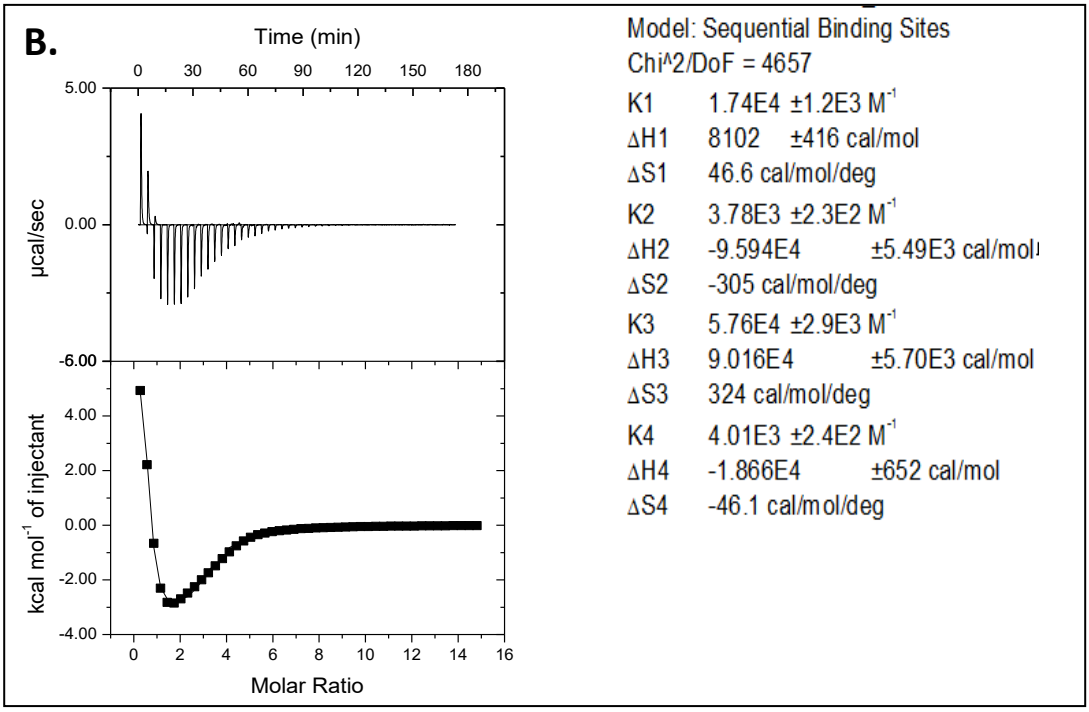

Figure 20B: Titration of 75µM hSCGN A216V with 5mM Calcium in the presence of 1mM TCEP

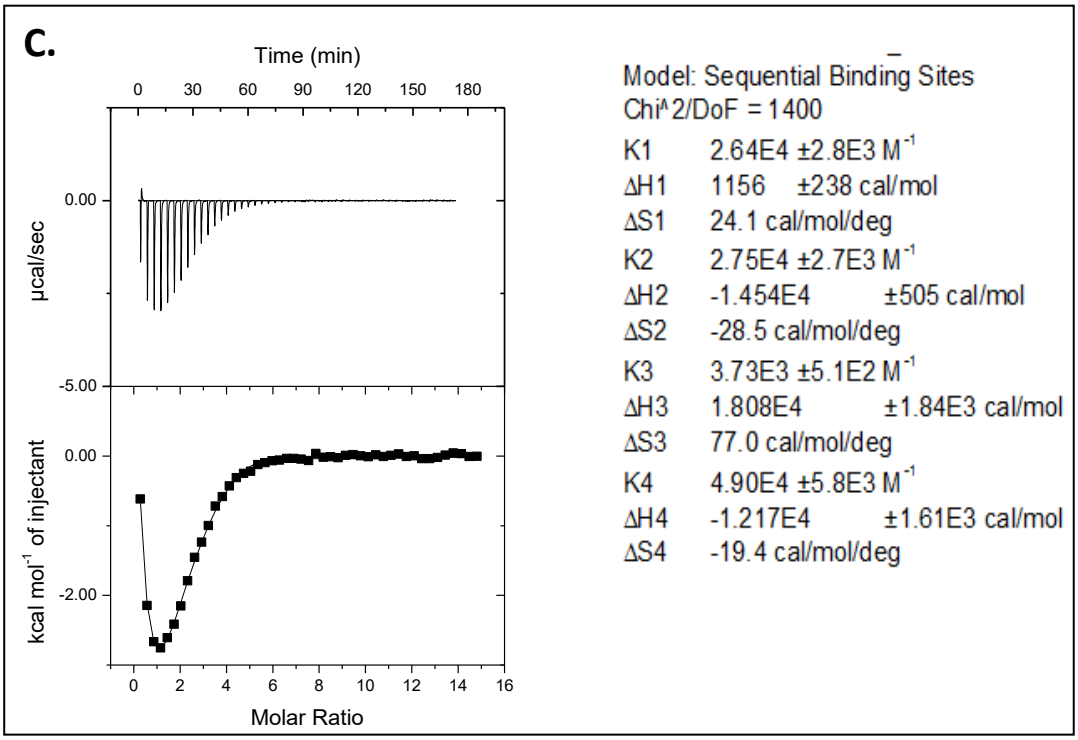

Figure 20C: Titration of 75µM hSCGN R77H with 5mM Calcium in the presence of 1mM TCEP

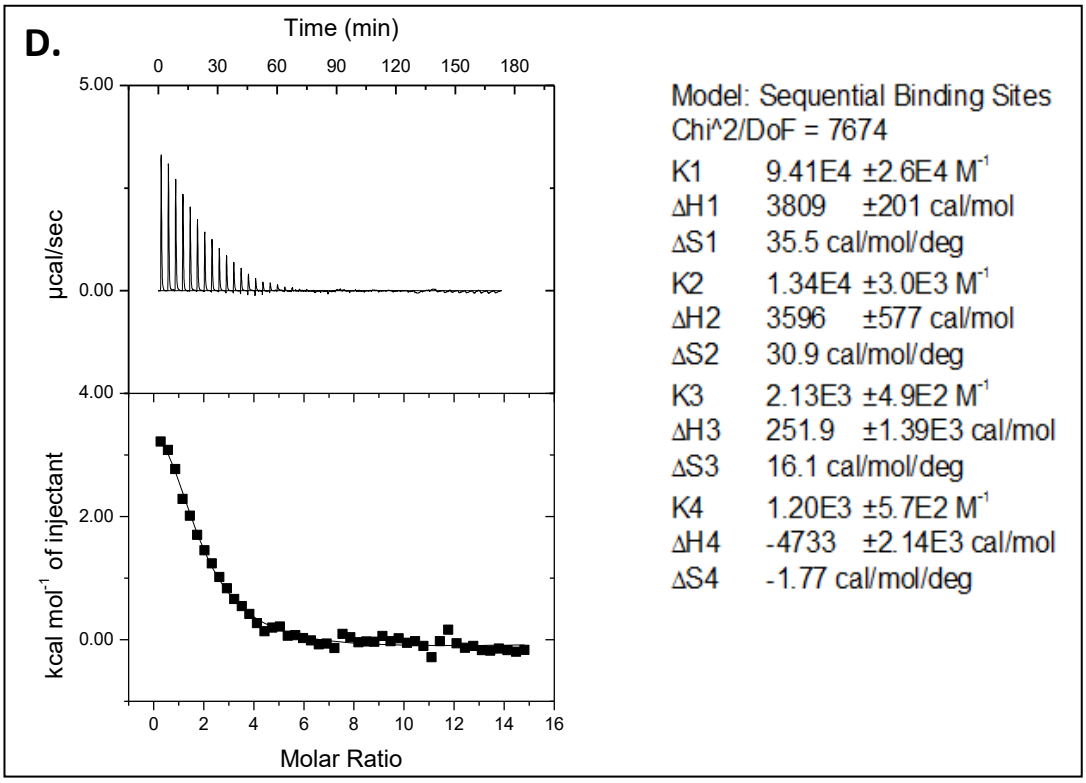

Figure 20D: Titration of 75µM hSCGN V108M with 5mM Calcium in the presence of 1mM TCEP

In both the cases the WT and two mutants R77H and V108M seems to show cooperative binding with calcium which is indicated by small heat change followed by greater heat change in the beginning and then the heat change seemed to be decreasing due to saturation of binding sites (Fig. 19 and 20). But in case of V108M, the cooperative binding of calcium seems to be lost as the binding isotherm shows large heat change in the beginning and small heat change later.

4.10 Interaction with insulin

4.10.1 Tryprophan fluorescence

i) Titration of apo form of protein with insulin

All the proteins including the WT and three mutants in apo form showed decrease in fluorescence intensity along with small blue shift upon titration with insulin showed 11% decrease, A216V showed 16%, R77H showed 31% and V108M showed 32% decrease in F.I. indicating that all the proteins bind insulin (Fig. 21A, B, C and D). R77H and V108M show greater change in F.I. upon insulin titration which means greater change in conformation of these proteins in apo form.

A.

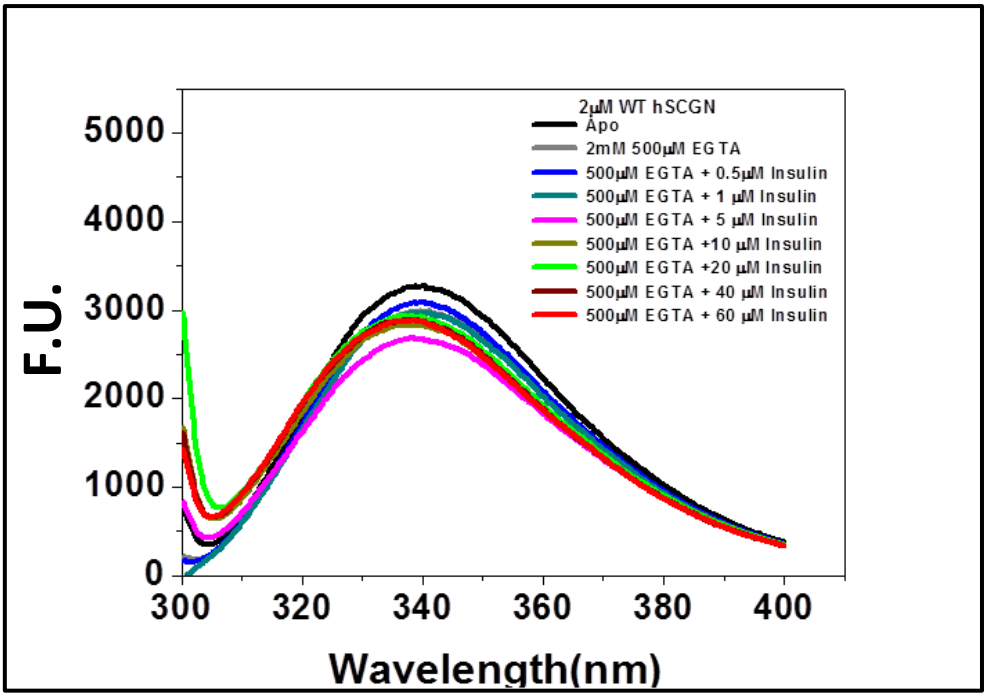
2μM WT hSCGN
Apo
2mM 500μM EGTA
500μM EGTA + 0.5μM Insulin
500μM EGTA + 1 μM Insulin
500μM EGTA + 5 μM Insulin
500μM EGTA +10 μM Insulin
500μM EGTA +20 μM Insulin
500μM EGTA + 40 μM Insulin
500μM EGTA + 60 μM Insulin
F.U.
5000
4000
3000
2000
1000
0
300
320
340
360
380
400
Wavelength(nm)

B.

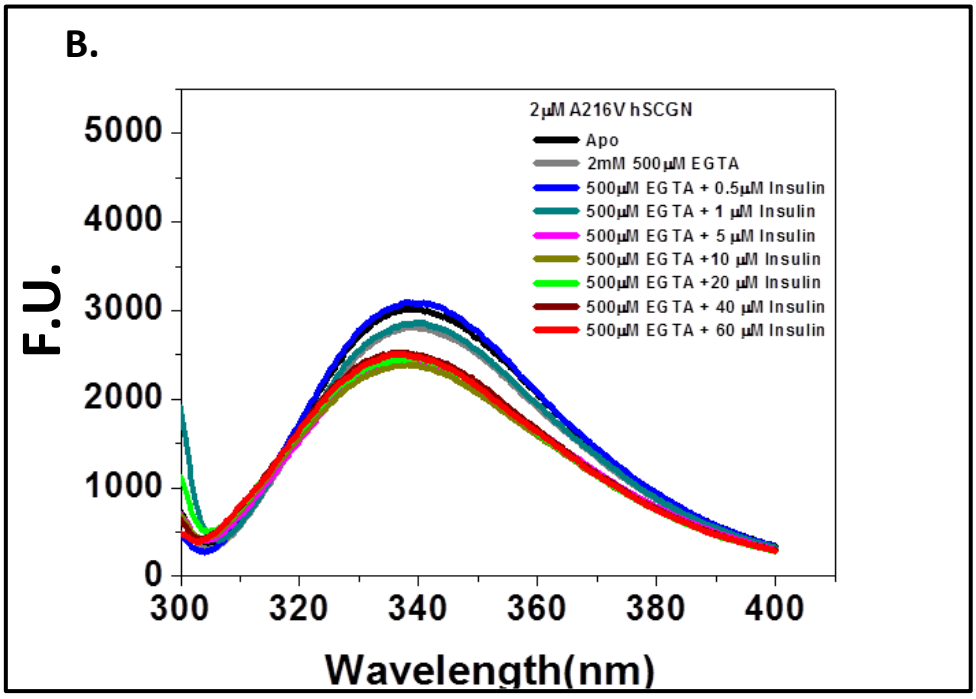
2μM A216V hSCGN
Apo
2mM 500μM EGTA
500μM EGTA + 0.5μM Insulin
500μM EGTA + 1 μM Insulin
500μM EGTA + 5 μM Insulin
500μM EGTA +10 μM Insulin
500μM EGTA +20 μM Insulin
500μM EGTA + 40 μM Insulin
500μM EGTA + 60 μM Insulin
F.U.
5000
4000
3000
2000
1000
0
300
320
340
360
380
400
Wavelength(nm)

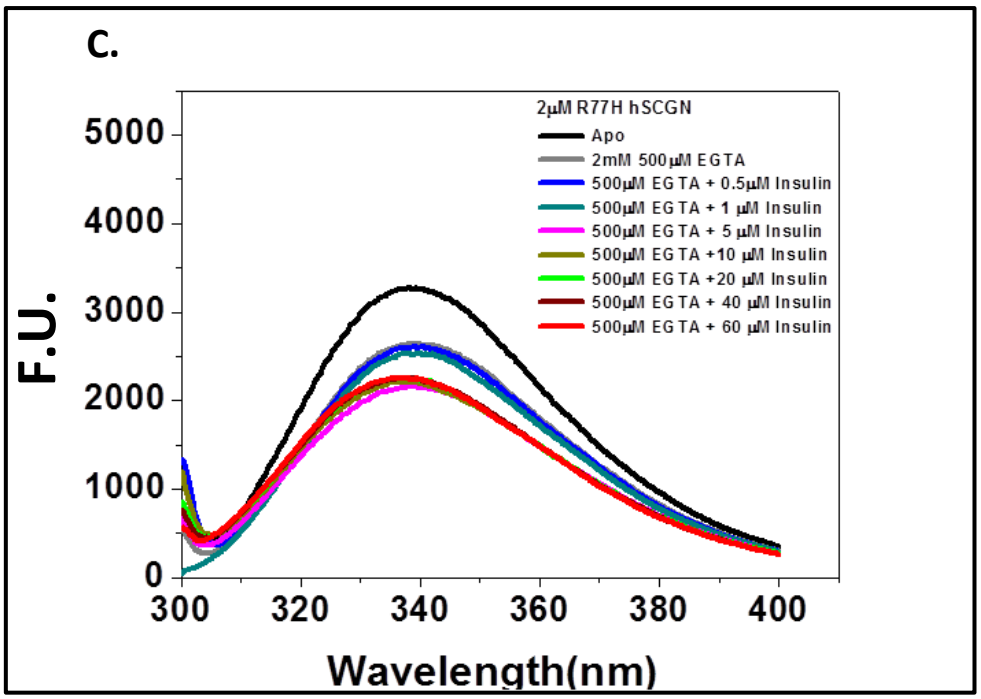

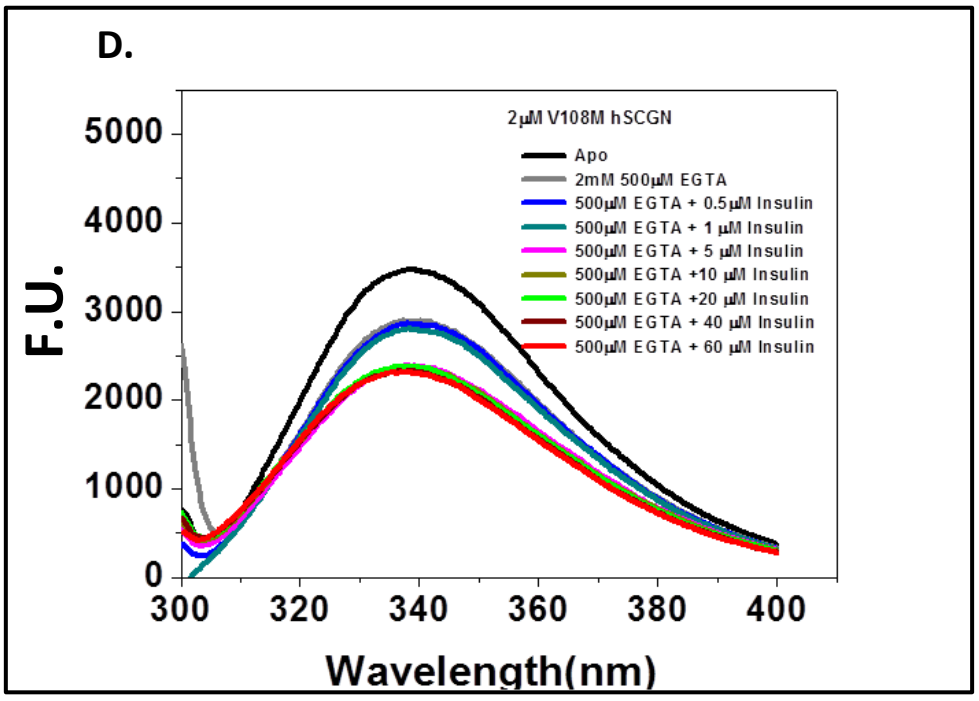

Figure 21: Titration of apo form of protein with different concentration of insulin denoted by different coloured lines. **Figure 21A:** WT hSCGN, **Figure 21B:** A216V hSCGN , **Figure 21C:** R77H hSCGN and **Figure 21D:** V108M hSCGN. **F.U.:** Fluorescence unit

.

ii) Titration of holo form of protein with insulin

The holo form of protein showed more prominent reduction in F.I. than apo form. Holo form of WT hSCGN, A216V and R77H showed 50% decrease in F.I. along with 3nm red shift (Fig. 22A, B and C) whereas V108M shows only 35% decrease with 1nm red shift (Fig. 22D). At low concentration of insulin (till 10µM), the blue shift in spectra due to Calcium binding was retained whereas at higher concentration of insulin, the blue shift in the spectra was reverted back to the state as the apo form of protein due to insulin binding (Fig 22).

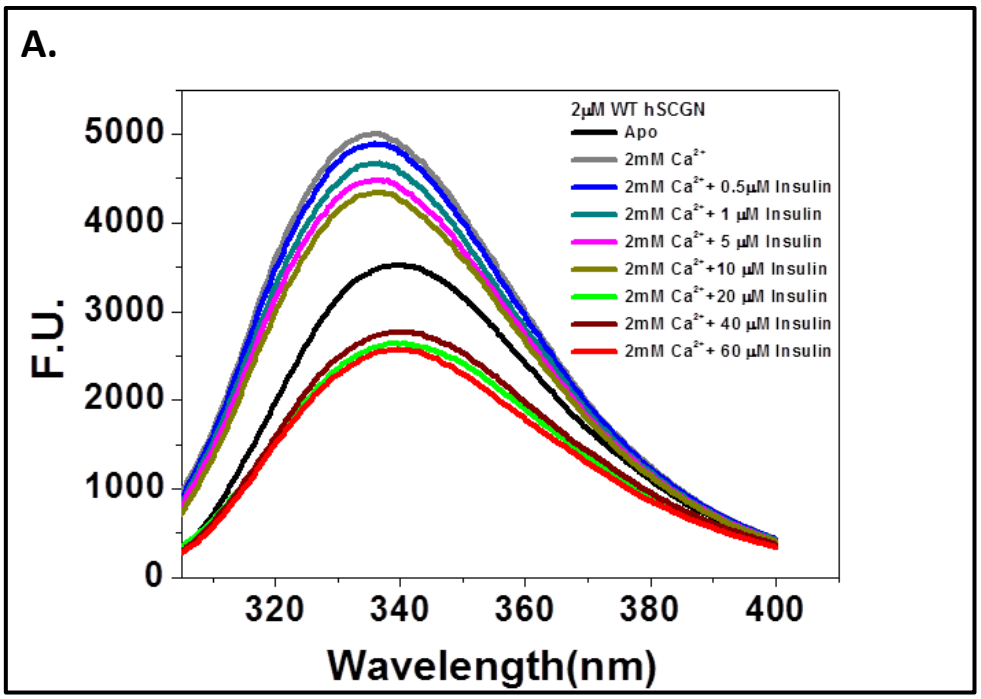

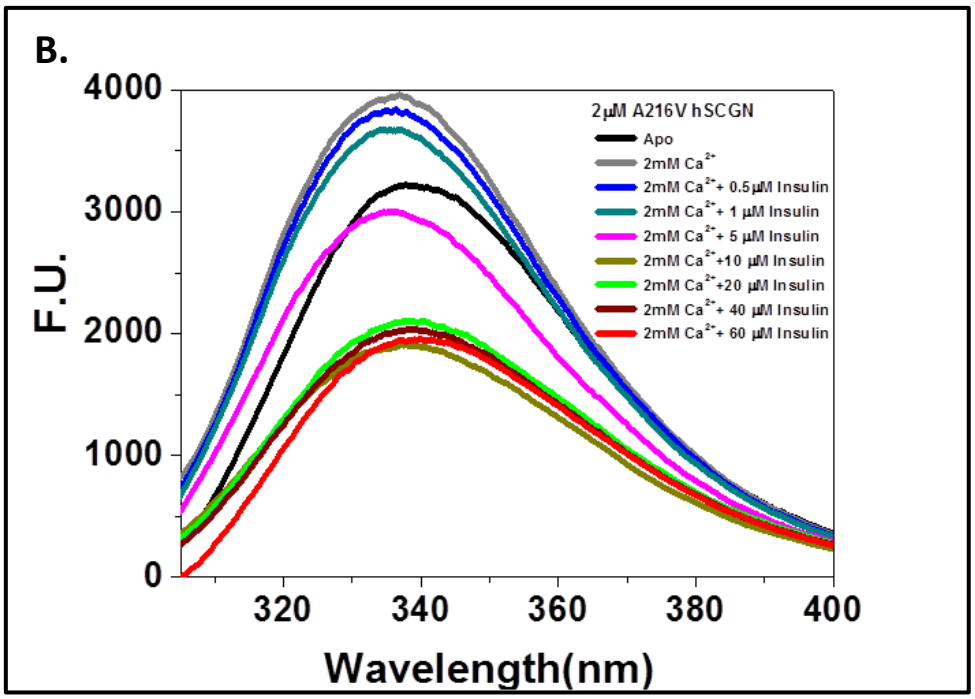

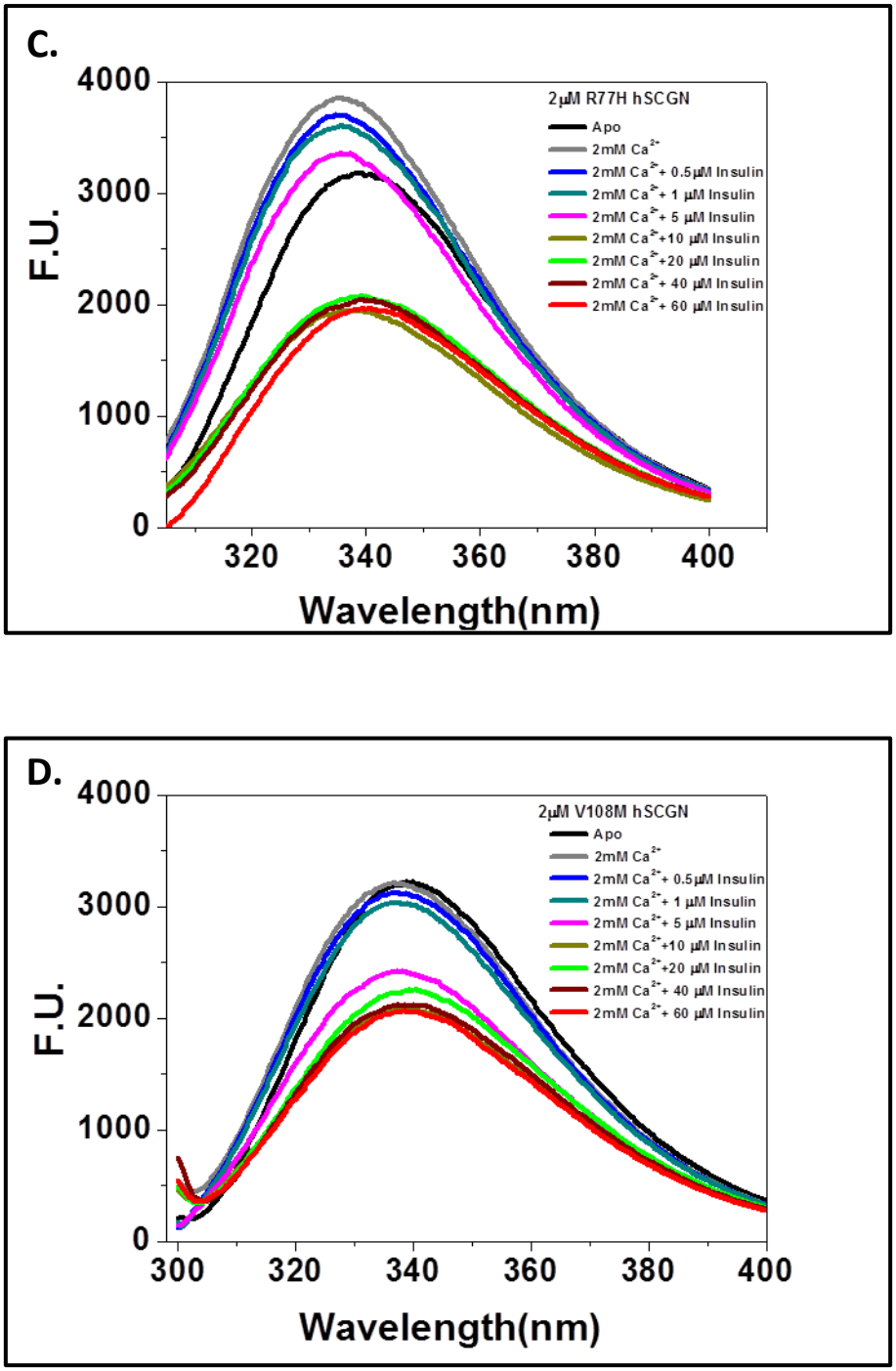

Figure 22: Titration of holo form of protein with different concentration of insulin denoted by different coloured lines. **Figure 22A:** WT hSCGN, **Figure 22B:** A216V hSCGN , **Figure 22C:** R77H hSCGN and **Figure 22D:** V108M hSCGN. **F.U.:** Fluorescence unit

4.10.2 Cirular Dichroism for studying insulin interaction

i) Titration of apo form of protein with insulin

In apo form, all the mutants and wild type protein showed structural change upon addition of insulin. Signals from 250-270nm are attributed to phenyl alanine, signalas from 270-290nm and 280-300nm are attributed to tryptophan and tyrosine residues. In all the cases maximum change is found to be seen around phenyl alanine and tyrosine

regions. Wild type protein shows maximum change in spectra upon insulin addition (i.e. from MRE from -8 to +8) whereas V108M mutant showed least structural change (MRE increased from -8 to -3). hSCGN A216V and R77H showed increase in ellepticity from -8 to +3 and -9 to +5 respectively (Fig. 23 B and C).

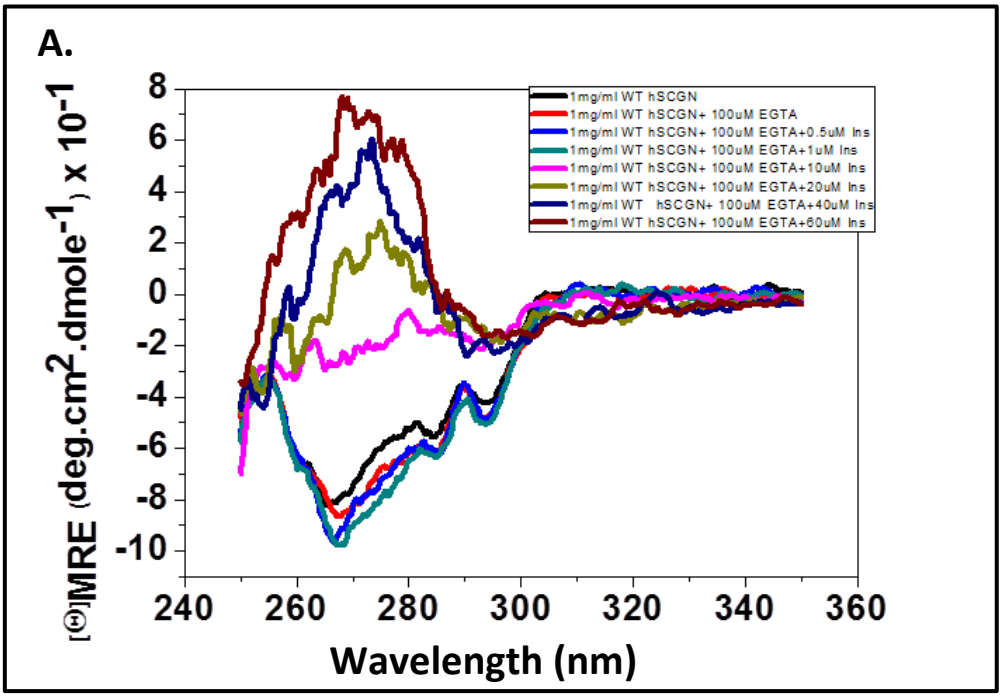

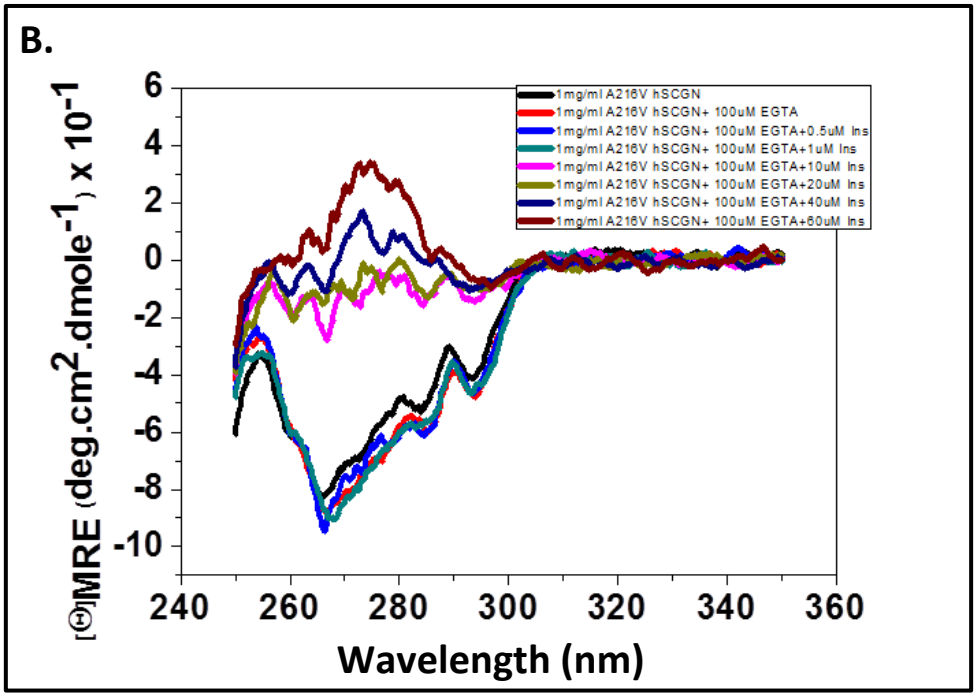

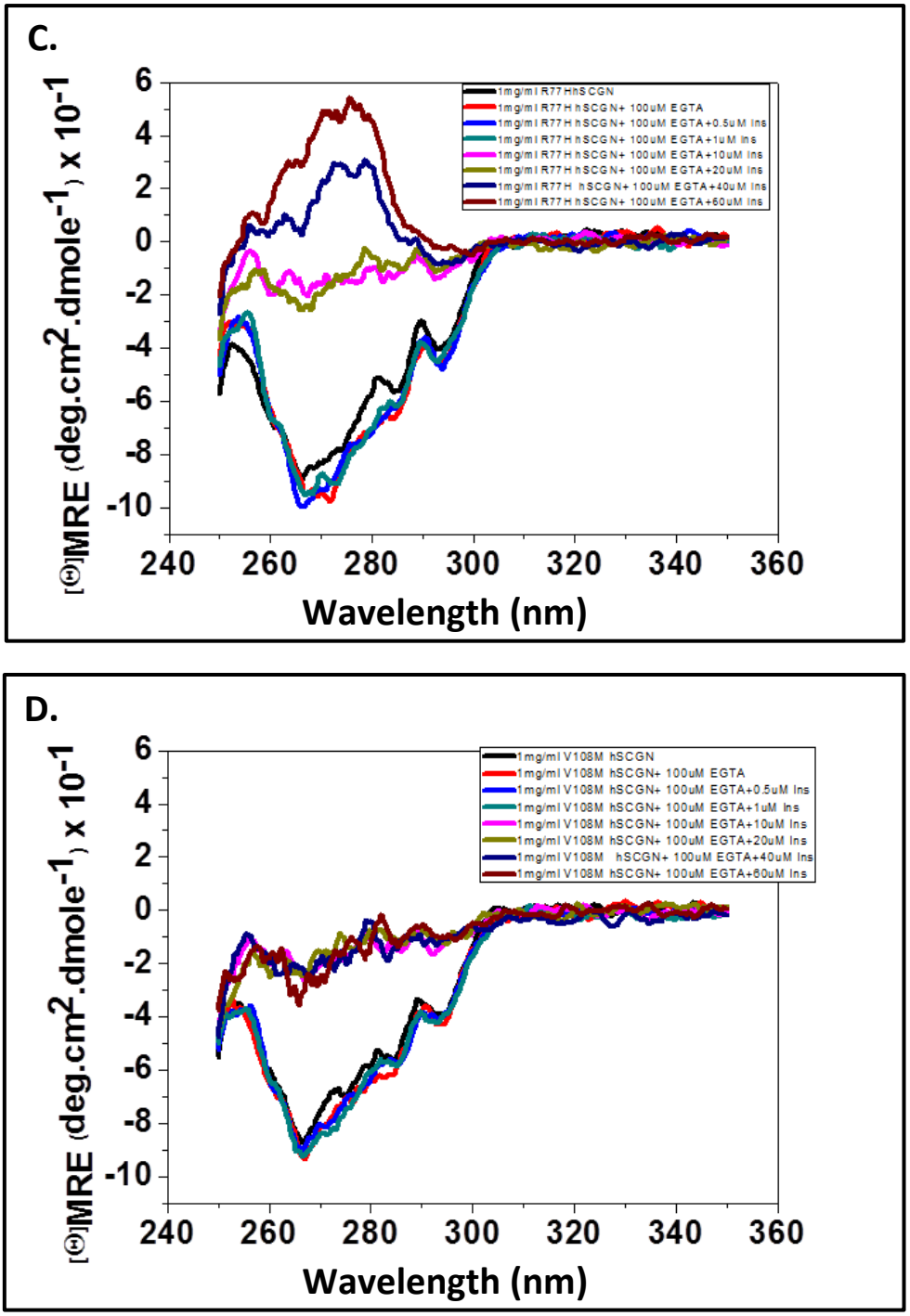

Figure 23: Titration of apo form of protein with different concentration of insulin denoted by different coloured CD spectra. **Figure 23A:** WT hSCGN, **Figure 23B:** A216V hSCGN , **Figure 23C:** R77H hSCGN and **Figure 23D:** V108M hSCGN

ii) Titration of holo form of protein with insulin

In holo form, both WT and mutant hSCGN shows greater affinity towards insulin. The structural change upon addition of small concentration has become more pronounced in holo form (Fig 24). This was clearly evident in the mutant V108M where the MRE has increased from -9 to -2 in apo form and -9 to +6 in holo form in the presence of 10µM insulin. WT hSCGN and R77H mutant showed increased affinity to insulin in holo form

and became saturated at lower concentration on insulin shown by only minor change in CD spectra after 10µM insulin titration. A216V and V108M mutants

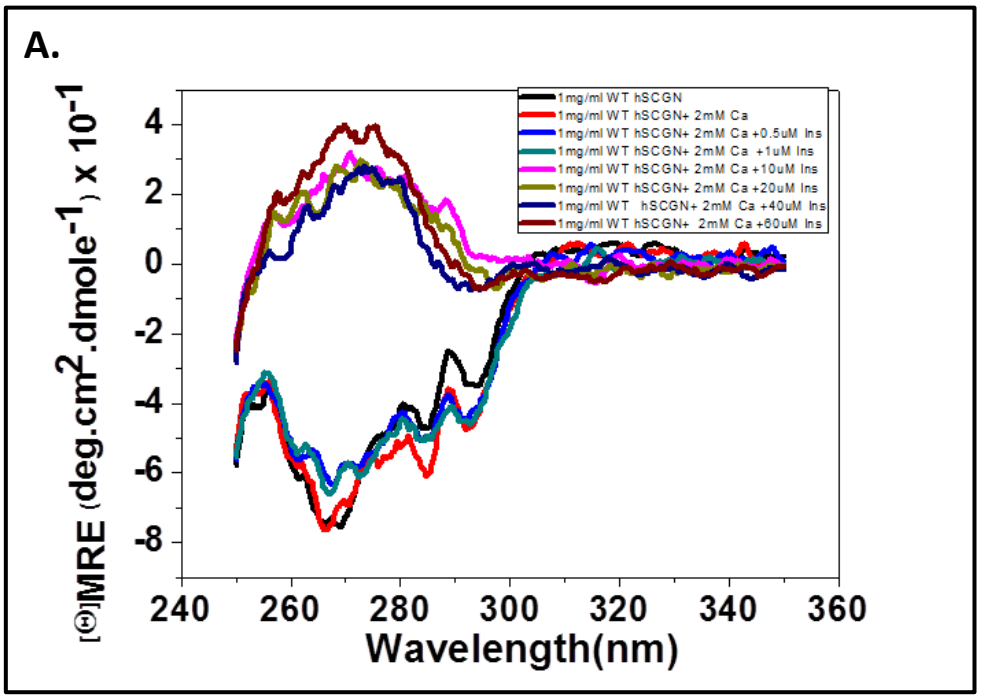

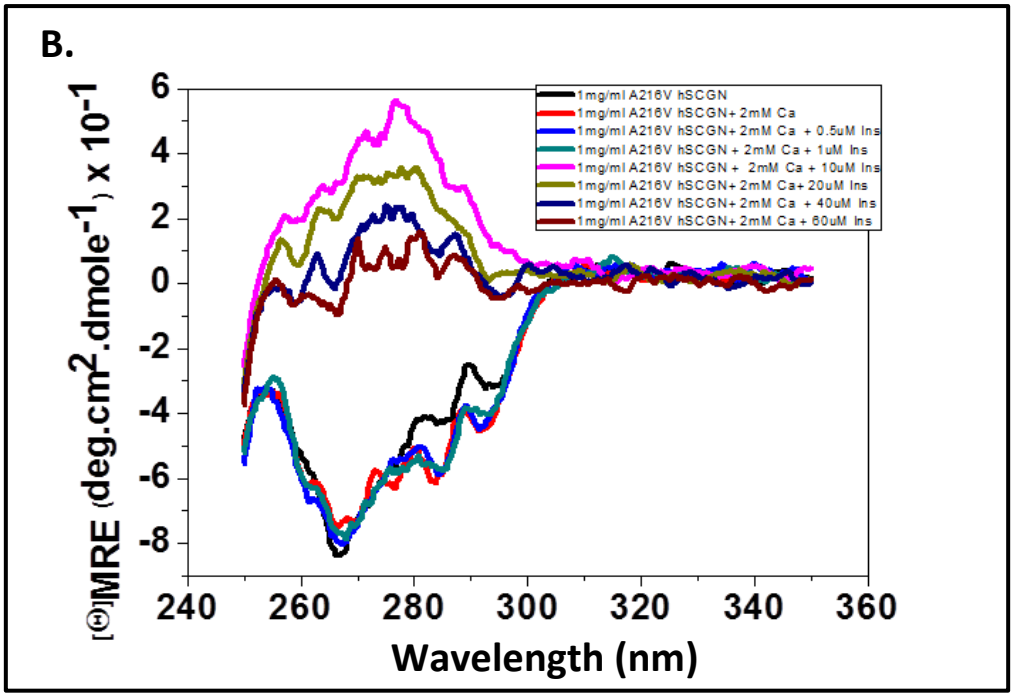

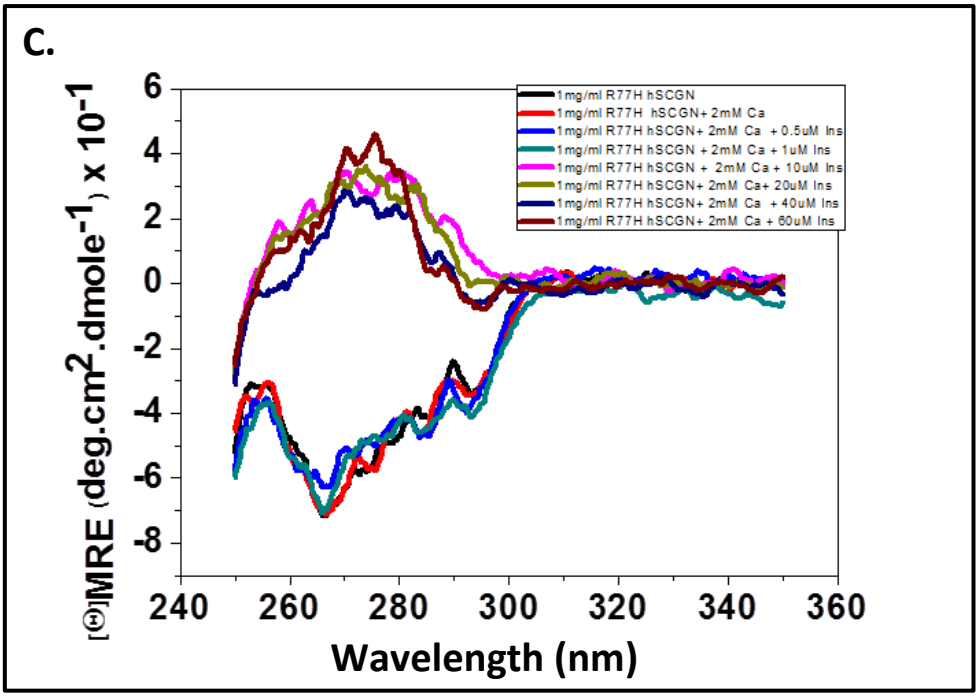

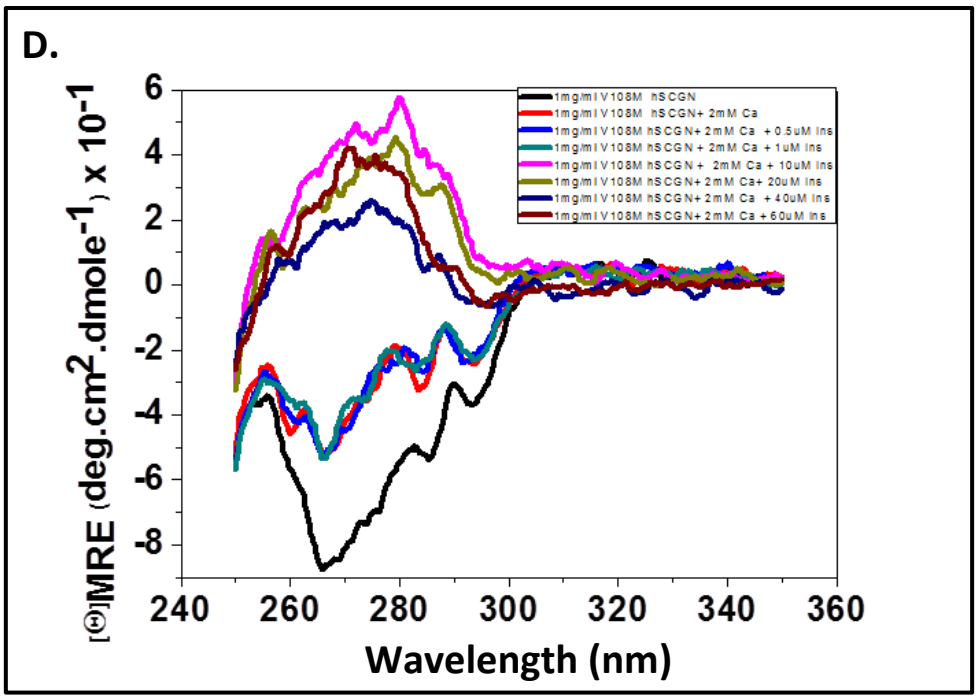

Figure 24: Titration of holo form of protein with different concentration of insulin denoted by different coloured CD spectra. **Figure 24A:** WT hSCGN, **Figure 24B:** A216V hSCGN , **Figure 24C:** R77H hSCGN and **Figure 24D:** V108M hSCGN

4.10.3 Far western blotting

Both the WT hSCGN (lane 6) and mSCGN (lane 5), gave positive band in the blot after 3 minutes of incubation with TMB substrate. The mutants A216V, R77H and V108M (lanes 7, 8 and 9) did not give any band. hSCGN WT gave darker band than that of the mSCGN because human insulin was used for probing that's why the binding of insulin with hSCGN might have occurred with higher affinity or stability. The positive control insulin

(lane 1) gave a huge blotch. This result signifies that the binding of mutants with insulin did not form a stable complex due to which the bound insulin might have been washed off in the washing step but the binding of hSCGN WT and insulin formed a stable complex which and could retain the washing step.

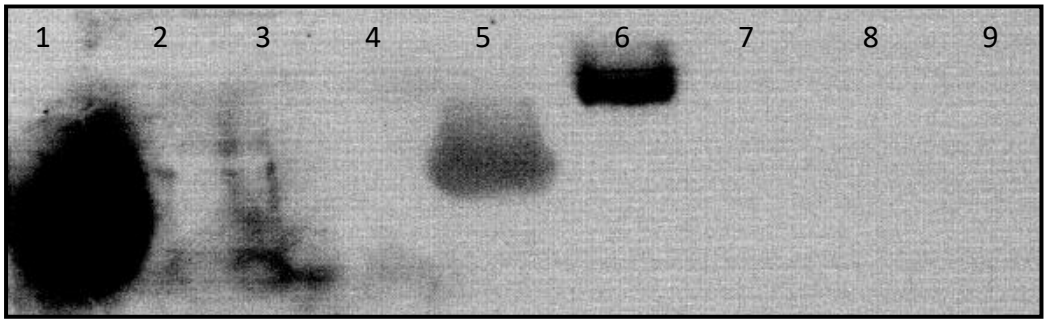

Figure 25: Far western blotting of proteins to study their interaction with insulin where insulin is used as baiting agent and primary antibody used against insulin. **Lane 1:** Insulin**,** **Lane 2**: Prestained marker, **Lane 3:** BSA, **Lane 4:** Negative control, **Lane 5:** mouse SCGN, **Lane 6:** hSCGN WT, **Lane 7:** A216V, **Lane 8:** R77H and **Lane 9:** V108M

4.11 Partial trypsin digestion

The gel pictures show that the holo form of all the proteins is highly digested (Fig. 26B). Binding of calcium causes exposure of arginine and lysine residues in the loops and flexible regions which corresponds to greater digestion in the presence of calcium. In digested apo form of all the proteins, low molecular weight bands are more prevalent indicating the protein structure is loose and thus more typsin got access to the structure. The digested holo form of all the proteins give greater quantity of high molecular weight bands indicating the core of the protein had become compact with higher exposure of loops which was readily accessed by trypsin. V108M mutant shows greatest digestion and R77H is second most digested indicating large change in conformation of these proteins upon mutation. V108M mutation causes change in conformation in such a way that the protein becomes more flexible with the exposure of loops where trypsin can cut and this structural perturbation becomes more pronounced when the protein binds calcium.

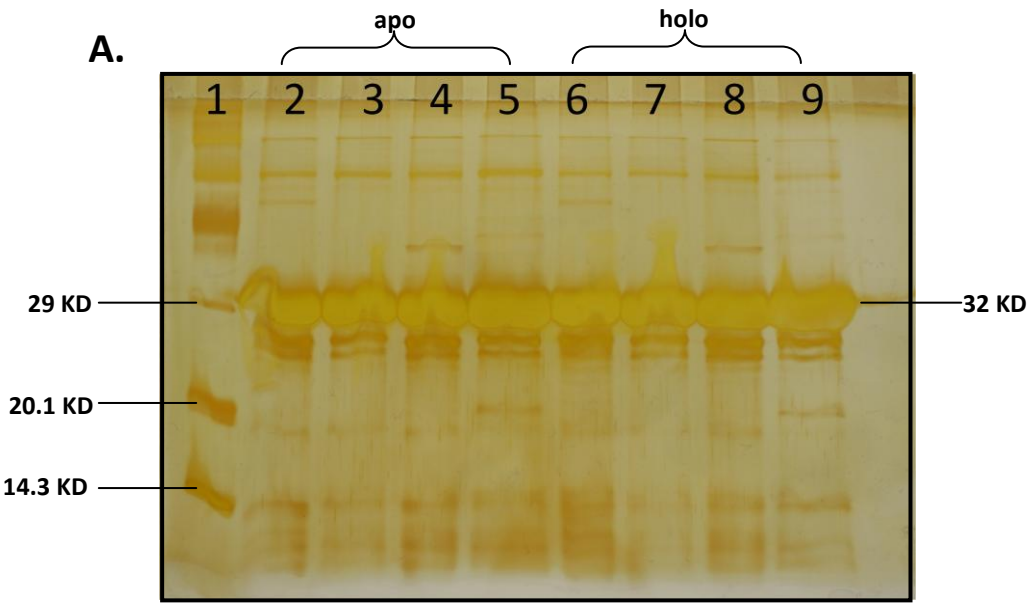

Figure 26A: Wild type and mutant proteins (20µg) in the presence and absence of Ca (Loading control). Lane 1: low range marker (Clonetech), Lane 2, lane 3, lane 4, lane 5: WT, A216V, R77H and V108M respectively with 100µM EDTA, Lane 6, lane 7, lane 8 and lane 9: WT, A216V, R77H and V108M respectively with 2mM Calcium

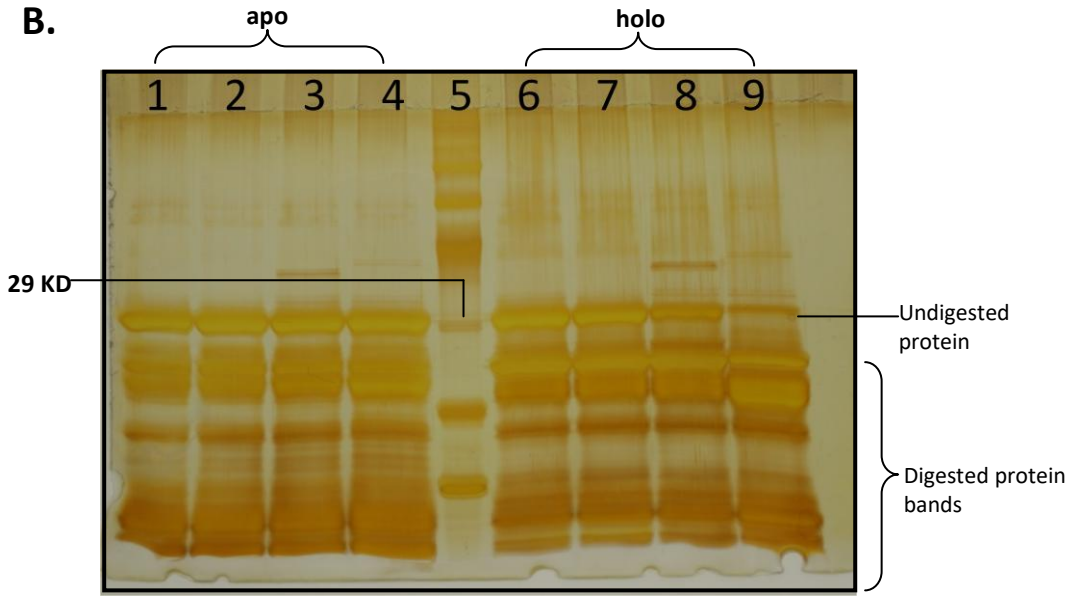

Figure 26B: Digestion with 0.4µg of Trypsin . Lane 1, lane 2, lane 3, lane 4: WT, A216V, R77H and V108M respectively with 100µM EDTA, Lane 5: low range marker (Clonetech), Lane 6, lane 7, lane 8 and lane 9: WT, A216V, R77H and V108M respectively with 2mM Calcium

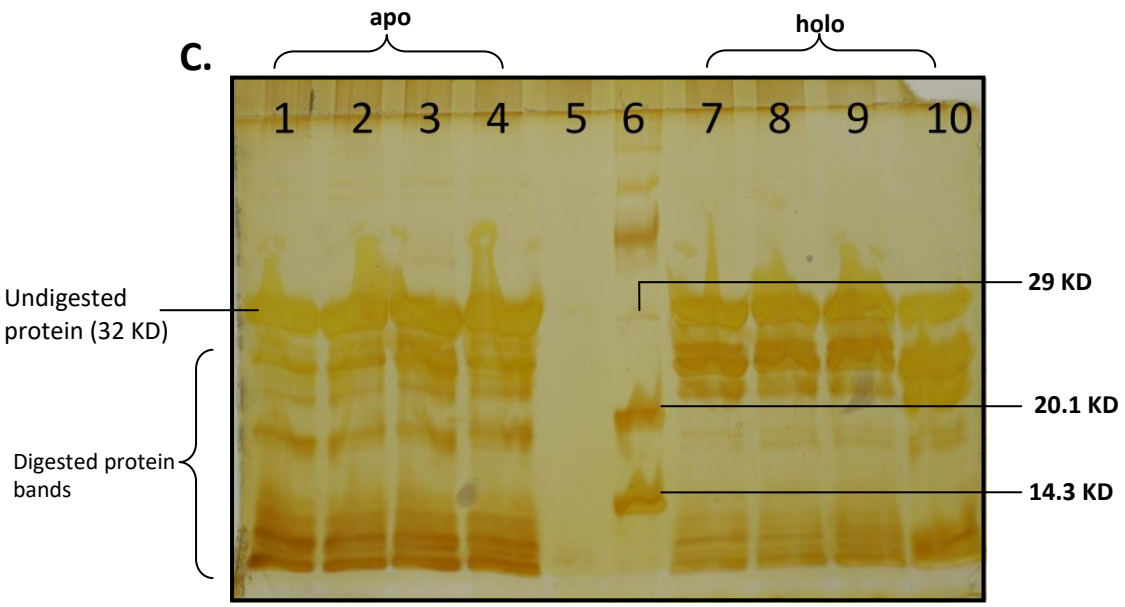

Figure 26C: Digestion with 0.1µg of Trypsin. **Lane 1, lane 2, lane 3, lane 4:** WT, A216V, R77H and V108M respectively with 100µM EDTA, **Lane 5:** empty, **Lane 6:** low range marker (Clonetech), Lane 7, lane 8, lane 9 and lane 10: WT, A216V, R77H and V108M respectively with 2mM Calcium

4.12 Glutaraldehyde crosslinking of protein

All the proteins were capable of crosslinking and formed oligomers in the presence of glutaraldehyde. The diffused bands of protein in the presence of glutaraldehyde indicate intramolecular cross linking occurring at different positions. In oxidized state, all the four proteins form mostly dimer and some amount of higher oligomers in apo form (Fig. 27A, lanes 1, 3, 4 and 5) but the presence of calcium increases the higher molecular weight oligomers (Fig. 27A, lanes 6-9). Monomeric form is most abundant in hSCGN WT(Fig.27 lane 1). It was expected that in the presence of DTT, the monomer population would increase. In reduced Apo form, the protein forms monomer dimer, trimer, tetramer as well as higher oligomers to some extent (Fig 27B, lanes 1-4)). But in the presence of calcium, the reduced protein showed very less monomer and dimers and more of higher oligomers (Fig. 27B, lanes 6-9) which suggest that the reduced protein is forming cysteine independent oligomers in the presence of Calcium.

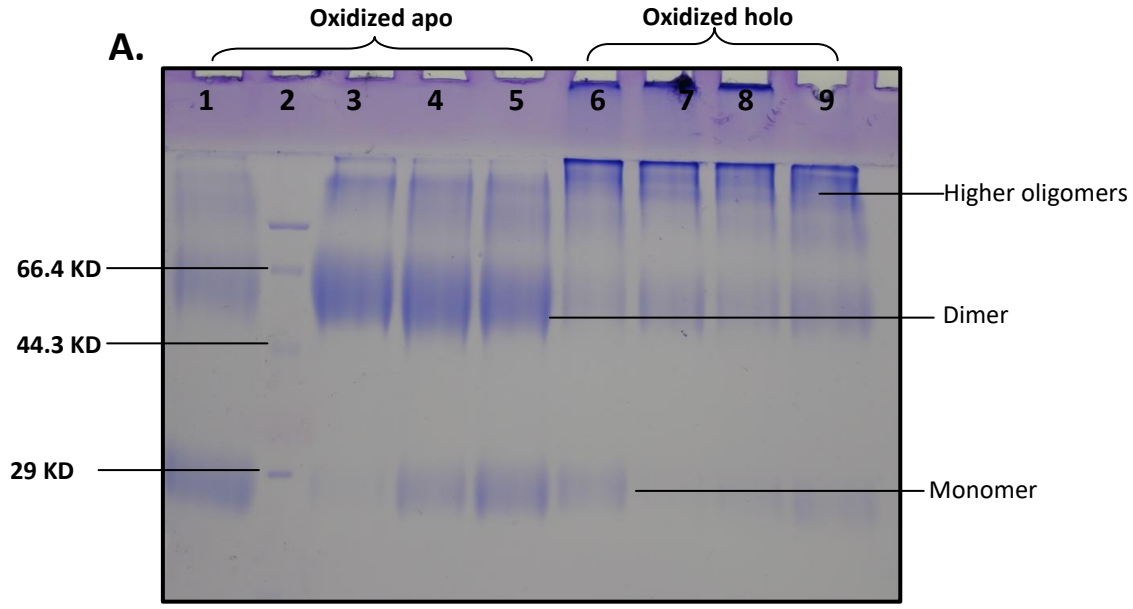

Figure 27A: Glutaraldehyde crosslinking (0.12%) in oxidized condition. **Lane 1, lane 3, lane 4, lane 5:** WT, A216V, R77H and V108M respectively with 100µM EDTA, **Lane 2:** low range marker (Clonetech), **Lane 6, lane 7, lane 8 and lane 9:** WT, A216V, R77H and V108M respectively with 2mM Calcium

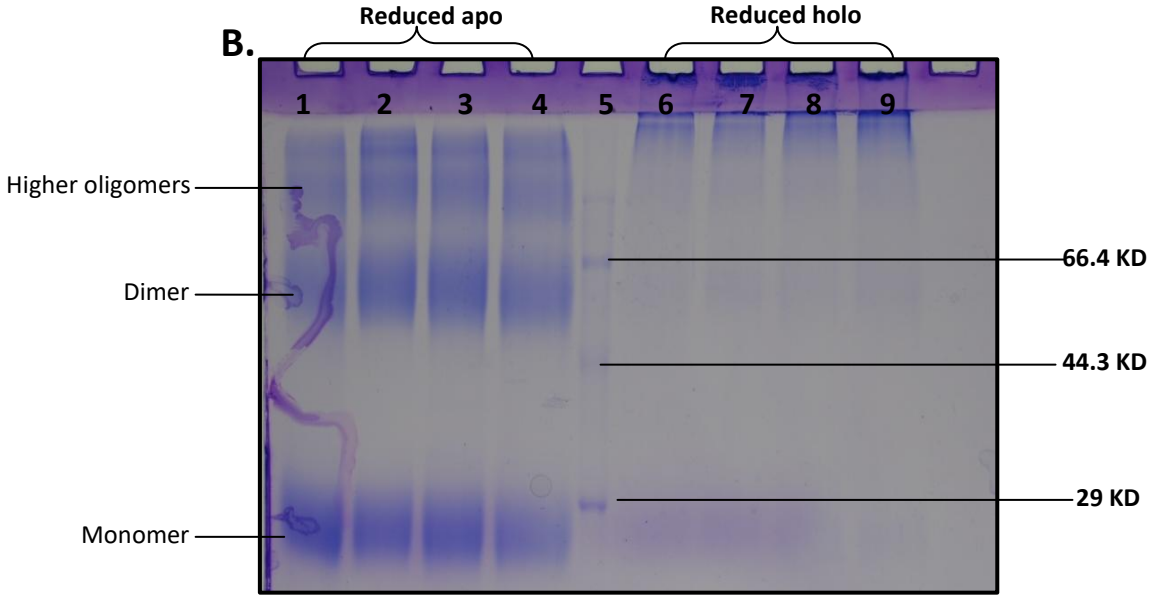

Figure 27B: Glutaraldehyde crosslinking (0.12%) in reduced condition (1mM DTT). **Lane 1, lane 2, lane 3, lane 4:** WT, A216V, R77H and V108M respectively with 100µM EDTA, **Lane 5:** low range marker (Clonetech), **Lane 6, lane 7, lane 8 and lane 9:** WT, A216V, R77H and V108M respectively with 2mM Calcium

4.13 GdmCl unfolding of protein

As the concentration of GdmCl was increased, fluorescence intensity of protein was decreased along with the increase in λmax i.e. red shift. At completely denatured state,

the λmax of the protein became equal to the λmax of tryptophan amino acid alone in aqueous environment which is about 350nm. The unfolding profile of all the proteins plotted in the form of F.I. versus wavelength is shown in appendix 7.

In apo form, all the proteins followed similar route of unfolding except R77H which shows a slight shift compared to other proteins (Fig 28A). All the proteins had similar λmax at starting point (39 to 40nm) followed by a baseline before the transition started. Unfolding started at about 1.5mM concentration of GdmCl in case of WT and A216V hSCGN whereas in case of R77H unfolding starts at 1.5mM concentration of GdmCl (Fig. 28A). The $C_{1/2}$ value of unfolding for apo form of WT, A216V, R77H and V108M is manually estimated from the plot as 2.65M, 2.65M, 2.46M and 2.66M respectively which indicates that apo form of WT, A216V and V108M hSCGN are more stable. R77H which has lowest $C_{1/2}$ in apo form is the least stable.

In holo form, the λmax was 335nm for WT, A216V and R77H whereas for V108M, it was 337nm indicating less blue shift. The baseline before transition was smaller in holo form than the apo form. Transition started from 0.5mM concentration of GdmCl in case of holo WT, A216V and R77H whereas in case of V108M transition started from about 0.05mM concentration of GdmCl indicating lower stability of this protein than others. At low concentration of GdmCl, holo V108M followed different path of unfolding (Fig 28B). The $C_{1/2}$ for both WT and A216V hSCGN was estimated to be 2.74M whereas for R77H and V108M it was estimated to be 2.7M and 2.68M respectively. The $C_{1/2}$ value for all the proteins was found to be increased in holo form indicating holo form was more stable than apo form except in case of V108M where the $C_{1/2}$ value was similar in apo and holo form. This indicated that calcium binding did not impart stability to V108M mutant protein. The F.I. (360/320) versus GdmCl concentration plot was also plotted for confirmation which showed similar nature of unfolding as that of the λmax versus GdmCl plot (Fig 28C and 28D).

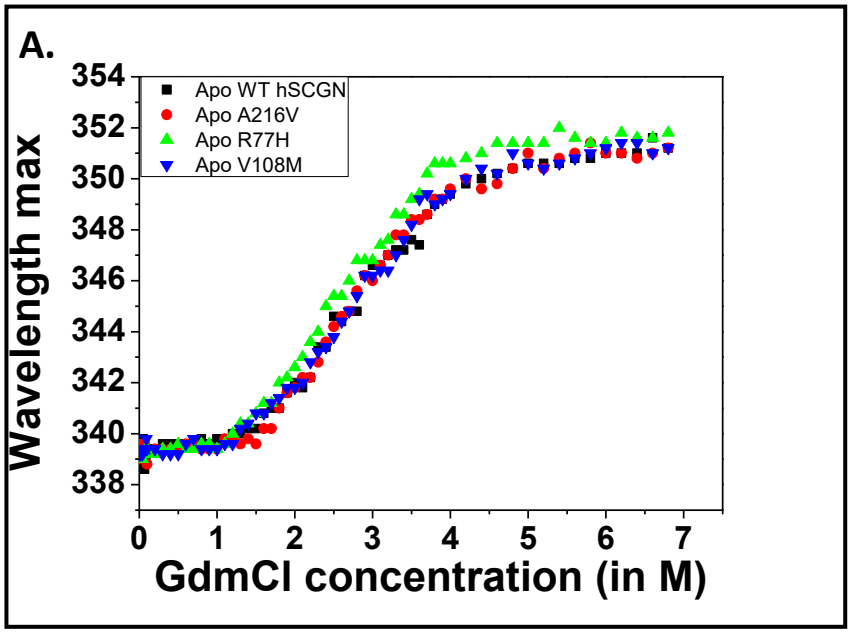

Figure 28A: Unfolding plot of four proteins in apo form (100µM EDTA) represented in the form of Wavelength max. (λmax) versus GdmCl concentration, each line denoting different proteins. **Black:** WT hSCGN, **Red:** A216V hSCGN, **Green:** R77H hSCGN and **Blue:** V108M hSCGN

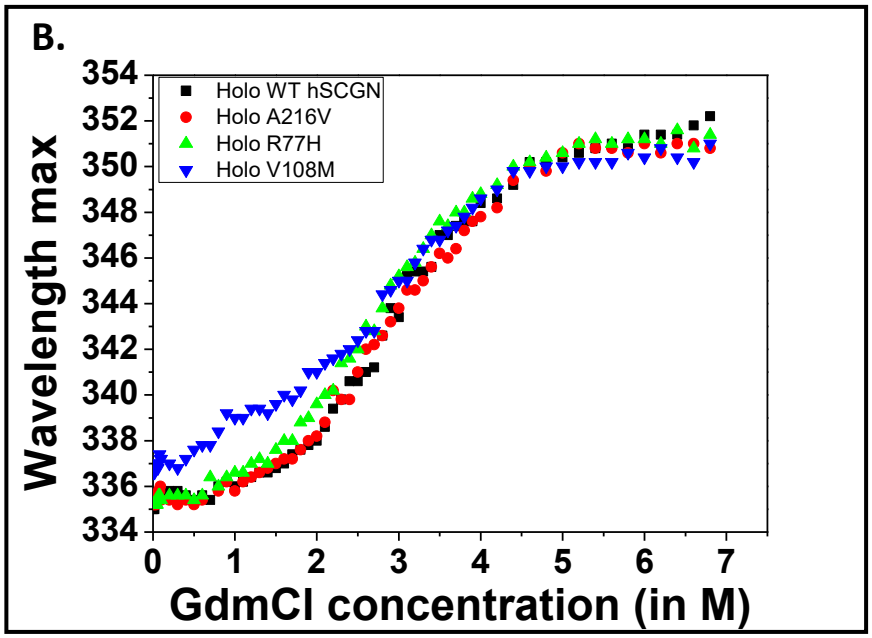

Figure 28B: Unfolding plot of four proteins in holo form (2mM Ca^{+2}) represented in the form of Wavelength max. (λmax) versus GdmCl concentration, each line denoting different proteins. **Black:** WT hSCGN, **Red:** A216V hSCGN, **Green:** R77H hSCGN and **Blue:** V108M hSCGN

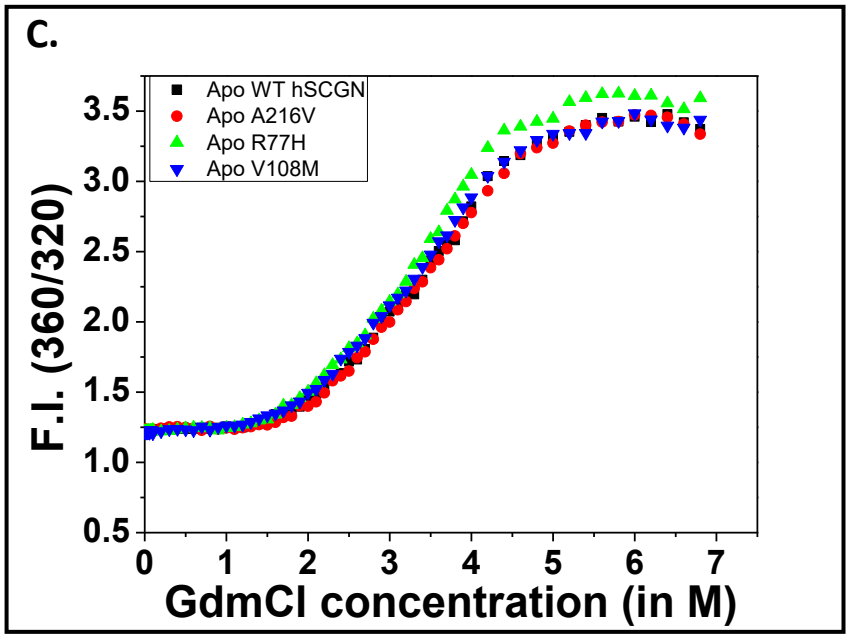

Figure 28C: Unfolding plot of four proteins in apo form (100µM EDTA) represented in the form of F.I. (360/320) versus GdmCl concentration, each line denoting different proteins. **Black:** WT hSCGN, **Red:** A216V hSCGN, **Green:** R77H hSCGN and **Blue:** V108M hSCGN

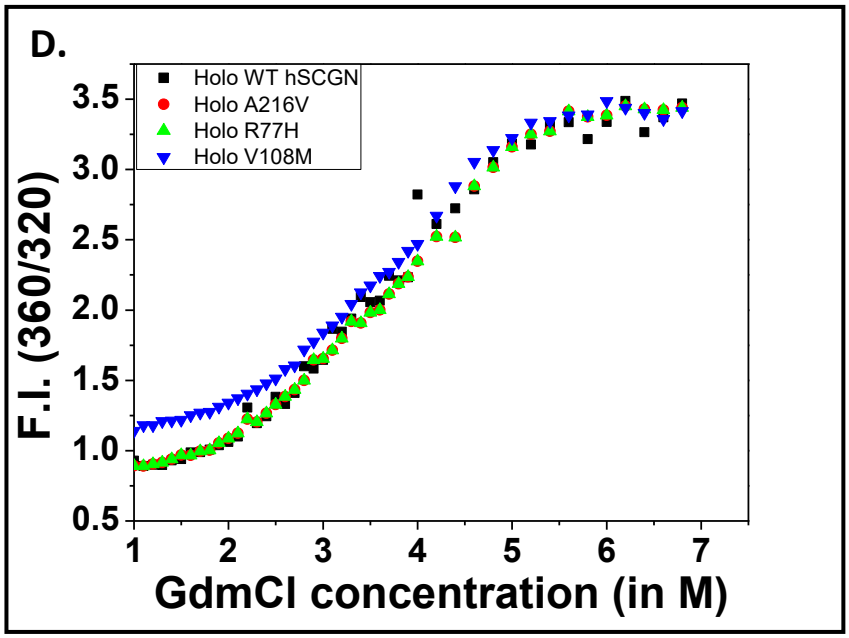

Figure 28D: Unfolding plot of four proteins in holo form (2mM Ca^{+2}) represented in the form of Wavelength max. (λmax) versus GdmCl concentration, each line denoting different proteins. **Black:** WT hSCGN, **Red:** A216V hSCGN, **Green:** R77H hSCGN and **Blue:** V108M hSCGN

4.14 Restriction free cloning to insert hscgn WT and its mutant in pEGFP-N3 vector and tranfection of construct in MIN6 cell line

After restriction free cloning was performed, the amplicon of second PCR was given for sequencing. The sequencing result revealed Secretagogin was well as the mutant genes were placed just before EGFP tag (Fig. 31). The conformation of the tagged protein was also carried out by using expasy translate tool (Appendix 10). The confirmed constructs were used for transfection into MIN6 cell line. Successful transfection of MIN6 cells with pEGFP h*scgn* WT as well as mutants was indicated by green fluorescence in MIN6 cell culture under fluorescence microscope (Fig. 29).

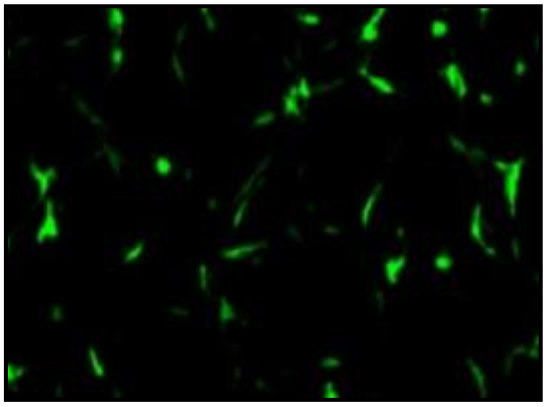

Figure 29: EGFP signal in MIN6 cell line after 21days of transfection by pEGFP-N3 *hscgn* WTusing Gentamicin (1000µg/ml) as selection agent

A.

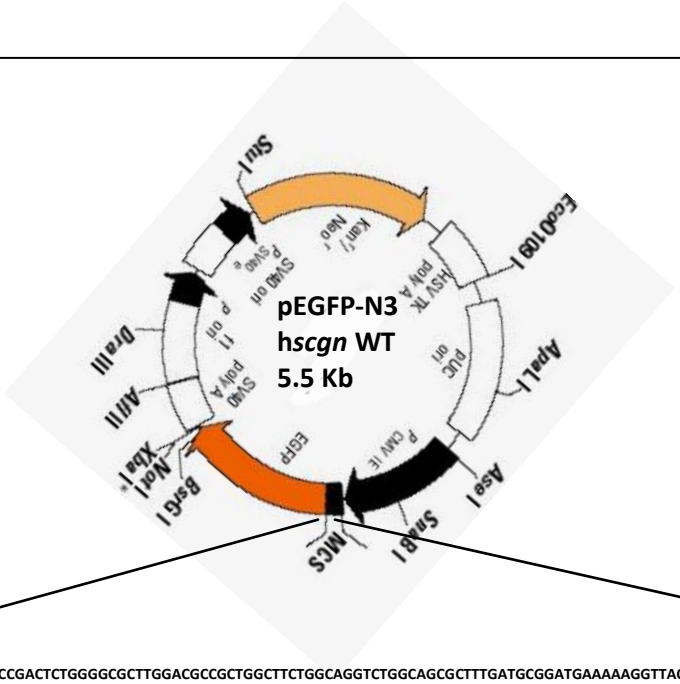

5'_ATGGACAGCTCCCGGGAACCGACTCTGGGGCGCTTGGACGCCGCTGGCTTCTGGCAGGTCTGGCAGCGCTTTGATGCGGATGAAAAAGGTTACATAGAAGAGAAGGAACTCGATGCTTTCTTT
CTCCACATGTTGATGAAACTGGGTACTGATGACACGGTCATGAAAGCAAATTTGCACAAGGTGAAACAGCAGTTTATGACTACCCAAGATGCCTCTAAAGATGGTCGCATTCGGATGAAAGAGCTT
GCTGGTATGTTCTTATCTGAGGATGAAAACTTTCTTCTGCTCTTTCGCCGGGAAAACCCACTGGACAGCAGCGTGGAGTTTATGCAGATTTGGCGCAAATATGACGCTGACAGCAGTGGCTTTATAT
CAGCTGCTGAGCTCCGCAACTTCCTCCGAGACCTCTTTCTTCACCACAAAAAGGCCATTTCTGAGGCTAAACTGGAAGAATACACTGGCACCATGATGAAGATTTTTGACAGAAATAAAGATGGTCG
GTTGGATCTAAATGACTTAGCAAGGATTCTGGCTCTTCAGGAAAACTTCCTTCTCCAATTTAAAATGGATGCTTGTTCTACTGAAGAAAGGAAAAGGGACTTTGAGAAAATCTTTGCCTACTATGAT
GTTAGTAAAACAGGAGCCCTGGAAGGCCCAGAAGTGGATGGGTTTGTCAAAGACATGATGGAGCTTGTCCAGCCCAGCATCAGCGGGGTGGACCTTGATAAGTTCCGCGAGATTCTCCTGCGTCA
CTGCGACGTGAACAAGGATGGAAAAATTCAGAAGTCTGAGCTGGCTTTGTGTCTTGGGCTGAAAATCAACCCAGTGAGCAAGGGCGAGGAGCTGTTCACCGGGGTGGTGCCCATCCTGGTCGAGC
TGGACGGCGACGTAAACGGCCACAAGTTCAGCGTGTCCGGCGAGGGCGAGGGCGATGCCACCTACGGCAAGCTGACCCTGAAGTTCATCTGCACCACCGGCAAGCTGCCCGTGCCCTGGCCCACC
CTCGTGACCACCCTGACCTACGGCGTGCAGTGCTTCAGCCGCTACCCCGACCACATGAAGCAGCACGACTTCTTCAAGTCCGCCATGCCCGAAGGCTACGTCCAGGAGCGCACCATCTTCTTCAAGG
ACGACGGCAACTACAAGACCCGCGCCGAGGTGAAGTTCGAGGGCGACACCCTGGTGAACCGCATCGAGCTGAAGGGCATCGACTTCAAGGAGGACGGCAACATCCTGGGGCACAAGCTGGAGTA
CAACTACAACAGCCACAACGTCTATATCATGGCCGACAAGCAGAAGAACGGCATCAAGGTGAACTTCAAGATCCGCCACAACATCGAGGACGGCAGCGTGCAGCTCGCCGACCACTACCAGCAGA
ACACCCCCATCGGCGACGGCCCCGTGCTGCTGCCCGACAACCACTACCTGAGCACCCAGTCCGCCCTGAGCAAAGACCCCAACGAGAAGCGCGATCACATGGTCCTGCTGGAGTTCGTGACCGCCGC
CGGGATCACTCTCGGCATGGACGAGCTGTACAAG-3'

B.

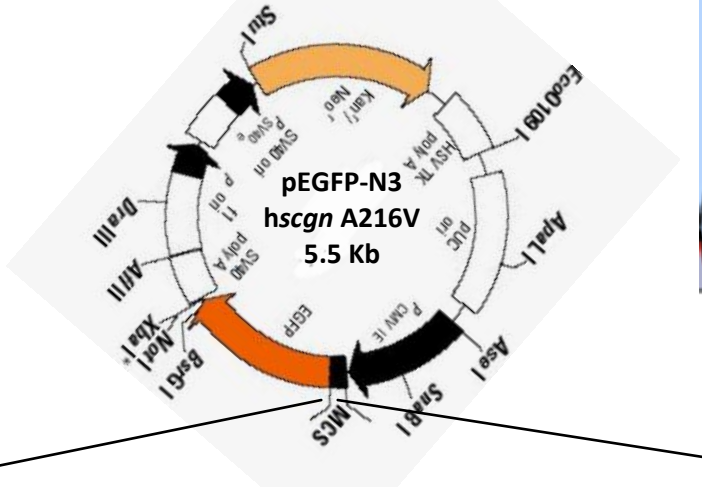

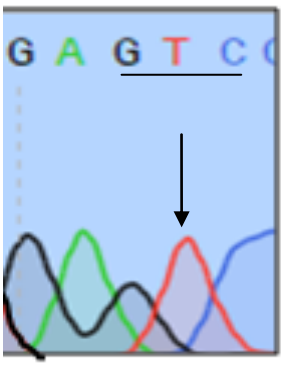

5'_ATGGACAGCTCCCGGGAACCGACTCTGGGGCGCTTGGACGCCGCTGGCTTCTGGCAGGTCTGGCAGCGCTTTGATGCGGATGAAAAAGGTTACATAGAAGAGAAGGAACTCGATGCTTTCTTT
CTCCACATGTTGATGAAACTGGGTACTGATGACACGGTCATGAAAGCAAATTTGCACAAGGTGAAACAGCAGTTTATGACTACCCAAGATGCCTCTAAAGATGGTCGCATTCGGATGAAAGAGCTT
GCTGGTATGTTCTTATCTGAGGATGAAAACTTTCTTCTGCTCTTTCGCCGGGAAAACCCACTGGACAGCAGCGTGGAGTTTATGCAGATTTGGCGCAAATATGACGCTGACAGCAGTGGCTTTATAT
CAGCTGCTGAGCTCCGCAACTTCCTCCGAGACCTCTTTCTTCACCACAAAAAGGCCATTTCTGAGGCTAAACTGGAAGAATACACTGGCACCATGATGAAGATTTTTGACAGAAATAAAGATGGTCG
GTTGGATCTAAATGACTTAGCAAGGATTCTGGCTCTTCAGGAAAACTTCCTTCTCCAATTTAAAATGGATGCTTGTTCTACTGAAGAAAGGAAAAGGGACTTTGAGAAAATCTTTGCCTACTATGAT
GTTAGTAAAACAGGAGTCCTGGAAGGCCCAGAAGTGGATGGGTTTGTCAAAGACATGATGGAGCTTGTCCAGCCCAGCATCAGCGGGGTGGACCTTGATAAGTTCCGCGAGATTCTCCTGCGTCA
CTGCGACGTGAACAAGGATGGAAAAATTCAGAAGTCTGAGCTGGCTTTGTGTCTTGGGCTGAAAATCAACCCAGTGAGCAAGGGCGAGGAGCTGTTCACCGGGGTGGTGCCCATCCTGGTCGAGC
TGGACGGCGACGTAAACGGCCACAAGTTCAGCGTGTCCGGCGAGGGCGAGGGCGATGCCACCTACGGCAAGCTGACCCTGAAGTTCATCTGCACCACCGGCAAGCTGCCCGTGCCCTGGCCCACC
CTCGTGACCACCCTGACCTACGGCGTGCAGTGCTTCAGCCGCTACCCCGACCACATGAAGCAGCACGACTTCTTCAAGTCCGCCATGCCCGAAGGCTACGTCCAGGAGCGCACCATCTTCTTCAAGG
ACGACGGCAACTACAAGACCCGCGCCGAGGTGAAGTTCGAGGGCGACACCCTGGTGAACCGCATCGAGCTGAAGGGCATCGACTTCAAGGAGGACGGCAACATCCTGGGGCACAAGCTGGAGTA
CAACTACAACAGCCACAACGTCTATATCATGGCCGACAAGCAGAAGAACGGCATCAAGGTGAACTTCAAGATCCGCCACAACATCGAGGACGGCAGCGTGCAGCTCGCCGACCACTACCAGCAGA
ACACCCCCATCGGCGACGGCCCCGTGCTGCTGCCCGACAACCACTACCTGAGCACCCAGTCCGCCCTGAGCAAAGACCCCAACGAGAAGCGCGATCACATGGTCCTGCTGGAGTTCGTGACCGCCGC
CGGGATCACTCTCGGCATGGACGAGCTGTACAAG-3'

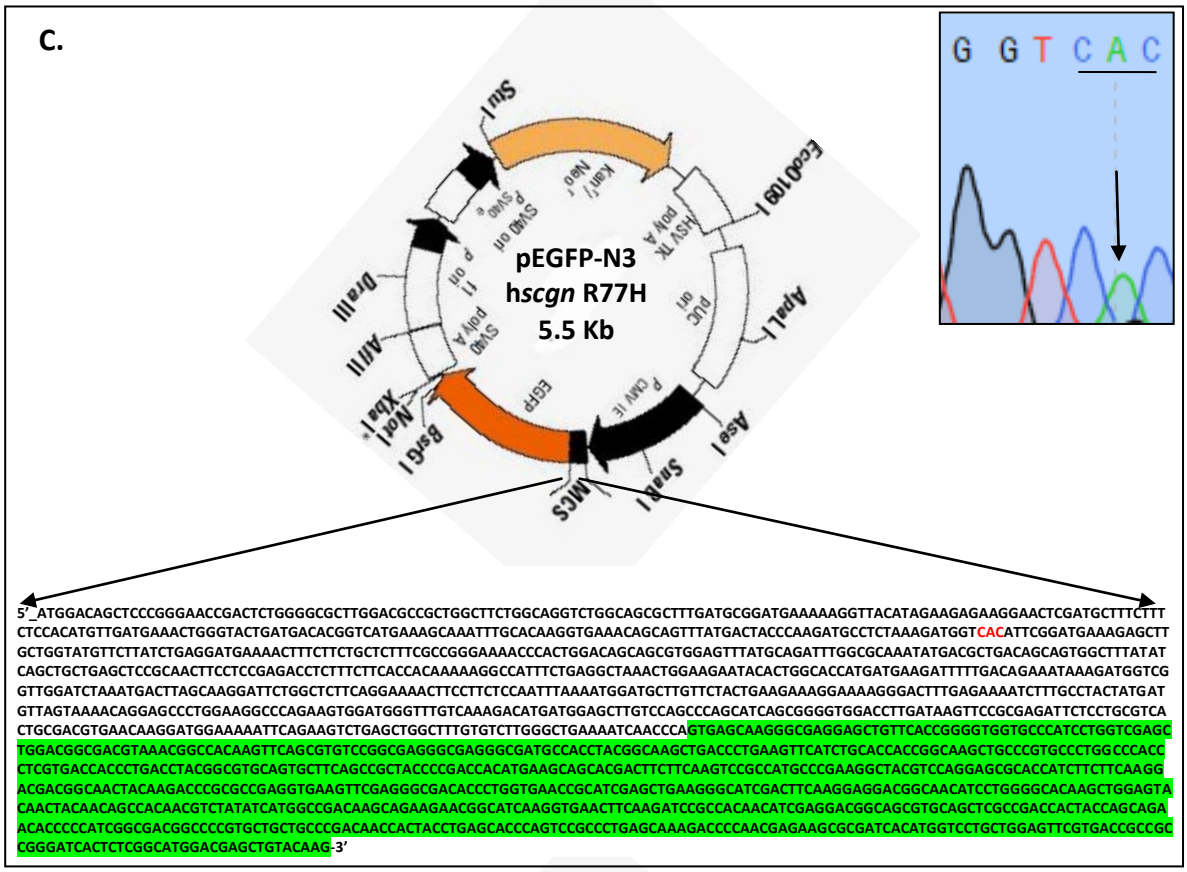

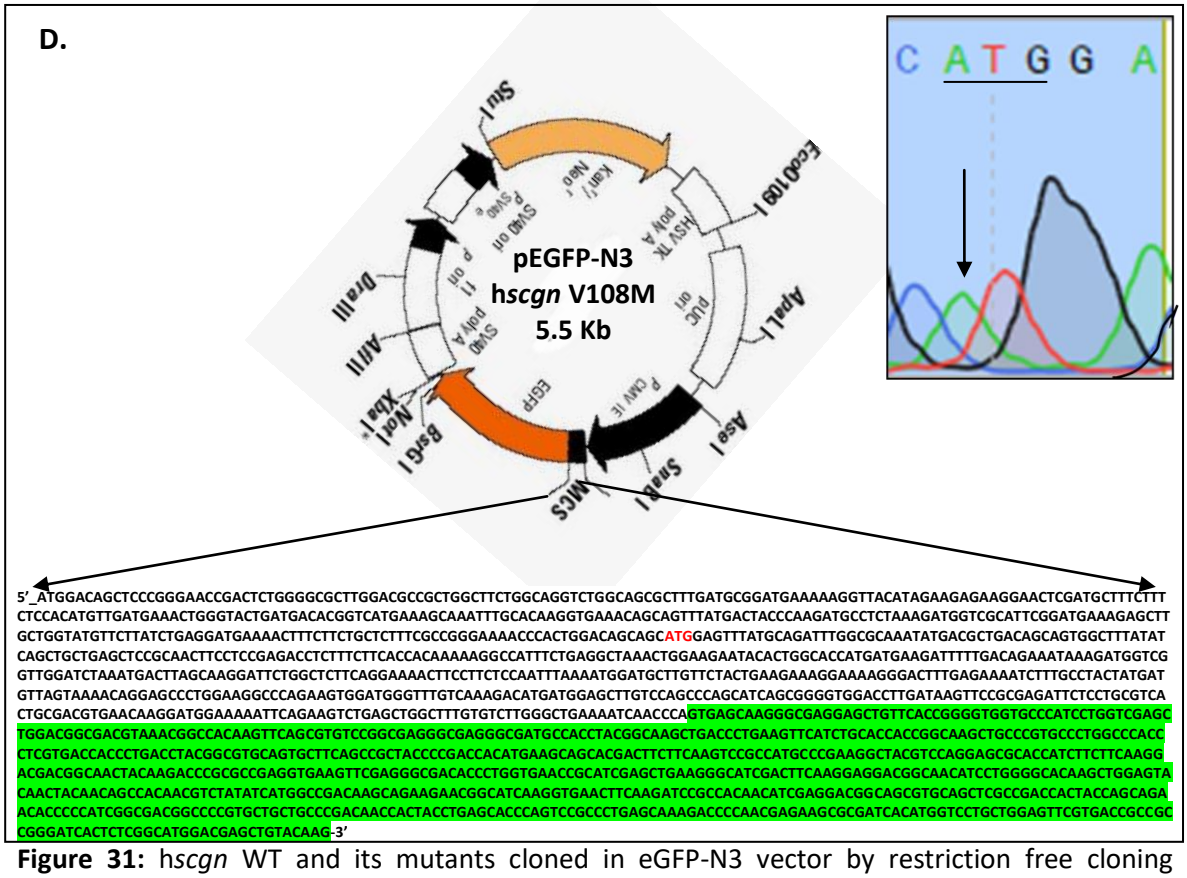

Figure 31: h*scgn* WT and its mutants cloned in eGFP-N3 vector by restriction free cloning method. The protein is inserted just in front of EGFP tag. The point of each mutations marked by red nucleotides and EGFP tag highlighted in green. **Figure A**: pEGFP-N3 h*scgn* WT, **Figure B:** pEGFP-N3 h*scgn* A216V, **Figure C:** pEGFP-N3 h*scgn* R77H and **Figure D:** pEGFP-N3 h*scgn* R77H.

CHAPTER 5

DISCUSSION

Secretagogin is a recently discovered protein with multiple functions. Being calcium binding sensor protein, the protein undergoes conformational changes in the presence of calcium which is the main basis of its function. Most of the function of Secretagogin yet discovered is calcium dependent. Recently the therapeutic role of Secretagogin in treatment of Diabetes has been discovered (Kumar Sharma et al., n.d.). Scientists believe that this protein has a potential role as transcription factors and chaperones but these functions still needs to be worked on and verified. This protein being recently discovered, not much information is available on the mutations related to this protein and its consequences. Thus this study is an approach to provide better insights on the mutants of Secretagogin and how the mutation affects the structure and function of the protein.

5.1 Cloning, overexpression and purification of hSCGN and its mutants (A216V, R77H, V108M)

The pET system is the most robust system for the cloning and expression of recombinant protein in *E.coli*. Almost 50% of the cell total protein is converted into the desired protein within few hours after induction. The system also allows one to choose N-terminal and C-terminal fusion tags for detection, purification and localization of expressed protein. pET-21b is one of the translational vectors which contain efficient translation initiation signal and allows one to keep C-terminal histidine tag in the protein. Since the gene of interest is under the control of T7 promoter, host bearing the T7 polymerase gene is selected over protein expression. The amount of protein expressed depends upon the plasmid and host combination. BL21 (DE3) is the host commonly used for this system which is deficient in both *lon* and *OmpT* (Novagen, 2003). After desired protein has been expressed it needs to be purified for further use. Different factors needs to be considered for protein purification like molecular weight, charge, hydrophobicity, pI value of the protein, fusion tag if present, and quantity of impurities present. Single or multiple step purification process can be carried out depending upon the extent of purity required. For high purity, usually affinity chormatography is used. For fusion protein with a tag, respective affinity based column is used for purification. As our protein was untagged, purification process was optimized using hydrophobic interaction chromatography followed by anion exchange chromatography (Q-sepharose). HIC was selected as secretagogin has number of hydrophobic amino acid residues. Anion exchange chromatography was performed at p^H 7.5 as the pI of this protein is 5.25 and thus possesses negative charge at p^H 7.5. Even after two step purification, some low molecular weight impurities were still present. Size exclusion chromatography was then performed to remove low molecular weight impurities. As our protein is calcium binding, it binds calcium with high affinity. Before

performing any biophysical experiment it is necessary to ensure that the protein is free from calcium to study its properties in apo form and then compare it in holo form. In order to remove calcium already bound to the protein, EDTA is added at the concentration 10 times greater than the concentration of calcium binding sites. The protein consists of 3 tryptophan residues at 18, 21 and 114 position. The presence of tryptophan in protein has made the biophysical study much easier.

5.2 Expression check and leaky expression

It is necessary to carry out expression check for each mutant individually as the expression level and stability of protein might have changed due to mutation. All the mutant proteins showed similar expression level as that of the WT protein i.e. there was no compromised expression of mutant proteins. The mutant proteins could be purified in the same manner as the wild type protein. During overexpression, it is necessary to grow the cell culture till the optical density reaches 0.6 (when the cell is in exponential phase of growth) before induction with IPTG in order to ensure maximum population of cell has been achieved before driving them into protein production. Large amount of leaky expression was observed even in the uninduced cell culture. The host strains such al *E.coli* BL21 contains T7 RNA polymerase under the control of *lacUV5* promoter which allows some degree of transcription even in uninduced state. Moreover the yeast extract used in the LB media might contain inducer galactose which contributes to high basal expression. In case if the protein of interest is toxic or has innocuous effect on cell growth, more stringent control is required. For this glucose containing media can be used where glucose prevents the basal expression. Host carrying pLyS plasmids can be used which encodes lysozyme, a natural inhibitor of RNA polymerase. As our protein was non-toxic, basal level expression could be neglected (Novagen, 2003).

5.3 Study of protein behaviour by fluorescence spectroscopy and Circular Dichroism

Biophysical characterization of protein is the first step into understanding the properties of any protein. The protein should at least be 90% pure for reliable characterization. The first step involves the fluorescence spectroscopy to determine whether the protein contains tryptophan or not. The protein containing tryptophan gives fluorescence emission spectra with wavelength maxima at around 350nm when excited with light of wavelength 395nm. Fluorescence spectra can be used to study change in structure of protein upon ligand binding. The freshly prepared WT hSCGN showed 29% increase in fluorescence intensity along with significant blue shift whereas the two mutants A216V and R77H (5.33% and 0.44%) showed lesser increase in fluorescence with similar blue shift of nearly 4nm upon calcium titration (Fig 11A, B and C). This response shows that mutants have become less responsive to calcium. Upon ageing, the WT protein also lost pronounced increase in F.I. upon calcium addition like the mutant protein (only 8.8% increase in F.I. of WT upon ageing) but blue shift was still retained (Fig 12A) and the mutant A216V and V108M showed similar changes as freshly prepared protein (Fig 12B

and C). When the protein was reduced using 1mM DTT, WT hSCGN as well as the mutants A216V and R77H regained the ability to show the response to calcium by prominent increase in F.I (25.5%, 33.9% and 25.4% respectively) along with blue shift of nearly 4nm (Fig 13A, B and C). Circular Dichroism spectra also showed similar result. WT and mutants A216V and R77H, in oxidized state did not show prominent change in tertiary spectra upon calcium addition (Fig 13 A, B and C). When these proteins were reduced with 1mM DTT, they still did not show marked change in tertiary spectra (result not shown) but upon reduction with 4mM DTT and incubation for 1 hour, there was markable increase in positive signal upon titration with calcium i.e. increase of MRE by 5units, 2units and 2units respectively for WT, A216V and R77H (Fig 14 A, B and C). This clearly shows that, secretagogin is less responsive to calcium in dimeric or higher oligomeric state. Upon treatment with DTT, the disulphide bonds were broken and the protein was converted to monomeric state which shows greater response towards calcium. This result corresponds with the fact that in reducing condition such as cytosol, SCGN has greater affinity for calcium whereas in oxidizing condition of ER, it has lesser affinity for calcium (Khandelwal *et al*., 2017). This Ca^{2+}-redox switch can be an important mechanism to regulate protein function. The WT protein, upon ageing undergoes oligomerization showing less response to calcium. This gives us the idea that *in vivo,* when Secretagogin becomes old, it undergoes dimerization and becomes less responsive to calcium due to which its calcium dependent properties might get disrupted. The change in tertiary CD spectra was greatest in WT protein than the two mutants which again states that WT protein is more responsive to calcium than the two mutants.

5.4 Anomalous behaviour of hSCGN V108M mutant

The V108M on the other hand displayed completely different characteristics than the WT as well as A216V and R77H mutant proteins. This mutant did not show increase in F.I. although small blue shift was observed in Fluorescence spectra upon calcium titration either in oxidized or reduced state (11D, 12D and 13D). There seemed to be a serious alteration in Ca^{2+} responsive/binding properties of the protein. Unlike other proteins, V108M mutant showed much prominent increase of 3.5 units in positive signal upon calcium titration in oxidized state (Fig.15D) whereas the increase became less prominent when the protein was reduced to 2.5units (Fig. 16D). The dimeric form this protein seems to show stronger response towards Calcium than the monomeric form of protein. This character surprised us completely because it directs us to the result that the Ca^{2+}-redox switch of this protein might have been reversed by this mutation. As seen in ANS fluorescence spectroscopy, V108M seems to have most exposed hydrophobic surface than WT and other mutants (Fig. 14D) with highest quantum yield and blue shift. This gives us the clue that V108M might have gained function with greater exposed hydrophobic patches which provides binding sites for its ligand. In the condition when WT hSCGN is not active, this mutant Secretagogin might remain active causing hyperactivation which might lead too abnormality.

5.5 Study of oligomeric property of protein by analytical gel filtration

In apo form of WT hSCGN, monomeric fraction was dominant (60%) but calcium induced dimerization of the protein increasing the population of dimer to 50% (Fig. 18A and B). The dimer was redox responsive as this dimer forming property of Ca^{2+} was lost in reduced condition (Fig. 18 C and D). In apo form of all the mutants, about 90% of the population was dimeric and upon binding calcium, the dimer population was increased (Fig. 18 A and B). The dimers formed by mutants were also redox responsive. It is already known that Ca^{2+} induced dimerization occurs due to structural changes in the N-terminal region of Secretagogin inducing the protein to form C-193 linked dimers more efficiently. This dimer formation is directly related to biological protein function such as insulin secretion (Lee *et al.*, 2017). These mutations might also have caused structural changes in N-terminal increasing the propensity of the mutant proteins to form dimer. This oligomeric state might be the major cause for altered calcium response which might alter the protein's biological function. If it is so, reducing stress in the cell, might reduce the dimeric fraction of mutants to monomeric fraction which is more Calcium responsive. Thus *in vivo*, the use to reducing pharmaceuticals may help these Secretagogin mutants to regain the normal functional state.

5.6 Interaction with Insulin

All the wild type and mutant proteins were found to interact with insulin. This interaction with insulin suggests that secretagogin might have role in other functions related to insulin other than exocytosis like insulin maturation or insulin oligomerization properties. The red shift that occurs in protein due to insulin binding states that tryptophan is exposed to the hydrophilic environment (Fig 21). The interaction of hSCGN WT and mutants is more effective in the presence of calcium as the reduction in F.I. was more prominent in holo form (Fig. 22). The binding affinity is increased by calcium which is defined by greater change in tertiary structure in holo form upon addition of same amount of insulin. Previous work done on mSCGN showed that the binding site of insulin and calcium in mSCGN is independent of each other and insulin binding with mSCGN does not affect calcium binding (Kumar Sharma *et al*., 2017). But the current analysis, the binding of insulin to holo form reverts the blue shift caused by Calcium (Fig. 22) on the protein indicating that insulin binding opposes the binding of calcium with hSCGN WT and mutant. The binding sites of the two might be dependent or the bound calcium might be replaced or allosterically removed by insulin. As hSCGN WT only was able to form stable complex with insulin as indicated by positive band in western blot (Fig. 25) biologically only the WT of protein might be able to induce the function downstream to insulin binding whereas mutants though having potential to bind insulin, might not be able form stable complex with it and might get outcompeted by other ligands of insulin and hence might not be able to induce the downstreaming functions.

5.7 Partial trypsin digestion and Glutaraldehyde crosslinking

All the protein showed greater digestion by trypsin in holo forms (Fig 26B and C). This indicates that the holo form of all the proteins have flexible parts more solvent exposed to the periphery which might directly be linked to the calcium dependent functions of the protein. The result from ANS fluorescence also indicates that Calcium bound holo form has more surface exposed hydrophobic patches (Fig. 14). This gives us the idea that the loops might be hydrophobic in nature and solvent exposure of these loops might help in protein function by exposing the ligand binding sites of Secretagogin. The holo form of V108M mutant shows highest digestion which implies that calcium binding causes greater exposure of hydrophobic loop and flexible region which is also supported by its ANS fluorescence spectra that shows highest F.I. in both apo and holo form. This gives suggests that hSCGN V108M mutant protein might be more active than WT protein and this hyperactivity might lead to pathological conditions.

Upon crosslinking by glutaraldehyde all the proteins formed oligomers (Fig 27). All the protein has the ability to form cysteine independent oligomers *in vitro*, as we could see large fraction of dimer even in the reduced form of protein crosslinked by glutaraldehyde. Whether this happens in the biological system or not is yet to be discovered. But if this happens, it would change the whole perspective of redox dependent monomeric-dimeric switch of this protein which is considered as the basis of its function.

5.6 Accessing calcium binding affinities by ITC

All the mutants bind calcium to some extent but the binding affinity or mechanism or redox response seems different than the wild type of protein. Though the Calcium binding affinity of hSCGN was previously determined to be log k_1= 7.1±0.4, log k_2= 4.7±0.6, logk_3= 3.6±0.7 and log k_4= 4.6±0.6 at physiological pH (Rogstam *et al*., 2007), in the current analysis it was determined to be k_1=1.89E^4±1.0E^{3}M^{-1}, k_2=4.61E^4±2.9E^{3}M^{-1}, k_3=2.55E^5±1.7E^{4}M^{-1} and k_4= 4.98E^5±2.7E^{4}M^{-1}. This might have occurred to different salt conditions used in the two experiments. Though mutant R77H binds Calcium with similar Ka values as that of WT hSCGN in oxidizing condition (Fig 19 A and C), calcium binding in reduced condition shows different Ka values (Fig 20 A and C). In reduced state, one site in the wild type protein shows highest binding affinity towards calcium (Ka 10^{5}M^{-1}) which acts as the calcium sensor site. Even in the oxidized state one site in WT proteins shows lowest free energy change value as shown in appendix 8 and 9 (-11.25 X 10^{3}cal Mol^{-1}) upon calcium binding and this site might act as calcium sensor site in oxidizing condition. This property was absent in mutant. This result leads us to the assumption that the mutant might have lost the calcium sensor property that is shown by the wild type of protein. V108M mutant which shows distinct properties in all the cases, shows lowest binding to Calcium even in ITC compared to WT as well as other mutant proteins in terms of both Ka and free energy change.

5.7 Stability analysis of protein by GdmCl unfolding assay

In GdmCl unfolding assay, though the apo form of V108M mutant has stability similar to that of other proteins (2.66M for V108M and 2.65M, 2.65M and 2.46M respectively for WT, A216V and R77H), the calcium bound form (holo) of V108M was most stable and started unfolding even with small concentration of GdmCl with a very small baseline (Fig. 28B and D). This is the indication that the calcium binding properties of V108M mutant is severely distorted by misfolding of protein due to mutation. Though this mutant binds calcium, but the affinity of binding along with the stability of holo form after binding Calcium is very less. This indicates that the binding of calcium might cause distortion in the structure of V108M mutant. Thus physiologically, this mutation might affect the calcium related function of Secretagogin severely which might lead to disease or malignancies such as cancer. R77H mutant shows lowest stability in apo form terms of its $C_{1/2}$ value i.e.2.46M which might have occurred due to misfolding because of mutation. This might result in stressed protein which might get degraded easily *in vivo* or have impaired functions. GdmCl unfolding assay can also be used to study the intermediate states formed during unfolding of protein but it could not be carried out in the current analysis.

R77H mutant that is found to be different from the wild type of protein in terms of calcium binding affinity, oligomeric state and stability has been found to be implicated in Ulcerative colitis and Cronh's disease. Though these structural perturbations gives idea that the protein normal function is altered by R77H mutation, the actual mechanism of how this mutation leads to these disease is yet to be discovered. A216V mutation that is also found to be different from WT protein in many aspects including calcium binding affinity, oligomeric state and insulin binding, might cause disruption in the function of protein though it is not yet found to be associated with any abnormalities yet. The detailed picture of how these mutations affect the overall 3D- structure of protein can only be studied by high resolution techniques like NMR and crystallography that provides further insights into the consequences of these mutations.

CHAPTER 6

SUMMARY

The multifunctional protein Secretagogin has come into limelight after the recent finding that its level is decreased in case of diabetic individuals and the chronic injection of Secretagogin not only improves insulin response but also can alleviate diabetes. Many mutations in this gene have been reported which are found to be associated with several disease and malignancies such as cancer. Q22R, A216V, R77H, V108M, R135Q, P276Q are some mutations that are clinically important. The mutation in Secretagogin that is studied in the current project are A216V, R77H and V108M.

To characterize the clinically important mutants of human secretagogin, the gene was first cloned in pET-21b vector. The WT secretagogin gene was used as to induce mutations at desired point using site directed mutagenesis technique. Mutants were also cloned in pET 21b vector. These WT and mutant proteins were then overexpressed from *E.coli* BL21 cells. The protein was then purified using hydrophobic interaction chromatography, anion exchange chromatography followed by preparative gel filtration. These proteins were decalcified and characterized using fluorescence spectroscopy, circular dichroism and isothermal titration calorimetry, analytical gel filtration chromatography, trypsin digestion and glutaraldehyde crosslinking. These genes were then transferred into mammalian vector pEGFP-N3 using restriction free cloning. These constructs were then used for transfection into MIN6 cells to produce stably transfected cell line.

It was found that mutation brings structural perturbation in the protein which results in alteration in properties of the mutants from the wild type protein. A216V and R77H were different from WT protein in terms of calcium binding affinity though both of them were found to bind calcium (as determined result of ITC) and dominant oligomeric state. Dimeric state was more prominent in these proteins but the monomeric form showed a greater response to calcium. R77H is also different form wild type of Secretagogin in terms of stability as its $C_{1/2}$ value is lesser than that of WT protein. V108M was different from WT and other mutants in many aspects such as calcium binding affinity, structural change upon calcium binding, oligomeric state as well as the state that binds calcium. This protein bound calcium less efficiently than others and interestingly it was found that the dimeric population was more calcium responsive. Calcium binding in all the proteins cause exposure of the flexible regions and loops, but the effect was most prominent in V108M mutant. In V108M mutant, the binding of calcium could not impart stability to the V108M mutant protein's structure as in case of other protein. hSCGN WT and all the mutants taken in the study showed interaction with insulin, but only wild type protein was able to form stable complex with insulin.

CHAPTER 7

CONCLUSION

Thus, it was possible to achieve the aim of the project since the mutants could be successfully overexperssed, purified and characterized. The study shows that a single mutation in the amino acid composition of the protein could bring a huge alteration in its structure which could directly affect the protein function and the cell physiology as a whole. This could be the basis of many genetic defects. In this study, the mutants were found to be different from the wild type protein in one way or the other. A216V and R77H mutation, though occurring in the calcium binding region did not cause loss of calcium binding properties in these mutants. But V108 mutant, which occurs in the helix region, causes perturbation in the protein structure in such a way that the behaviour of the protein as a whole is changed. The wild type of protein could form a stable complex with insulin which might have important physiological function. All the mutations affected the interaction of the protein with insulin which can have serious biological impact. The mutants were found to be dominantly present in dimeric state which can be the major cause of pathological condition. The reduction of dimeric form of mutants to monomeric form in the presence of reducing agent gives us the hope that the functional properties of mutants can be regained by the use of reducing pharmaceutical drugs. V108M which seemed to be hyperactive than WT protein, has dimer which is more Calcium responsive. Thus the use of reducing pharmaceutical drugs might reduce its more functional dimeric form of hSCGN V108M to less functional monomeric form. Mutant study not only helps to figure out the disease associated with the mutation in the gene but also may help to discover the unknown functions of the protein. Thus, the study of these mutants might provide deep insights into the diseases associated with the mutation in Secretagogin gene and indirectly help to figure out new function of the protein.

Limitations

- Because of the limitation of time, Q22R, R135Q and P276Q mutants could not be characterized.
- The digested fragments after trypsin digestion could not be given for mass spectrometry because of complexity and resources limitation.
- Though low resolution techniques like fluorescence spectroscopy and circular dichroism reveals some structural aspects of the protein, detailed structural analysis can only be done by high resolution techniques like Nuclear magnetic resonance/ X-ray crystallography.

Recommendations and future work

1. Overexpression, purification and characterization of remaining mutants (Q22R, R135Q and P276Q).

2. The interacting partners of the wild type and mutant secretagogin can be determined by differential pull down experiment.
3. The interaction of mutant protein with SNAP-25 could be studied by co-transfection of these genes into MIN6 cell line and co-localization study of the two proteins.
4. The effect of these mutations in the secretion of insulin can be studied in pancreatic cell by ELISA using anti-insulin Antibody.

CHAPTER 8

REFERENCES

Adolf, K., Wagner, L., Bergh, A., Stattin, P., Ottosen, P., Borre, M.,Tørring, N. (2007). Secretagogin is a new neuroendocrine marker in the human prostate. *The Prostate*, *67*(5), 472–484. https://doi.org/10.1002/pros.20523

Aghajanian, S., Hovsepyan, M., Geoghegan, K. F., Chrunyk, B. A., & Engel, P. C. (2003). A thermally sensitive loop in clostridial glutamate dehydrogenase detected by limited proteolysis. *The Journal of Biological Chemistry*, *278*(2), 1067–74. https://doi.org/10.1074/jbc.M206099200

Agilent Technologies. (2015). *SIZE EXCLUSION CHROMATOGRAPHY FOR BIOMOLECULE ANALYSIS*. © Agilent Technologies, Inc. Retrieved from https://www.agilent.com/cs/library/primers/public/5991-3651EN_LR.pdf
amersham pharmacia biotech. (n.d.). *Gel filtration Principles and Methods* (8th ed.).

Birkenkamp-Demtröder, K., Wagner, L., Brandt Sørensen, F., Bording Astrup, L., Gartner, W., Scherübl, H., … Ørntoft, T. F. (2006). Secretagogin Is a Novel Marker for Neuroendocrine Differentiation. *Neuroendocrinology*, *82*(2), 121–138. https://doi.org/10.1159/000091207

Bitto, E., Bingman, C. A., Bittova, L., Frederick, R. O., Fox, B. G., & Phillips, G. N. (2009). X-ray structure of *Danio rerio* secretagogin: A hexa-EF-hand calcium sensor. *Proteins: Structure, Function, and Bioinformatics*, *76*(2), 477–483. https://doi.org/10.1002/prot.22362

Brini, M., Ottolini, D., Brini, M., Ottolini, D., Calì, T., & Carafoli, E. (2013). *Interrelations between Essential Metal Ions and Human Diseases* (Vol. 13). https://doi.org/10.1007/978-94-007-7500-8

CanProVar 2.0:Human Cancer Proteome Variation Database. (n.d.). Retrieved September 15, 2017, from http://lilab.life.sjtu.edu.cn:8080/canprovar2/inforprotein.php?id=SCGN&display%5B3%5D=COSMIC&display%5B4%5D=TCGA&display%5B5%5D=HPI&display%5B6%5D=OMIM&display%5B7%5D=Biomart&display%5B2%5D=DEP&display%5B1%5D=snp

Carafoli, E., & Krebs, J. (2016). Why calcium? How calcium became the best communicator. *Journal of Biological Chemistry*, *291*(40), 20849–20857. https://doi.org/10.1074/jbc.R116.735894

Clapham, D. E. (2007). Calcium Signaling. *Cell*, *131*(6), 1047–1058. https://doi.org/10.1016/j.cell.2007.11.028

Correa, D. H. A., & Ramos, C. H. I. (2009). The use of circular dichroism spectroscopy to study protein folding , form and function. *African Journal of Biochemistry Research*, *3*(5), 164–173.

Dutta, A. K., Rosgen, J., & Rajarathnam, K. (2015). Using isothermal titration calorimetry to determine thermodynamic parameters of protein-glycosaminoglycan interactions. *Methods in Molecular Biology (Clifton, N.J.)*, *1229*, 315–24. https://doi.org/10.1007/978-1-4939-1714-3_25

Fadouloglou, V. E., Kokkinidis, M., & Glykos, N. M. (2008). Determination of protein oligomerization state: Two approaches based on glutaraldehyde crosslinking. *Analytical Biochemistry*, *373*(2), 404–406. https://doi.org/10.1016/j.ab.2007.10.027

Fontana, A., Polverino de Laureto, P., Spolaore, B., Frare, E., Picotti, P., & Zambonin, M. (n.d.). Probing protein structure by limited proteolysis. Retrieved from http://www.actabp.pl/pdf/2_2004/299.pdf

Freire, E., Mayorga, O. L., & Straume, M. (1990). Isothermal titration calorimetry. *Analytical Chemistry*, *62*(18), 950A–959A. https://doi.org/10.1021/ac00217a002

Garidel, Patrick & Kliche, Werner & Pisch-Heberle, Sandra & Thierolf, Michael. (2010). Chapter 2 Characterization of Proteins and Related Analytical Techniques. Protein Pharmaceuticals-formulation, Analytics & Delivery.

Gartner, W. (2001). Cerebral Expression and Serum Detectability of Secretagogin, a Recently Cloned EF-hand Ca2+ -binding Protein. *Cerebral Cortex*, *11*(12), 1161–1169. https://doi.org/10.1093/cercor/11.12.1161

Gerke, V., & Moss, S. E. (2002). Annexins: From Structure to Function. *Physiological Reviews*, *82*(2), 331–371. https://doi.org/10.1152/physrev.00030.2001

Ghisaidoobe, A. B. T., & Chung, S. J. (2014). Intrinsic tryptophan fluorescence in the detection and analysis of proteins: a focus on Förster resonance energy transfer techniques. *International Journal of Molecular Sciences*, *15*(12), 22518–38. https://doi.org/10.3390/ijms151222518

Greenfield, N. J. (2006). Using circular dichroism spectra to estimate protein secondary structure. *Nature Protocols*, *1*(6), 2876–90. https://doi.org/10.1038/nprot.2006.202.

Grindheim AK, Saraste J, V. A. (2017). Protein phosphorylation and its role in the regulation of Annexin A2 function. *Biochimica et Biophysica Acta (BBA) - General Subjects*, *1861*(11), 2515–2529. https://doi.org/10.1016/J.BBAGEN.2017.08.024

Hemsley, A., Arnheim, N., Toney, M.D., Cortopassi, G., and Galas, D. A simple method for site-directed mutagenesis using the polymerase chain reaction. Nucl. Acids Res. 17(16): 6545-6551 (1989).

Homo sapiens secretagogin, EF-hand calcium binding protein (SCGN), mRN - Nucleotide - NCBI. (n.d.). Retrieved September 15, 2017, from https://www.ncbi.nlm.nih.gov/nuccore/NM_006998.3

Jones, D.H., and Winistorfer, S.C. Site-specific mutagenesis and DNA recombination by using PCR to generate recombinant circles in vitro or by recombination of linear PCR products in vivo. Methods: A Companion to Methods in Enzymology 2(1): 2-10 (1991).

Jones, D.H., and Winistorfer, S.C. Recombinant circle PCR and recombination PCR for site-specific mutagenesis without PCR product purification. BioTechniques 12(4): 528-535 (1992).

Kapoor, M. (n.d.). How to cross-link proteins. Retrieved October 8, 2017, from http://www.fgsc.net/neurosporaprotocols/How to cross-link proteins.pdf

Khandelwal, R., Sharma, A. K., Chadalawada, S., & Sharma, Y. (2017). Secretagogin Is a Redox-Responsive Ca $^{2+}$ Sensor. *Biochemistry*, *56*(2), 411–420. https://doi.org/10.1021/acs.biochem.6b00761

Kumar Sharma, A., Khandelwal, R., Chadalawada, S., Sai Ram, N., Avinash Raj, T., Jerald Mahesh Kumar, M., & Sharma, Y. (2017). *SCGN Administration prevents Insulin Resistance and Diabetic Complications in High-Fat Diet Fed Animals*. *bioRXiv beta*. https://doi.org/10.1101/189324

Lee, J.-J., Yang, S.-Y., Park, J., Ferrell, J. E., Shin, D.-H., & Lee, K.-J. (2017). Calcium Ion Induced Structural Changes Promote Dimerization of Secretagogin, Which Is Required for Its Insulin Secretory Function. *Scientific Reports*, *7*(1), 6976. https://doi.org/10.1038/s41598-017-07072-4

Llano, E. M., Chan, L., Harrison, S. M., Li, H., Sifuentes-Dominguez, L., Park, J. Y., … Burstein, E. (2014). *Missense Mutation in SCGN (Secretagogin) as a Possible Cause of Ulcerative Colitis in Three Siblings*. Dallas, TX. Retrieved from https://repositories.tdl.org/utswmed-ir/bitstream/handle/2152.5/1486/Llano Poster.pdf?sequence=1&isAllowed=y

Norris, N., Sifuentes-Domínguez, L., & Burstein, E. (2016). *Mutant Secretagogin, a potential cause of ulcerative colitis, exhibits reduced affinity for SNARE complex protein SNAP-25 BACKGROUND and AIMS*. Dallas, TX

Novagen. (2003). pET System Tutorial. In *Protein Expression* (pp. 88–92). Retrieved from http://www.yrgene.com/documents/vector/c183-001.pdf

Rizo, J., & SuDhof, T. C. (1998). C 2 -domains, Structure and Function of a Universal Ca 2⁒ -binding Domain*. *The Journal of Biological Chemistry*, *273*(June 26), 15879–15882

Rogstam, A., Linse, S., Lindqvist, A., James, P., Wagner, L., & Berggård, T. (2007). Binding of calcium ions and SNAP-25 to the hexa EF-hand protein secretagogin. *Biochemical Journal*, *401*(1), 353–363. https://doi.org/10.1042/BJ20060918

SEGN_HUMAN | SNPeffect 4.0. (n.d.). Retrieved September 15, 2017, from http://snpeffect.switchlab.org/uniprot/SEGN_HUMAN.

Sharma, A. K., Khandelwal, R., Sharma, Y., & Rajanikanth, V. (2015). Secretagogin, a hexa EF-hand calcium-binding protein: High level bacterial overexpression, one-step purification and properties. *Protein Expression and Purification*, *109*, 113–119. https://doi.org/10.1016/j.pep.2015.02.011

Studer, R. A., Dessailly, B. H., & Orengo, C. A. (2013). Residue mutations and their impact on protein structure and function: detecting beneficial and pathogenic changes. *Biochemical Journal*, *449*(3), 581–594. https://doi.org/10.1042/BJ20121221

Tiber, P. M., Orun, O., Nacar, C., Sezerman, U. O., Severcan, F., Severcan, M., … Kan, B. (n.d.). Structural characterization of recombinant bovine Goα by spectroscopy and homology modeling. *Journal of Spectroscopy*, *26*(4–5), 213–229. https://doi.org/10.3233/SPE-2011-0543

Uversky, V.N and Permiakov, E. . (2007). *Methods in Protein Structure and Stability Analysis: Vibrational spectroscopy - - Google Books*. (V. N. U. and E. A.Permiakov, Ed.), *Nova Science Publishers, Inc.* New York

Vivian, J.T and Callis, P. R. (2001). Mechanisms of Tryptophan Fluorescence Shifts in Proteins. *Biophysical Journal*, *80*(5), 2093–2109. https://doi.org/10.1016/S0006-3495(01)76183-8

Wagner, L., Oliyarnyk, O., Gartner, W., Nowotny, P., Groeger, M., Kaserer, K., … Pasternack, M. S. (2000). Cloning and Expression of Secretagogin, a Novel Neuroendocrine- and Pancreatic Islet of Langerhans-specific Ca^{2+} -binding Protein. *Journal of Biological Chemistry*, *275*(32), 24740–24751. https://doi.org/10.1074/jbc.M001974200

Wang, Z., & Moult, J. (2001). SNPs, protein structure, and disease. *Human Mutation*, *17*(4), 263–270. https://doi.org/10.1002/humu.22

Yang, S.-Y., Lee, J.-J., Lee, J.-H., Lee, K., Oh, S. H., Lim, Y.-M., … Lee, K.-J. (2016). Secretagogin affects insulin secretion in pancreatic β-cells by regulating actin dynamics and focal adhesion. *The Biochemical Journal*, *473*(12), 1791–803. https://doi.org/10.1042/BCJ20160137

Zierhut, B., Daneva, T., Gartner, W., Brunnmaier, B., Mineva, I., Berggård, T., & Wagner, L. (2005). Setagin and secretagogin-R22: Posttranscriptional modification products of the secretagogin gene. *Biochemical and Biophysical Research Communications*, *329*(4), 1193–1199. https://doi.org/10.1016/j.bbrc.2005.02.093

APPENDICES

Appendix 1: Preparation of LB broth (1 litre)

10gm of tryptone, 10gm of NaCl and 5gm of Yeast extract was dissolved in 200ml of distilled water and then the volume was maintained to 1litre in a measuring cylinder. The media was then autoclaved and used.

Appendix 2: Preparation of LB Amp plates (250ml)

LB powder was directly added into 500ml of distilled water in a 500ml conical flask and autoclaved. The media was allowed to cool to about 45°C. 250µl of ampicillin solution (Stock concentration 100mg/ml) was added to the molten media and carefully swirled to mix. The media was then poured in Petri plates 20 to 25ml in each plates. The plates were then parafilmed and stored in the cold room.

Appendix 3: Preparation of 10X TAE buffer

48.4 gram of tris-base, 11.4ml of glacial acetic acid (17.4M) and 3.7gram of EDTA sodium salt was dissolved in 800ml of distilled water. The solution was diluted to 1000ml. Each time while using the buffer, the stock is diluted 10 times to bring the concentration to 1X.

Appendix 4: Preparation of 10X TGS buffer

30.2 gm of Tris-base and 122 gm of Glycine was dissolved in 500ml of distilled water. 10gm of SDS was dissolved in 50ml of warm distilled water. The two solutions were mixed and the volume was brought to 1 litre with distilled water.

Appendix 5: Preparation of transfer buffer (1 litre)

14.4 gm of Glycine and 3.33 gm of Tris-base was added to 500 ml of distilled water. 200ml of methanol was added to it just before use and the volume was brought to 1litre with distilled water.

Appendix 6: Preparation of DMEM media

13.3 grams of DMEM powder was dissolved in 900ml of autoclaved MilliQ water completely by stirring. 3.7 grams of sodium bicarbonate was dissolved into it. The p^H was adjusted to 7. The volume was adjusted to 1000ml with autoclaved MilliQ water. The media was then filtered using sterile filter membrane with porosity of 0.22 micron. Antibiotic (1X) was added according to requirement and 10% FBS was added to it to prepare the complete media.

Appendix 7: GdmCl unfolding profile of WT and mutants Secretagogin represented via tryptophan fluorescence spectra

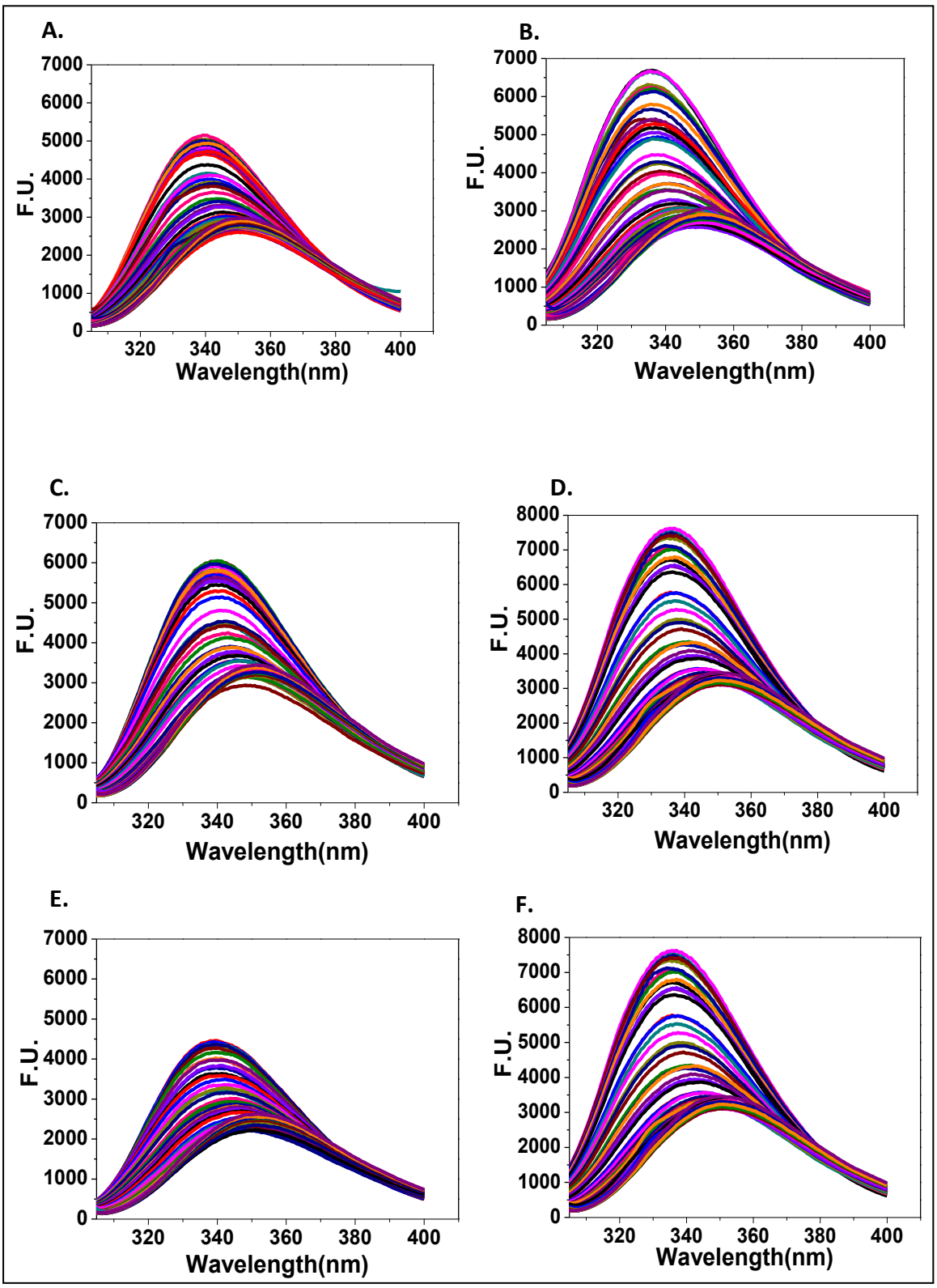

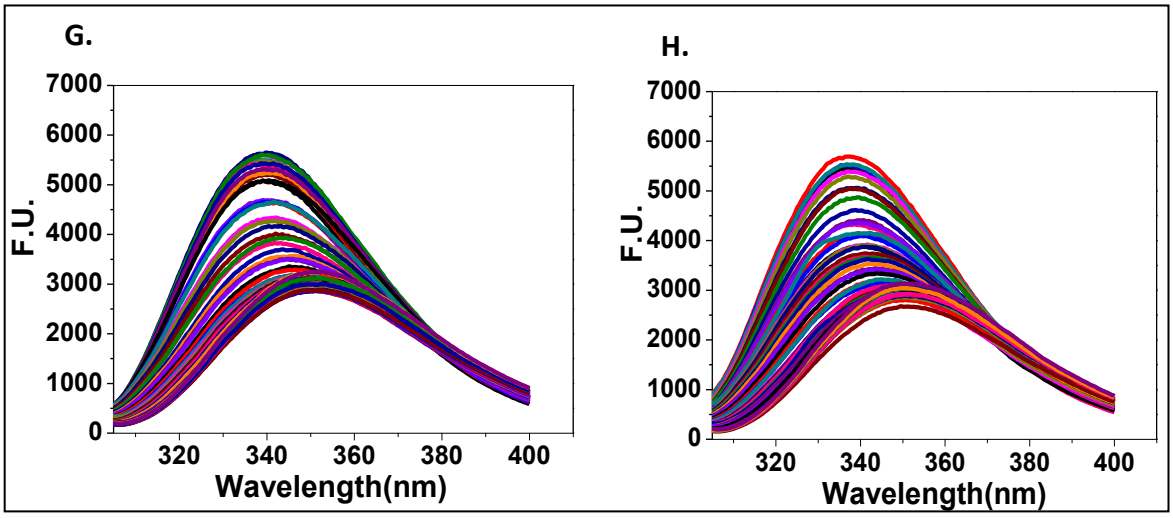

Figure 31: GdmCl unfolding profile of WT and mutant Secretagogin in oxidizing condition at apo and holo form studied by tryptophan fluorescence spectra. **Figure A:** Apo hSCGN WT, **Figure B:** Holo WT hSCGN, **Figure C:** Apo hSCGN A216V, **Figure D:** Holo hSCGN A216V, **Figure E:** Apo hSCGN R77H, **Figure F:** Holo hSCGN R77H, **Figure G:** Apo hSCGN V108M, **Figure H:** Holo hSCGN V108M

Appendix 8: Gibb's free energy value for four calcium binding sites of hSCGN WT and mutants upon calcium binding in oxidized condition.

hSCGN	ΔG1	ΔG2	ΔG3	ΔG4
WT	-5.59×10^3	-4.13×10^3	-11.25×10^3	-6.3×10^3
A216V	-6.97×10^3	-6.81×10^3	-5.81×10^3	-6.71×10^3
R77H	-7.28×10^3	-5.56×10^3	-6.65×10^3	-7.77×10^3
V108M	-6.4×10^3	-6×10^3	-5.36×10^3	-4.9×10^3

Appendix 9: Gibb's free energy value for four calcium binding sites of hSCGN WT and mutants upon calcium binding in reduced condition.

hSCGN	ΔG1	ΔG2	ΔG3	ΔG4
WT	-7.13×10^3	-5.63×10^3	-6.4×10^3	-6.25×10^3
A216V	-5.8×10^3	-5×10^3	-6.44×10^3	-4.92×10^3
R77H	-6.03×10^3	-6.94×10^3	-4.88×10^3	-3.39×10^3
V108M	-6.78×10^3	-5.62×10^3	-4.55×10^3	-4.21×10^3

Appendix 10: Confirmation of hscgn eGFP-N3 clones after sequencing by using expasy translate tool

MDSSREPTLGRLDAAGFWQVWQRFDADEKGYIEEKELDAFFLHMLMKLGTDDTVMKANLHKVKQQFMTT
QDASKDGRIRMKELAGMFLSEDENFLLLFRRENPLDSSVEFMQIWRKYDADSSGFISAAELRNFLRDLFLHHKK
AISEAKLEEYTGTMMKIFDRNKDGRLDLNDLARILALQENFLLQFKMDACSTEERKRDFEKIFAYYDVSKTGALE
GPEVDGFVKDMMELVQPSISGVDLDKFREILLRHCDVNKDGKIQKSELALCLGLKINPVSKGEELFTGVVPILVE
LDGDVNGHKFSVSGEGEGDATYGKLTLKFICTTGKLPVPWPTLVTTLTYGVQCFSRYPDHMKQHDFFKSAMP
EGYVQERTIFFKDDGNYKTRAEVKFEGDTLVNRIELKGIDFKEDGNILGHKLEYNYNSHNVYIMADKQKNGIKV
NFKIRHNIEDGSVQLADHYQQNTPIGDGPVLLPDNHYLSTQSALSKDPNEKRDHMVLLEFVTAAGITLGMTS

Figure 32: Confirmation of hscgn WT eGFP-N3 by expasy translate tool. Amino acid sequence of hSCGN WT followed by eGFP tag where EGFP tag is underlined

MDSSREPTLGRLDAAGFWQVWQRFDADEKGYIEEKELDAFFLHMLMKLGTDDTVMKANLHKVKQQFMTT
QDASKDGRIRMKELAGMFLSEDENFLLLFRRENPLDSSVEFMQIWRKYDADSSGFISAAELRNFLRDLFLHHKK
AISEAKLEEYTGTMMKIFDRNKDGRLDLNDLARILALQENFLLQFKMDACSTEERKRDFEKIFAYYDVSKTGVLE
GPEVDGFVKDMMELVQPSISGVDLDKFREILLRHCDVNKDGKIQKSELALCLGLKINPVSKGEELFTGVVPILVE
LDGDVNGHKFSVSGEGEGDATYGKLTLKFICTTGKLPVPWPTLVTTLTYGVQCFSRYPDHMKQHDFFKSAMP
EGYVQERTIFFKDDGNYKTRAEVKFEGDTLVNRIELKGIDFKEDGNILGHKLEYNYNSHNVYIMADKQKNGIKV
NFKIRHNIEDGSVQLADHYQQNTPIGDGPVLLPDNHYLSTQSALSKDPNEKRDHMVLLEFVTAAGITLGMDEL
YNKGL

Figure 33: Confirmation of hscgn A216V eGFP-N3 by expasy translate tool. Amino acid sequence of hSCGN A216V mutant followed by eGFP tag where the site of mutation is denoted by red coloured amino acid and EGFP tag is underlined.

MDSSREPTLGRLDAAGFWQVWQRFDADEKGYIEEKELDAFFLHMLMKLGTDDTVMKANLHKVKQQFMTT
QDASKDGHIRMKELAGMFLSEDENFLLLFRRENPLDSSVEFMQIWRKYDADSSGFISAAELRNFLRDLFLHHK
KAISEAKLEEYTGTMMKIFDRNKDGRLDLNDLARILALQENFLLQFKMDACSTEERKRDFEKIFAYYDVSKTGAL
EGPEVDGFVKDMMELVQPSISGVDLDKFREILLRHCDVNKDGKIQKSELALCLGLKINPVSKGEELFTGVVPILV
ELDGDVNGHKFSVSGEGEGDATYGKLTLKFICTTGKLPVPWPTLVTTLTYGVQCFSRYPDHMKQHDFFKSAM
PEGYVQERTIFFKDDGNYKTRAEVKFEGDTLVNRIELKGIDFKEDGNILGHKLEYNYNSHNVYIMADKQKNGIK
VNFKIRHNIEDGSVQLADHYQQNTPIGDGPVLLPDNHYLSTQSALSKDPNEKRDHMVLLEFVTAAGITLGMD
RSRTK

Figure 34: Confirmation of hscgn R77H eGFP-N3 by expasy translate tool. Amino acid sequence of hSCGN R77H mutant followed by eGFP tag where the site of mutation is denoted by red coloured amino acid and EGFP tag is underlined.

MDSSREPTLGRLDAAGFWQVWQRFDADEKGYIEEKELDAFFLHMLMKLGTDDTVMKANLHKVKQQFMTT
QDASKDGRIRMKELAGMFLSEDENFLLLFRRENPLDSSMEFMQIWRKYDADSSGFISAAELRNFLRDLFLHHK
KAISEAKLEEYTGTMMKIFDRNKDGRLDLNDLARVLALQENFLLQFKMDACSTEERKRDFEKIFAYYDVSKTGA
LEGPEVDGFVKDMMELVQPSISGVDLDKFREILLRHCDVNKDGKIQKSELALCLGLKINPVSKGEELFTGVVPIL
VELDGDVNGHKFSVSGEGEGDA

Figure 35: Confirmation of hscgn V108M eGFP-N3 by expasy translate tool. Amino acid sequence of hSCGN V108M mutant followed by eGFP tag where the site of mutation is denoted by red coloured amino acid and EGFP tag is underlined.

Table of contents